The Role of D-Serine in Normal Retinal Function and Implications for Psychiatry

A DISSERTATION
SUBMITTED TO THE FACULTY OF
UNIVERSITY OF MINNESOTA
BY

Nathalia Torres Jimenez

IN PARTIAL FULFILLMENT OF THE REQUIREMENTS
FOR THE DEGREE OF
DOCTOR OF PHILOSOPHY

Linda K. McLoon, Ph.D., Thesis Advisor

August 2019

Acknowledgements

I would like to acknowledge the mentorship of Dr. Robert F. Miller and Dr. Linda McLoon whose teachings shaped me as a scientist and person.

Dr. Robert Miller's interest and enthusiasm in understanding the neural network responsible for vison was contagious and fueled my desire to learn more about retinal circuitry. From his instruction, I learned the value of understanding science through a historical lens; appreciating current and old scientific literature as independent puzzle pieces that have not yet been connected to the whole. The time he spent discussing scientific papers with me provided the foundation for the work in this dissertation. I thank him greatly for the opportunity, support, instruction, time, and belief in me.

Dr. Linda McLoon's commitment to graduate level education allowed me to complete the investigation I started in Dr. Miller's laboratory. From her strong visual and written communication, my writing skills and this body of work were enriched. The time she spent listening to my scientific inquiries benefited my work and highlighted the importance of discussing ideas aloud. I thank her for taking me into her lab as a late graduate student, sponsoring my work, for pushing me to my full potential and for believing in me.

I am thankful to my committee members, Dr. Eric Newman, Dr. Paulo Kofuji, and Angus McDonald III for posing challenging questions that guided my research; conducting deep discussions of my work and providing unyielding support.

I thank the people from the Miller and the McLoon labs, past and present, for their technical instruction, support, and insight. This includes Dr. Manuel Esguerra, Dr. Eric Gustafson, Gabriel Romero, Amber Lockridge, Rachel Kueppers, and Dr. Heidi Roehrich.

I thank the GPN community and entering class of 2012. Special thanks to Dr. Steve McLoon for improving my public presentation skills since my first colloquium; Dr. Anna Ingebretson for the most interesting conversations on the English language I've ever had and unwavering moral support; to Dr. Craig Moodie for convincing me to come to Minnesota and adopting me as a little sister; to Dr. Marc Pisansky for bouncing around scientific ideas with me and always having the perfect playlist; Dr. David Zhang for blending creativity with science in ways I didn't imagine possible; to Dr. Adele DeNicola for advocating for others and riding this roller coaster till the end with me; to Justin Lines for answering my signal processing questions and providing great moral support; to Dr. Martha Streng, Dr. Zoé Christenson Wick, and Zach Zeidler for instantaneous moral support and advice, especially during tough times in Ethahall; to Alex Doyle and Gerardo Rodriguez Orellana for endless streams of Takis, candy, and support throughout graduate school and, love for Python.

I thank my Twin Cities family for making Minnesota a little bit less cold through their warmth, community, and love; if it were not for them, I would have returned to Colombia long ago. Special thanks to Eliza Rasheed, Mary Delorié, Lanka Dasanayaka, and Liam Callahan for feeding me, encouraging me, and dancing with me! To Dan Newsom and Dr. Natalie Newsom for striving to reach one's maximum potential and speaking Spanish with me. To Anna Min and Tina Cho for taking amazing professional headshots free of charge and feeding me. To Mark Komen and Lynda Cannova for supporting me professionally and sharing your personal struggles with schizophrenia, it fueled me to continue my work despite the obstacles. To Can Do Canines, for training the most incredible hearing dog, Darla to be my faithful companion. And last, but not least, thank you to my in-laws: Ken Kitchen, Jane Kitchen, Gillean Kitchen, Dr. Diego Hernando, and Anastasia Raykova for loving and caring for me above all else.

Dedication

Para mi familia, soy la primera, pero no la última. Se suele decir que << se necesita una aldea para criar un niño o una niña>> y, en mi caso lo ha sido. Les quiero agradecer por cuidar, alimentar, y hasta castigar a mí hermano y a mi cuando hacíamos maldades, travesuras o incumplíamos con nuestras tareas mientras nuestros padres estaban trabajando. Ha sido posible llegar a esta cima por su apoyo y cariño incondicional. Nunca lo olvidaré.

To my parents, Jairo Efrain Torres and Maria Fanny Jimenez, whose indisputable love and support gave me the strength to know that a dream could become a possibility.

To my brother, Miguel Angel Torres Jimenez, whose stern love equipped me with technological savviness that aided my ability to troubleshoot experimental problems.

To Ian James Kitchen, my husband and best friend, for everything.

Abstract

There is a lack of objective measurements for assessing the progression of mental disorders such as schizophrenia. Biomarkers for schizophrenia would be an invaluable asset to identify at-risk individuals objectively, which should consequently improve the person's prognosis and treatment. One such candidate for becoming a biomarker for schizophrenia is the flash-electroretinogram (fERG), an ophthalmological tool that assesses retinal integrity. Prior research had conflicting results, with some studies showing that people with schizophrenia have a reduced response from photoreceptors and bipolar cells. However, it has been unclear why abnormalities would occur that early in the retinal pathway when mouse studies that investigated monoamine deprivation, such as dopamine, did not reflect those deficits. An alternative reason for an altered fERG is that it may reflect reduced N-methyl-d-aspartate receptor (NMDAR) function, which has been postulated to explain some of the pathology exhibited in people with schizophrenia. However, no retinal field potentials in the outer retina had been attributed to NMDAR function. One way to induce hypofunction of the NMDAR is by reducing the availability of its co-agonist, either glycine or D-serine, since the NMDAR needs both glutamate and a co-agonist for activation. I examined how D-serine deprivation and its excess affects the outer retinal field potentials, and whether it has implications for psychiatry. We report the first fERG study in a genetic mouse model of schizophrenia characterized by NMDAR hypofunction from genetic silencing of serine racemase expression ($SR^{-/-}$), an enzyme that converts L-serine to D-serine. We analyzed fERG components under mesopic-adapted conditions that reflect outer retinal function, the a-wave and the b-wave, to determine the resemblance to the human fERG from people with schizophrenia. In all the analyses, I included sex as a factor, due to the

sex differences underlying the disease. We tested pharmacologically-induced hyperfunction of the NMDAR in WT mice by introducing D-serine. Lastly, we analyzed human fERG and pattern-electroretinogram (PERG) studies to assess outer and inner retinal function. I report that hypo- or hyper-function of the NMDAR, through changes in available D-serine, profoundly affects the temporal scale of photoreceptor and bipolar cell signaling, as well as the amplitude of bipolar cell currents. This work mirrors the deficits observed in people with schizophrenia. Including sex as a factor in analyses showed that D-serine affects male mice more profoundly regardless of genotype, suggesting that NMDAR and D-serine are involved in the retinal field potentials of the outer retina and are dependent on the animal's sex. These studies also suggest that either there is a functional NMDAR component to the outer retinal field potentials or that D-serine has another role in the retina aside from being an endogenous co-agonist for the NMDAR. This implicates the involvement of gonadal hormones and D-serine in retinal functional integrity. Our human analyses reflect deficits in the retinal ganglion cell layer, and a trending reduction of the signal corresponding to bipolar cells. Furthermore, the human data analyses also showed an interaction between sex, with deficits affecting males with schizophrenia more profoundly. This work elevates the potential of the fERG to differentiate between healthy controls and subjects with schizophrenia, and to detect sex differences known to be present in schizophrenia.

Table of contents

Page

Abstract iv

List of tables viii

List of figures x

Chapter 1: Introduction

Significance 1

Schizophrenia: NMDAR hypofunction hypothesis 3

NMDAR, serine racemase and D-serine expression in the retina 6

Developmental differences in expression and distribution 8

NMDAR, D-serine and serine racemase function in the retina 10

Flash-electroretinogram 11

Flash-electroretinogram in people with schizophrenia 15

My aims and contributions 20

Chapter 2: Electroretinographic Abnormalities and Sex Differences in an NMDAR Hypofunction Mouse Model of Schizophrenia: A and B Wave Analysis

Synopsis 24

Introduction 26

Methods 30

Results 35

Discussion 47

Supplementary material 55

Chapter 3: Effects of D-Serine in Outer Retinal Function

Synopsis 58

Introduction 59

Methods 60

Results 62

Discussion 82

Chapter 4: Electroretinographic Evidence of Retinal Ganglion Cell Dependent Function in Schizophrenia

Synopsis 85

Introduction 87

Methods 93

Results 102

Discussion 113

Supplementary materials 120

Chapter 5: Conclusion 127

Bibliography 133

List of tables

Page

Chapter 1: Introduction

Table 1.1 Summary of fERG abnormalities in people with schizophrenia 16

Chapter 2: Electroretinographic Abnormalities and Sex Differences in an NMDAR Hypofunction Mouse Model of Schizophrenia: A and B Wave Analysis

Table 2.1 A-wave implicit time in WT and $SR^{-/-}$ mice 36

Table 2.2 A-wave implicit time in WT and $SR^{-/-}$ mice depending on sex.....37

Table 2.3 B-wave amplitudes in WT and $SR^{-/-}$ mice 40

Table 2.4 B-wave amplitudes in WT and $SR^{-/-}$ mice depending on sex.....40

Table 2.5 B-wave implicit time in WT and $SR^{-/-}$ mice 42

Table 2.6 B-wave implicit time in WT and $SR^{-/-}$ mice depending on sex.....42

Table 2.7 B/a wave ratio in WT and $SR^{-/-}$ mice 44

Table 2.8: Low frequency component in WT and $SR^{-/-}$ mice 46

Table 2.9 Low frequency component in WT and $SR^{-/-}$ mice depending on sex 46

Supp. Table 2.1: A-wave amplitudes in WT and $SR^{-/-}$ mice depending on sex 55

Chapter 3: Effects of D-serine in Outer Retinal Function

Table 3.1 Statistical analysis of the a-wave amplitude 64

Table 3.2 Effect of D-serine on the a-wave amplitude for each group.....66

Table 3.3 Statistical analysis of the a-wave implicit time 68

Table 3.4 Effect of D-serine on the a-wave implicit time for each group 70

Table 3.5 Statistical analysis of the b-wave amplitude 73

Table 3.6 Effect of D-serine on b-wave amplitude for each group.....75

Table 3.7 Statistical analysis of b-wave implicit time 78

Table 3.8 Effect of D-serine for the b-wave implicit time for each group 80

Chapter 4: Electroretinographic Evidence of Retinal Ganglion Cell Dependent Function in Schizophrenia

Table 4.1 Clinical and demographic characteristic of the participants.....93

Table 4.2 Parameters of the visual stimuli used for data collection 95

Table 4.3 Statistical analysis of the PhNR-fERG 103

Table 4.4 Statistical analysis of the oscillatory potentials 106

Table 4.5 Statistical analysis of the PERG evoked using the CRT display 109

Table 4.6 Statistical analysis of the PERG evoked by LED display 109

Supp Table 4.1 Variability measurements 119

Supp Table 4.2 Statistical analysis for the b-wave amplitude and b/a ratio 120

Supp Table 4.3 Statistical analysis for a-wave, b-wave, and PhNR implicit time.....120

Supp Table 4.4 Analysis of the PhNR/b-wave ration 121

List of figures

Page

Chapter 1: Introduction

Figure 1.1 Schematic of a mouse flash-electroretinogram 13

Figure 1.2 Schematic of retinal currents reflected in a fERG 14

Chapter 2: Electroretinographic Abnormalities and Sex Differences in an NMDAR Hypofunction Mouse Model of Schizophrenia: A and B Wave Analysis

Figure 2.1 Representative fERG recordings from WT and $SR^{-/-}$ mice.....34

Figure 2.2 A-wave implicit time analysis 36

Figure 2.3 B-wave amplitude analysis.....39

Figure 2.4 B-wave implicit time analysis 41

Figure 2.5 b/a wave ratio analysis 43

Figure 2.6 Fourier transform analysis.....45

Supplementary Figure 2.1 A-wave amplitude analysis 56

Supplementary Figure 2.2 Retinal layer height calculations 57

Chapter 3: Effects of D-serine in Outer Retinal Function

Figure 3.1 Effects of D-serine on the a-wave amplitude 65

Figure 3.2 Effects of D-serine on the a-wave implicit time.....69

Figure 3.3 Effects of D-serine on a-wave implicit time: sex, genotype, and treatment.....71

Figure 3.4 Effects of D-serine on b-wave amplitude 74

Figure 3.5 Effects of D-serine on b-wave amplitude: sex, genotype, and treatment 76

Figure 3.6 Effect of D-serine on b-wave implicit time.....79

Table 3.7 Effects of D-serine on b-wave implicit time: sex, genotype, and treatment 81

Chapter 4: Electroretinographic Evidence of Retinal Ganglion Cell Dependent Function in Schizophrenia

Figure 4.1 Individual PhNR-fERG waveform for a single subject at a single flash strength ...95

Figure 4.2 Filtered PhNR-fERG for every subject at the brightest flash strength.....102

Figure 4.3 PhNR-ffERG N72 and PhNR component: amplitude and time 105
Figure 4.4 Oscillatory potentials 107
Figure 4.5 Filtered PERG traces for every subject 110
Figure 4.6 N35 component of the PERG: amplitude and time 111
Supplementary Figure 4.1 Scatterplot of BPRS as a function of age.....122
Supplementary Figure 4.2 Histograms representing time of recording 123
Supplementary Figure 4.3 a-wave and b-wave: amplitude and time 124

.

Chapter 1

Introduction

One of the overarching goals in medicine today is the attempt to understand the etiology of diseases to increase our ability to diagnose conditions that affect the central nervous system. This will potentially allow us to detect conditions earlier and design treatments to decrease illness and disability. Currently, there is a lack of objective measures for assessing various medical conditions at various stages of the disease (Slikker Jr, 2018). In response to this need, the United States' medical research agency, the National Institute of Health (NIH), has made it its mission to support research in "understanding of causes, diagnosis, prevention of and cure of human diseases", setting a national quest to find objective markers in medicine to serve as biomarkers. Biomarkers are biological features that can provide information about risk, occurrence, and/or progression of disease. Medical conditions where biomarkers can have tremendous impact are in the diagnosis and prognosis of psychiatric diseases such as schizophrenia. Clinical interviews are the current method of diagnosing schizophrenia; however, despite being able to identify the disease once present, it fails to detect people with schizophrenia prior to symptom onset (Weickert, Weickert, Pillai, & Buckley, 2013). Identifying at risk individuals would be invaluable for earlier prognostic and symptom-specific treatment.

Significance

Schizophrenia is a chronic and severe disease that affects between 0.25% - 0.65% of people in the United States (Desai, Lawson, Barner, & Rascati, 2013; Kessler et al., 2005; Wu, Shi, Birnbaum, Hudson, & Kessler, 2006). Despite the small

percentage of the American population afflicted with the disease, it is quite disabling, and the economic cost is high. In 2002, Schizophrenia's economic burden to the United States was calculated at $67.2 billion dollars (Wu et al., 2005) rising in 2013 to $155.7 billion dollars (Cloutier et al., 2016). In part, this cost is attributed to the chronic nature of the disease as the exact cause of schizophrenia is not known, and current treatments only relieve symptoms but do not cure the disease. At present, people with schizophrenia must live with the disease throughout their lives, which implies a long-term commitment from families, who may lack the means to pay for unending treatments and to care for their loved one. The long-term nature of the disease yields an accumulated direct health care and non-health care related cost of $43.7 billion dollars due to the significant expense of hospital inpatient, outpatient, and emergency room visits along with the cost of prescription drugs, assistance from law enforcement, and often, homeless shelters (Chong et al., 2016). Although it is easy to acknowledge the direct costs associated with the disease, schizophrenia's burden to society as a whole is huge, due to the indirect cost from the lost productivity attributed to unemployment or decision of caregivers to leave jobs. This indirect cost, not caused directly by the disease, is estimated to be $117.3 billion dollars (Chong et al., 2016). Unfortunately, society must endure the consequences of this chronic, and yet incurable, disease with unending treatment because the etiology of schizophrenia is unknown. The current treatments for schizophrenia are anti-psychotic drugs that effectively reduce psychosis and relapse, but do not ameliorate other symptoms and have significant negative side effects (Luby et al., 1962). Many of these treatments are based on the dopamine hypothesis for the etiology of schizophrenia, using antipsychotic drugs, which work by blocking dopamine D2/3 receptors (Li et al., 2016; Snyder, 1976). A more recent hypothesis suggests loss of

function of the N-Methyl-D-Aspartate receptor (NMDAR) as a potential etiology for schizophrenia, and this has opened-up possibilities of new treatments.

Schizophrenia: NMDAR hypofunction hypothesis

There have been multiple hypotheses for the cause of schizophrenia, but one is based on the clinical observation of recreational use of dissociative anesthetics that caused patients to exhibit symptoms resembling schizophrenia (Luby et al., 1962). Since these dissociative anesthetics antagonized a subclass of glutamate receptors called the NMDAR, it was conjectured that schizophrenia could result, in part, from hypoactivity of the NMDAR. From these observations, a new hypothesis emerged that is attractive for the understanding the etiological underpinnings of schizophrenia: the NMDA receptor hypofunction hypothesis. Since the hypothesis inception, new studies from various fields provide evidence that in at least one large group of individuals, the pathophysiology of schizophrenia can be attributed to NMDAR hypofunction.

NMDAR

The NMDAR is an ionotropic glutamate receptor that is essential for information transfer at many synapses in the brain and retina. In structure, the NMDAR is a heterotetramer assembled from various combinations of its subunits: NR1, four variants of NR2 (A, B, C, D), and two variants of NR3 (A, B) (Das et al., 1998; Moriyoshi et al., 1991; Sugihara et al., 1992) To have a functional NMDAR channel, two obligatory NR1 subunits and two NR2 subunits, or a mixture of NR2 and N3 subunits, must be in place (Meguro et al., 1992). The NMDAR has several unique properties that underlie its physiological function. First, two ligands are required to activate the receptor, glutamate and a co-agonist (Kleckner and Dingledine, 1988; Paoletti, 2011), glycine or D-serine.

The binding site differs between the subunits; glutamate binds to the NR2 subunit, while D-serine and glycine bind to the NR1 subunit (Blanke and Van Dongen, 2009). Second, it is voltage-sensitive due to the presence of magnesium ion (Mg^{2+}) that blocks the receptor channel at resting potential and prevents any current flow at the NMDAR until the cell is depolarized, despite having both the agonist and co-agonist bound. Lastly, the NMDAR has a high permeability to calcium (Ca^{2+}), which activates a plethora of intracellular cascades that can result in synaptic depression, potentiation, or excitotoxicity depending on the amount of Ca^{2+} influx (Malenka and Bear, 2004). Although these properties are unique to the NMDAR, differing subunit composition adds to the complexity of this receptor because the NMDAR properties are determined by the subunit composition. This multifaceted receptor has been implicated in the etiological underpinnings of schizophrenia from evidence in proteomic and genomic studies that showed abnormalities in both the NMDAR and in NMDAR-interacting molecules at the synapse in people with schizophrenia (Föcking et al., 2015). This knowledge augments the necessity in understanding the NMDAR and its ligands as these are critical for shedding light on the mechanisms by which NMDA receptors can become hypoactive or hyperactive.

Co-agonist site and D-serine

One unique property of the NMDAR is the requirement of another agonist, other than glutamate, to activate the ion channel, which makes both co-agonists, glycine and D-serine, indispensable for NMDAR function. The co-agonist site of the NMDAR was previously known as the ‘strychnine-insensitive glycine site,’ which as the name suggests, reflects the bewilderment that originated from knowing that glycine bound to this site (Johnson and Ascher, 1987), but in the presence of strychnine, a glycine

antagonist, NMDAR currents were not abolished (Bristow et al., 1986; Kishimoto et al., 1981). At first, D-serine was not suspected as a candidate for co-agonist because D-amino acids were believed to play a role in lower organisms only (Corrigan, 1969). However, in 1992 substantial levels of D-serine were discovered in the rat brain (Hashimoto et al., 1992b), with a high correlation between D-serine and NMDAR binding in the brain (Hashimoto et al., 1993). More support for the presence of D-serine came from the development of a stereoselective antibody for D-serine that strongly labeled the hippocampus and frontal lobes of the rat brain, brain regions with a high density of NMDAR (Schell et al. 1995). The biosynthesis of D-serine requires the racemization of L-serine through the synthesizing enzyme serine racemase (Wolosker et al., 1999), while D-amino acid oxidase (DAAO) is the degradation enzyme in both the brain and retina (Beard et al., 1988; Jules et al. 1992; Neims et al., 1966; Schell et al., 1997). Functional relevance of D-serine for modulating the NMDAR came from experiments showing that exogenous addition of DAAO on to brain slices reduced NMDAR currents (Mothet et al., 2000). This suggested that, similar to glycine, D-serine serves as an endogenous co-agonist to the NMDAR. One possibility of invoking a reduction in NMDAR function would be limiting the amount of D-serine or glycine. Corroborating evidence in NMDAR hypofunction as an etiological component of schizophrenia comes from studies showing a difference in levels of both serine racemase and D-serine in people with schizophrenia. The levels of D-serine to total serine were lower in people with schizophrenia in both serum (Hashimoto et al., 1993; Yamada et al., 2005) and cerebral spinal fluid (Bendikov et al., 2007; Hashimoto et al., 2005). Post-mortem studies showed that protein levels of serine racemase were reduced in the hippocampus by 39% and in the frontal cortex by 21% in people with schizophrenia. In the hippocampus, the

serine racemase/DAAO ratio was 34% lower in schizophrenics (Bendikov et al., 2007). Furthermore, single nucleotide polymorphisms in the serine racemase gene have been associated with schizophrenia (Goltsov et al., 2006). On the treatment side, there was an improvement in schizophrenic symptoms when subjects received D-serine (Kantrowitz et al., 2010). Understanding of the NMDAR composition in the retina has increased since the postulation of the NMDAR hypofunction hypothesis, and the discovery of the ability of D-serine to act as an endogenous co-agonist for the NMDAR expanded the potential implications in Psychiatry.

NMDAR, D-serine, and serine racemase expression in the retina

NMDAR

Functional NMDARs were found in both outer and inner layers in the retina. In the outer layers, functional NMDARs were localized to horizontal cells (O'Dell and Christensen, 1989); while in the inner layers of the retina, NMDARs were present on retinal ganglion cells (RGCs) (Grünert et al., 2002; Hartveit et al., 1994; Zhang and Diamond, 2006) and amacrine cells (Hartveit and Veruki, 1997). Other cell types in the retina, such as photoreceptors and bipolar cells, expressed NMDAR subunits but functionality on these neurons is still in question. In photoreceptors, a polyclonal antibody for the alternative C-terminus of the NR1 (N1C2'), that recognized splice variants 3a,3b,4a, and 4b, was used to detect these splice variants on both cone pedicles and rods spherules in rats (Fletcher et al., 2000) and rabbits (Kalloniatis et al. 2004). *In situ* hybridization studies demonstrated that the NR1 and NR2B subunits had similar distribution patterns, both expressed in the inner nuclear and ganglion cell layer in rats (Brandstätter et al., 1994). Positive immunolabeling of the NR1 subunit in rod

bipolar cell has been confirmed in mice (Hartveit, 1996); while NRC2' labeling has been confirmed in flat midget bipolar cells in primates (Kalloniatis et al., 2004). Despite expressing both NR1 and NR2 subunits, the subunits required to make a functional NMDR channel, there is no evidence of NMDAR-mediated currents from retinal slice preparations (Hughes, 1997; Karschin and Wässle, 1990); however, isolated rat bipolar cells do reflect NMDA-mediated responses (E. Hartveit, 1996). Therefore, while there are NMDAR subunits are expressed throughout the retina, it is uncertain where these individual subunits form the functional NMDAR complex.

Serine racemase and D-serine

The expression of serine racemase and D-serine in the retina was studied, but results were inconsistent. A multi-species, immunofluorescence study showed positive labeling of D-serine in Müller glial cells, with high immunoreactivity in the inner nuclear and inner plexiform layers; this was confirmed in tiger salamander, mudpuppy, rat, and mouse retinas (Stevens et al., 2003). Serine racemase had a similar distribution pattern to D-serine, with positive expression in Müller cell proximal stalks and processes (Stevens et al., 2003). A second study demonstrated expression of serine racemase and D-serine in neurons and Müller cells in the adult mouse retina (Dun et al., 2008). To identify which cell type reflected positive immunoreactivity in the ganglion cell layer, immunoreactivity from cultured retinal ganglion and Müller cells was analyzed. There was a positive expression of serine racemase in Müller and ganglion cells, while D-serine was positive in retinal ganglion cells (Müller cells were not examined) (Dun et al., 2008). Taken together, these results suggest that the expression pattern of D-serine and serine racemase is not confined to glial cells.

Developmental differences in expression and distribution

There is evidence reflecting developmental changes in NMDAR, D-serine, and serine racemase expression in the retina (Dun et al., 2008; Romero et al., 2014) This is important because it is well-established that there are genetic factors contributing to high-risk for schizophrenia, which suggest a neurodevelopmental component to the pathophysiology of the disease (Lewis and Lieberman, 2000; Rapoport et al., 2012). The fact that developmental changes in the NMDAR, serine racemase, and D-serine are present in the retina suggest that neurodevelopmental changes pertinent to the disease may be reflected in the electroretinogram.

NMDAR

In mice, NMDAR subunit expression increases throughout retinal development, and both serine racemase and D-serine decrease (Dun et al., 2008; Romero et al., 2014; Watanabe et al., 1994). A study of developmental changes in the NMDAR examined with *in situ* hybridization during embryonic and post-natal development showed that the NR1 and NR2B subunits, the subunits required to make a functional NMDAR channel, were both expressed at E15 in the internal neuroblastic layer, the layer that eventually becomes the retinal ganglion cell layer and inner nuclear layer, and increased thereafter in expression (Watanabe et al., 1994). A gradual increase of NMDAR expression was seen until P14, but distribution changes of the NMDAR in adulthood were not evaluated in this study. It is unclear whether there are differences in the NMDAR distribution pattern in the NMDAR-hypofunction model in comparison to control. This question is intriguing when considering the involvement of NMDAR in the developmental plasticity of the somatosensory (Schlaggar et al., 1993) and auditory cortex (Bear et al., 1990), and

how retinal networks may change/adapt in response to reduced functionality of the NMDAR.

Serine racemase and D-serine

In contrast to the NMDAR, serine racemase and D-serine declined with age (Dun et al., 2008). In young retinas (3 weeks old), serine racemase was abundantly expressed in the ganglion cell layer, inner nuclear layer, and inner segments of photoreceptors; however, this expression was drastically reduced in adult mice (18-week-old). Reduced serine racemase expression in the adult retinas was seen in the inner nuclear layer when compared to expression levels at 3 weeks of age. Like serine racemase, immunoreactivity of D-serine declined with age but was primarily detected in the outer layers rather than the inner layers (Dun et al., 2008). Positive immunostaining for D-serine in 3-week-old mice was observed in the outer plexiform layers and outer limiting membrane; by 18-weeks of age, a minimal reactivity of D-serine in all layers was observed. Analysis of D-serine at an even earlier age, 3-days-old, showed positive immunodetection in the inner portion of the inner nuclear layer, retinal ganglion cell layer, and outer plexiform layer (Dun et al., 2008). This study suggests that the distribution pattern changes location for D-serine, from an inner-retinal distribution pattern earlier in development, to an outer-retinal distribution pattern later in development. Capillary electrophoresis studies of D-serine levels in wild type and serine racemase knockout ($SR^{-/-}$) showed that the amount of serine racemase and D-serine in the retina declined in development. In wild-type retinas, D-serine levels gradually declined from birth until the first month of life (Romero et al., 2014). At postnatal day 2, D-serine levels in the wild type retinas were in the range of 1,014-1,208 nmol/g and dropped to 27-43 nmol/g range at one month. Similarly, in $SR^{-/-}$ retinas D-serine levels

declined with age, but they were statistically significantly smaller than those from age-matched WT retinas. At postnatal day 2, $SR^{-/-}$ D-serine level ranged from 542-768 nmol/g and dropped to 2-5 nmol/g in adulthood. Cumulatively, these studies suggest that in the retina the distribution of serine racemase and D-serine expression decreased in development, which fuels the question of why serine racemase and D-serine are so abundant early in development? It is unclear how changes in serine racemase and D-serine affect retinal networks but understanding this process may provide insights into fERG abnormalities in schizophrenia.

NMDAR, D-serine, and serine racemase function in the retina

In the retina, it is well established that NMDAR currents contribute to light-evoked activity from retinal ganglion cells (Coleman and Miller, 1988). Glycine, one of the co-agonists for the NMDAR, is involved in inhibitory neurotransmission in the retina and continuously available (Coull and Cutler, 1978). Due to glycine's role in inhibitory neurotransmission, it was thus speculated that D-serine might be the endogenous co-agonist instead. Evidence supporting the role of D-serine as an endogenous co-agonist for the NMDAR came from studies that showed NMDAR currents in retinal ganglion cells were potentiated with addition of exogenous D-serine (Stevens et al., 2003). Abolition of NMDAR current through application of exogenous DAAO, D-serine degrading enzyme (Gustafson et al., 2007), with a several fold increase of NMDAR in response to D-serine and not glycine at the same concentration (Stevens et al., 2003). Although D-serine and glycine are present in the retina, the co-agonist site of the NMDAR in retinal ganglion cells was not saturated (Daniels and Baldridge, 2010; Gustafson et al., 2007; Kalbaugh et al., 2009; Stevens et al., 2003). This led investigators to hypothesize that dynamic

release of D-serine may serve to recruit the NMDAR to meet light intensity demands (Sullivan et al., 2011). While much is known about the NMDAR contribution to the physiological response of retinal ganglion cells, much remains to be resolved regarding NMDAR function in vision (Miller and Slaughter, 1986; Slaughter and Miller, 1983; Lukasiewicz and McReynolds, 1985). For instance, in the brain, it is well established that increasing the frequency of activation of NMDAR in mature synapses results in long lasting effects that underlie the mechanisms for learning and memory and synaptic plasticity (Malenka and Bear, 2004). The brain takes advantage of the infrequent activation of the NMDAR to produce these long-lasting changes; however, this does not appear to be the case in the retina. In the brain, NMDAR activation results from substantial pre-synaptic glutamate release. In the retina, NMDAR is expressed by many neuronal types, and it is active in the absence (Gottesman and Miller, 2003) and presence of light (Diamond and Copenhagen, 1993). Further work needs to be performed to establish more clearly how the NMDAR contributes to the circuits and networks involved in vision and how these circuits differ in individuals with mental disorders.

Flash-electroretinogram

Electrical signaling from biological systems

Electricity from biological systems results from ion concentration changes across membrane. The presence of ions in the intra- and extracellular space give the solution electrical conductivity (Plonsey and Barr, 2007). In biological systems, sodium and potassium ions, and calcium and chloride ions to a smaller degree, are key players in deriving charged currents in the central nervous system. The differences in their ionic

concentrations inside and outside of the membrane are important for excitability of cells. In neurons, potassium concentration is higher intracellularly than extracellularly, while sodium concentration is higher extracellularly than intracellularly. Hence, when a neuron is activated, sodium enters the cell, which generates a current sink (-), a flow of positive ions away from the extracellular space, and at another retinal depth, potassium exits the cell where it generates a current source (+), a flow of positive ions into the extracellular space. These opposite charge currents, when separated by a distance, is called a dipole. In the mammalian retina, the vertical transmission of glutamate results in a sequential activation of cells whose dipoles add, and this is reflected in the flash-electroretinogram. Hence, the flash-electroretinogram (fERG) is a measurement of the electrical signaling in the retina in response to a flash of light. It is thus the sum of local conductance changes from activated retinal cells, which upon activation give rise to inward and outward currents that generate an extracellular potential change large enough to be measured at a distance. The flash-electroretinogram is a complex visual signal representing light-evoke, electrical potential changes from the retina; enabling the understanding of retinal events through measurements from the surface of the eye, the cornea.

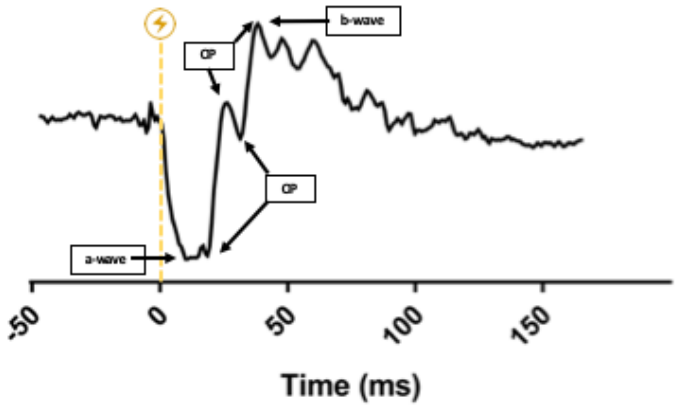

Fig 1.1 Schematic of a mouse flash-electroretinogram. *Yellow lightning bolt represents flash on-set.*

The flash-electroretinogram and components

The fERG signal is composed of distinct waves that originate from different retinal structures that are time-locked to stimulus onset (Figure 1). The a-wave is the earliest component; it is a corneal-negative deflection representing the photocurrent generated in the outer segments of photoreceptors upon light activity. When light enters the retina, it terminates the dark current, a current generated by rods under complete darkness (Figure 2A), and results in an inversion in photoreceptors' dipole. Light stops sodium from crossing the membrane of the photoreceptors, resulting in a flow of positive ions into the extracellular space, source (+); while potassium stops flowing out of the cell, resulting in a decrease in positive charge in the extracellular space, sink (-) (Figure 2A). Since the sink (-) is closest to the cornea, photoreceptor activity is reflected in a negative deflection. Following the a-wave, there is a corneal-positive potential known as the b-wave that reflects membrane potential changes in on-bipolar cells. When light hits,

sodium enters the cell creating a sink (-) and potassium leaves the cell creating a source (+) (Figure 2B). Superimposed in the rising edge of the b-wave are small amplitude, rhythmic wave that are collectively known as the oscillatory potentials. Their origin is uncertain, but it has been narrowed down to cells in the inner retina: bipolar terminals, amacrine cells, and retinal ganglion cells. Following the b-wave, the slowest latency potential reflects the difference the potentials from Müller cells and retinal pigment epithelium called the c-wave (not reflected in Figure 1.1). The c-wave could be a corneal positive, negative, or neutral depending on which of the subcomponents is dominating. A corneal-positive c-wave is dominated by activity from retinal pigment epithelium; while a cornea-negative c-wave is dominated from Müller cells, no potential reflects equal contributions from both subcomponents (Frishman and Wang, 2010)

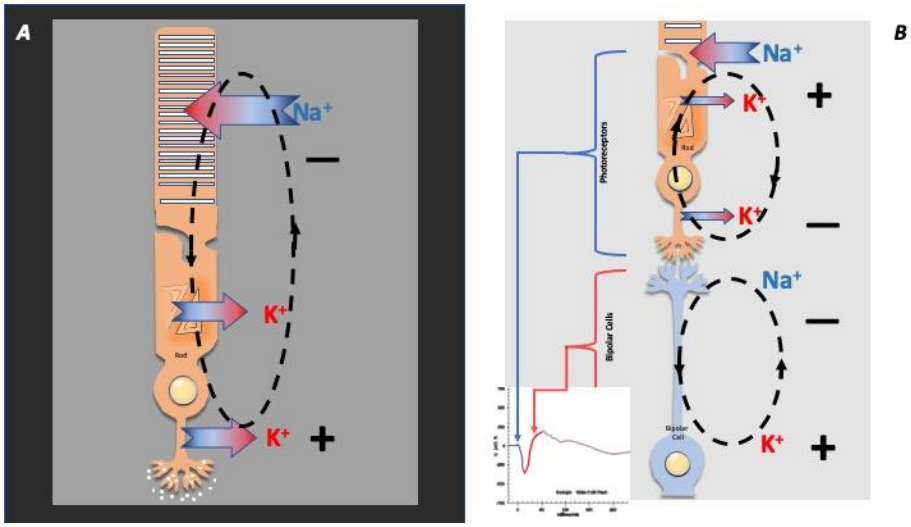

Figure 1.2 ***Schematic of retinal currents reflected in a fERG.*** (A) Depicts depolarization of rods in the dark, otherwise known as the dark-current. Sodium (Na+) flows into the cell, creating a sink, flow of position ions away from extracellular space (-). Potassium flows out, creating a source (+), flow of positive ions into the extracellular space. White dots reflect glutamate release (B) Depicts retinal currents in response to light and its contribution to the fERG (insert). Red/Blue arrows indicate movement of ions from low (blue) to high concentration (red).

Changes in the fERG due to light adaptation

The cellular origins of the fERG differ depending on the light adapting conditions. As mentioned previously, the a-wave is a negative response associated with photoreceptors, but it can be driven by either rods or cones, depending on the intensity of the background light. A dark-adapted a-wave is a response driven by rods because it is the response to a light stimulus from total darkness. A light-adapted a-wave is a response driven by cones, because the bright background is bright enough to saturate rod photoreceptors (McCulloch et al., 2015). In both the light- and dark- adapted a-wave, the positive component that follows is the b-wave, which predominantly originates form ON bipolar cells.

Flash- electroretinogram in people with schizophrenia

In the past 28 years, studies showed electroretinographic differences between people with schizophrenia and healthy controls (Balogh et al., 2008; Demmin et al., 2018; Gerbaldo et al., 1992; Hebert et al., 2010; Hebert et al., 2015; Marmor et al., 1988; Raese et al., 1982; Schechter et al., 1987; Warner et al., 1999). These studies demonstrated abnormalities in people with schizophrenia that are differentially manifested in the retina and, therefore, could be assessed by an objective, non-invasive method, the fERG. However, despite the growing evidence that the fERG of people with schizophrenia is different from healthy controls, there are disagreements on which fERG components are reliably different. Nonetheless, these studies hold promise for using components of the fERG as a biomarker for schizophrenia and are summarized below (Table 1.1).

Table 1.1	a-wave		b-wave		OPs		a-wave		b-wave		OPs		a-wave		b-wave		OPs	
	Amp.	Time	Amp.	Time	Amp.	Time	Amp.	Time	Amp.	Time	Amp	Time	Amp.	Time	Amp.	Time	Amp.	Time
Raese (1982)	X	X	X	X	SZ=↓	SZ=↑	X	X	X	X	X	X	X	X	X	X	X	X
Schechter (1987)	N.S.	X	N.S.	X	N.S.	X	X	X	X	X	X	X	N.S.	X	N.S.	X	N.S.	X
Marmor (1988)	N.S.	X	N.S.	X	N.S.	X	X	X	X	X	X	X	N.S.	X	N.S.	X	N.S.	X
Gerbaldo (1992)	X	X	N.S.	N.S.	X	X	X	X	X	X	X	X	X	X	phSZ =↓	X	X	X
Warner (1999)	SZ =↓	N.S.	SZ = ↓	X	X	X	X	X	X	X	X	X	SZ = ↓	N.S.	N.S.	X	X	X
Balogh (2008)	X	X	X	X	X	X	X	X	X	X	X	X	SZ = ↓	N.S.	N.S.	X	X	X
Hébert (2010)	oSZ =↓	X	oSZ =↓	X	X	X	X	X	X	X	X	X	N.S.	N.S.	N.S.	N.S.	X	X
Hébert (2015)	N.S.	X	SZ =↓	X	X	X	X	X	SZ = ↓	X	X	X	SZ = ↓	X	SZ =↓	SZ =↓	X	X
Demmin (2008)	N.S.	N.S.	N.S.	N.S.	X	X	bSZ =↓	N.S.	b,dSZ =↓	X	X	X	N.S.	N.S.	SZ =↓	SZ =↑	X	X

Table 1.1 Summary of fERG abnormalities in people with schizophrenia. *Meaning of symbols are as follows: [X] not measured, [N.S.] analyzed but not significant, [SZ] people with schizophrenia, [phSZ] people with schizophrenia with photophilic behavior, [oSZ] offspring of people with schizophrenia, [bSZ] people with schizophrenia exhibited a statistically significant difference only at the brightest flash strength, and [dSZ] people with schizophrenia exhibited a statistically significant difference only at the dimmest flash strength.*

Differences in a-wave

Both light- and dark- adapted a-wave have been measured in people with schizophrenia (Balogh et al., 2008; Demmin et al., 2018; Hebert et al., 2015; Marmor et al., 1988; Schechter et al., 1987; Warner et al., 1999). A reduced a-wave amplitude in both conditions was first observed in people with schizophrenia that exhibited low light sensitivity under dark and light adapted conditions (Warner et al., 1999). This reduced a-wave in both types of retinal adaptation was only observed in people with schizophrenia exhibiting photophilic behavior. Studies investigating people with schizophrenia that did not have photophilic behavior, showed a reduced light-adapted a-wave only. Although, follow-up studies demonstrated a reduction in the dark-adapted a-wave amplitude of high-risk offspring of people with schizophrenia (Hebert et al., 2010), but reduced dark-

adapted a-waves of people with schizophrenia have not been observed by others (Warner et al., 1999). Unlike the dark-adapted a-wave, the light-adapted a-wave showed statistically significant differences between people with schizophrenia and controls in several studies. (Balogh et al., 2008; Hebert et al., 2015; Warner et al., 1999). These results suggested the a-wave abnormalities are present in people with schizophrenia regardless of whether they have photophilic behavior, and that a-wave abnormalities are more commonly observed in light-adapted retinas.

Differences in b-wave

Reduction in the b-wave amplitude in people with schizophrenia has been reported in both dark- and light- adapted retinas with inconsistent results. In people with schizophrenia with photophilic behavior, a significant reduction in the light-adapted b-wave amplitude was reported (Warner et al., 1999). However, that significance disappeared when people with schizophrenia with and without photophilic behavior were pooled together. Two other groups evaluating fERG in people with schizophrenia did not replicate these findings in either light- or dark- adapted fERGs (Balogh et al., 2008; Warner et al., 1999). Other investigators measured fERGs in both dark- and light-adapted conditions but had inconsistent results. Two studies observed a reduction in the dark-adapted b-wave but not light-adapted; the other two studies observed a reduction in the light-adapted b-wave but not in the dark-adapted b-wave. Out of the seven research groups that measured the fERG in light- and dark-adapted conditions, only two observed a reduction in both conditions. In conclusion, we cannot state for certain whether changes in the b-wave amplitude were dependent on retinal adaptation, which would reflect differences in retinal neuron function; nonetheless, a reduced b-wave amplitude, regardless of light-adapting condition, is observed in people with schizophrenia.

Differences in OPs

The first study demonstrating differences between fERG of people with schizophrenia and controls examined the OPs in the dark-adapted retina, but did not evaluate the a- and b-wave. The group hypothesized that the OPs had higher potential in reflecting abnormalities because pharmacological fERG studies demonstrated that it was necessary to have intact dopamine and gamma-aminobutyric acid (GABA) transmission for the appearance of OPs (Raese et al., 1982), they hypothesized that desynchronization of dopamine feedback loops thought to occur in schizophrenia could be reflected in the OPs. Their results showed a statistically significant reduction in OP_{1-3} in people with schizophrenia in comparison to normal subjects as well as a statistically significant delay. Two other research groups evaluated the OPs but failed to replicate the original results. Schechter et al. (1979) measured OPs in schizophrenia in comparison to controls but extended their analyses to include the a- and b-waves as well. Their study differed in that it included three types of stimulus conditions: dark-adapted-dim light, dark adapted-bright light, light adapted-bright light. Unlike Raese et al. (1982), they did not observe any statistical differences in any of the dependent variables between OPs in people with schizophrenia and controls. Marmor et al. (1988) replicated the experimental design of measuring the fERG in three type of stimulus conditions, but only analyzed OP differences between people with schizophrenia and controls. They, too, reported no statistical significance in the OPs of people with schizophrenia and control subjects. Unfortunately, it is hard to interpret their lack of significance ad details of their statistical analyses were not adequate. Raese et al. (1992) conducted an unpaired t-test to compare the mean of the OP amplitudes between people with

schizophrenia and controls, providing *p*-values for each dependent variable measured. However, Schechter et al. (1987) measured significance by running a mixed ANOVA using group, schizophrenia vs. control, and light intensity as factors. It is unclear whether there was a lack of significance in the interaction effect between schizophrenia compared to controls, or in the main effects of each variable. Furthermore, no *p*-values or F-statistics were provided for the analyses completed. Marmor et al. (1988) had no mention of the statistical analyses in their methods for the human portion of their work.

Summary

Several major conclusions can be drawn from the studies performed thus far examining fERGs in people with schizophrenia and controls. Critical variables differ between these studies - light condition, flash intensity, medication - and the specific fERG components analyzed varied between studies. It is well established that these factors affect the fERG, which limits between study comparisons and global interpretation about the potential of the fERG as a biomarker for schizophrenia. No laboratory has specifically examined the potential role of NMDAR hypofunction on the ERG, despite recent studies suggesting that a large percentage of individuals with schizophrenia have known mutations in genes or signaling abnormalities that are related to some component of the NMDAR (Föcking et al., 2015; Kirov et al., 2012; Purcell et al., 2014). There are differences in the age of onset and severity of schizophrenic between men and women, with males showing an earlier onset, decreased treatment response, and greater severity of symptoms (Loranger, 1984; Peterson, 1968). Animal studies support this view, as they showed that NMDAR activity differs in the brains of male and female rats (Cyr et al., 2001; McEwen, 2002; McRoberts et al., 2007; Woolley, 1998). Thus, for my studies, sex is considered as a variable in the analyses.

My aims and contributions

Questions

The main question addressed in my thesis work was whether visual signals from the eye could demonstrate NMDAR signal deficiency that are hypothesized to account for schizophrenia, and as such, become a biomarker for the disease. My focus was on the flash-electroretinogram (fERG), a visual signal that had been demonstrated to be reduced in people with schizophrenia by the time I started my thesis, to understand if any of the fERG components had any NMDAR involvement that may be reflected in the fERG. Our current understanding about the function of NMDARs in the retina is based predominantly on its effects on the retinal ganglion cell layer, and not to its role in the outer retina. While functional NMDAR have been found in horizontal cells (O'Dell and Christensen, 1989), it was not clear whether NMDAR abnormalities would impact retinal currents earlier in the pathway, such as the a- and b-wave. This is the basis of the main focus of my thesis studies: *Were there any NMDAR-driven retinal network abnormalities earlier in the signal-transmission pathway that would explain the reduction in response observed in people with schizophrenia?* It was unclear if the reduction in the a- and b-wave amplitude observed in people with schizophrenia reflected any NMDAR abnormalities. Furthermore, I sought to understand whether there were any sex differences that could be reflected in the fERG. Earlier work on the fERG of healthy controls demonstrated longitudinal sex differences in the b-wave amplitude in humans (Bresnick and Palta, 1987; Tahara et al., 1993). With age, female and male b-wave amplitudes began to diverge, with females being higher than males. Simultaneously, literature on sex differences in people with schizophrenia, such as symptom onset being

later in females, stimulated my interest in learning whether any sex differences related to disease state could be detected by the fERG. Therefore, the aims of my experiments in this thesis were as follows:

- **Aim 1:** Evaluate the fERG in a genetically altered mouse strain that modeled NMDAR hypofunction caused by D-serine deprivation ($SR^{-/-}$), to identify whether there is a significant NMDAR component contribution to the fERG signal, specifically in the outer retina.
- **Aim 2:** Investigate whether exogenous D-serine would restore abnormalities in the fERG of the NMDAR hypofunction mouse model.
- **Aim 3**: Determine whether the sex of the animals would affect any of the fERG components in mice and humans
- **Aim 4:** Evaluate if there are any functional retinal ganglion cell abnormalities in people with schizophrenia by analyzing a type of fERG response that has a strong RGC contribution the pattern ERG and the Photopic Negative Response-ERG (PhNR-ERG).

Specifically, I performed a series of experiments focused on whether the fERG was altered in a mouse model of NMDAR hypofunction (Chapter 2). These mice had a mutation that made the enzyme serine racemase non-functional, and the decreased levels of D-serine were validated in the laboratory (Sullivan et al., 2011). Using a constitutive knockout mouse for serine racemase ($SR^{-/-}$) and littermate controls, I performed fERG under mesopic light conditions. The fERG waveforms were analyzed for the following parameters: a-wave amplitude and implicit time; b-wave amplitude and

implicit time; b/a ratio; Fourier transform. I also examined the fERGs from these two cohorts based on sex.

In a second series of experiments, I performed *in vivo* fERGs on the $SR^{-/-}$ and WT control mice followed by a topical application of D-serine (Chapter 3). The goal of this second set of experiments was to determine if D-serine treatment would rescue any alteration caused by the constitutive absence of D-serine in the retina.

The ultimate question is whether the fERG would be able to distinguish between people with schizophrenia and age-matched controls (Chapter 4). A large data set of subjects was collected using what is called the photopic negative response fERG (PhNR-fERG). The photopic negative response (PhNR) is produced in a light-adapted retina evoked by a red flash on a blue background, and it is a large negative wave that occurs after the b-wave in response to a brief light stimulus. It is considered to represent function of the retinal ganglion cells (Frishman et al., 2018). In these same subjects, pattern electroretinogram (PERG) was also performed. PERG is obtained in response to patterned visual stimuli presented at a contrast modulation and at a constant mean luminance (Luo and Frishman, 2011; Porciatti, 2015). The stimulus is typically contrast-reversing gratings or checkerboards. It is particularly indicative of retinal ganglion cell function, neurons known to have functional NMDAR (Cohen and Miller, 1994; Coleman and Miller, 1988; Gustafson et al., 2007). For the PhNR-fERG the following were analyzed: a-wave amplitude and implicit time, b-wave amplitude and implicit time, and the PhNR amplitude and implicit time. For the PERG the following was analyzed: N35, P50, and N95 amplitudes and implicit times, which are based on the time after retinal stimulation when these peaks normally occur.

Findings

My work shows that deprivation of D-serine affects the outer retina and is reflected in the fERG components, specifically a-wave implicit time, b-wave amplitude, and b/a ratio. These findings demonstrate that either the NMDAR participates in outer retinal networks or that D-serine has another role in the retina other than being the endogenous co-agonist to the NMDAR. Furthermore, my work shows that deprivation or elevation of exogenous D-serine affects male and female mice differently. This shed light on a possible interaction between hormones and D-serine that has not previously been identified. Specifically, D-serine has a profound effect on male mice (Chapters 2 and 3) and to a certain extent in human males (Chapter 3). This work elevates the fERG as a potential diagnostic tool for schizophrenia prior to symptom onset and identify specific approaches that are critical for success in these analyses.

Chapter 2

Electroretinographic Abnormalities and Sex Differences in an NMDAR Hypofunction Mouse Model of Schizophrenia: A and B Wave Analysis

Nathalia Torres Jimenez, Justin W. Lines, Paulo Kofuji, Henry Wei, Amy Rankila, Joseph T. Coyle, Linda K. McLoon, Robert F. Miller

Synopsis

Purpose: The flash-electroretinogram (fERG) as a tool to identify N-methyl-D-aspartate receptor (NMDAR) hypofunction in subjects with schizophrenia shows great potential. We report the first fERG study in a genetic mouse model of schizophrenia characterized by NMDAR hypofunction from genetic silencing of serine racemase expression (*SR*$^{-/-}$), an established risk gene for schizophrenia. We analyzed parameters of the fERG to determine the resemblance to human fERG from people with schizophrenia to determine the most significant variables to allow for early identification of individuals at high risk for schizophrenia, prior to symptom onset.

Methods: The fERG was analyzed in male and female mice in both *SR*$^{-/-}$ and wild type (WT) mice. Amplitude and implicit time of the a- and b-wave components, b/a wave ratio, and Fourier transform analysis of these components were analyzed.

Results: The a- and b-wave implicit times were significantly delayed, and b-wave amplitudes were significantly decreased in the male *SR*$^{-/-}$ mice compared to WT, but not female *SR*$^{-/-}$ mice. Fourier transform analysis and b/a wave ratio showed significant differences at multiple light intensities between all *SR*$^{-/-}$ and WT mice. The fERGs in the

SR$^{-/-}$ mouse model of schizophrenia show many of the same differences in fERGs as seen in people with schizophrenia.

Conclusions: The fERG prognostic capability may be improved by examination of a larger array of light intensities, considering sex as a variable, and performing Fourier transform analyses of all waveforms. This should improve ability to differentiate between healthy controls and subjects with schizophrenia, characterized by NMDAR hypofunction.

Introduction

As part of the central nervous system, the retina has been considered to be the "window to the brain" as the retina and brain share many neurophysiologic properties (London et al., 2013). Thus, prior studies have demonstrated electroretinographic differences between subjects with schizophrenia and healthy controls (Demmin et al., 2018; Gerbaldo et al., 1992). These findings point towards visual deficits in people with schizophrenia not limited to higher level visual-cognitive processing but manifested at earlier stages of the visual pathway, the retina. The significance of these findings focuses on the possibility of using retinal-evoked potentials as biomarkers for pre-symptomatic diagnosis of schizophrenia and for characterizing neurophysiologic abnormalities associated with schizophrenia or subgroups of schizophrenic subjects (Lavoie et al., 2014; Nguyen et al., 2017; Weickert et al., 2013). While clinical interviews for diagnosis of schizophrenia are effective at identifying schizophrenia once present, they have limited success in identifying pre-symptomatic individuals prior to the onset of psychosis (Savill et al., 2018). Thus, an objective measurement prior to symptom onset would be invaluable. Collectively, these studies suggest that the retinal-evoked potential, the flash-electroretinogram (fERG), may serve as a physiological metric for predicting schizophrenia in subjects at risk.

The fERG is a summed evoked potential from the retina in response to diffuse light. The advantage of the fERG as a diagnostic tool is that the technique is relatively non-invasive, easy to administer, and its major waves have a known cellular origin (Granit, 1933). The fERG response is well studied, and has been recorded in many species, including humans and mice. (Frishman and Wang, 2011) Despite clinical observations noting fERG abnormalities in people with schizophrenia, to date mouse

models of schizophrenia have not clearly defined what aspects of the fERG response might be most germane to use as a biomarker for schizophrenia or, specifically, a subtype associated with N-Methyl-D-aspartic acid receptor (NMDAR) hypofunction. Identifying which of the fERG waves to use as a biometric measurement for a potential diagnosis of schizophrenia can be achieved more readily in mice because of greater control of parameters such as age, sex, treatment, and genetic status, and there are now several excellent mouse models of schizophrenia to use for these analyses. Due to the importance of ensuring concordance between fERG abnormalities seen in people with schizophrenia and the mouse models with specific allelic variants similar to those seen in these individuals, we examined the fERG from a schizophrenic mouse model, a serine racemase knockout ($SR^{-/-}$), that has been extensively evaluated for mimicking and studying chronic brain pathology in schizophrenia (Basu et al., 2010). The $SR^{-/-}$ schizophrenia mouse model has a knockout of the gene for the enzyme serine racemase (SR), and has a reduced functionality of the NMDAR (Balu and Coyle, 2015) resulting in NMDAR hypofunction. SR is one of several risk genes for schizophrenia that affect NMDAR function and its downstream signaling (Balu & Coyle, 2015). Proteomic and genomic analyses of synapses in human brain samples from controls or people with schizophrenia found altered expression of multiple proteins with known specific roles in NMDAR function (Föcking et al., 2015; Tomasetti et al., 2017). While the proportion of people with schizophrenia in this subtype is not known, the NMDAR-related molecules are well represented in the identified risk genes (Föcking et al., 2015; Tomasetti et al., 2017).

The NMDAR is an ionotropic glutamate receptor that is critical for cellular communication and found in both brain and retina. In the brain, the NMDAR receptor is

critical for learning and memory. In the retina, NMDAR regulates light-evoked activity (Dixon and Copenhagen, 1992; Haverkamp and Wässle, 2000; Mittman et al., 1990). The hypothesized NMDAR relevance to schizophrenia originated after clinical observations of the recreational use of phencyclidine (PCP), which caused increased emergency room visits from patients exhibiting symptoms resembling schizophrenia (Luby et al., 1962). This new hypothesis for NMDAR hypofunction as a potential etiology of schizophrenia is supported by pharmacological (Goff et al., 1999; Goff et al., 1995), genetic (Chumakov et al., 2002; Yamada et al., 2005), clinical (Leiderman et al., 1996; Yurgelun-Todd et al., 2005) and postmortem studies (Hashimoto et al., 2005; Tsai et al., 1995; Weickert et al., 2013), and the hypothesis that reduced NMDAR activity can account, in part, for the etiology of schizophrenia (Javitt and Zukin, 1991b). In our study, we have utilized an NMDAR-hypofunction mouse model of schizophrenia ($SR^{-/-}$) to identify which of the fERG waves would best serve as a marker for NMDAR hypofunction. This mouse model for NMDAR-hypofunction has a null mutation for the SR gene (Labrie et al., 2009). SR synthesizes D-serine, the primary co-agonist of NMDARs in the forebrain (Stevens et al. 2010) and retina (Blokhuis et al., 2016). As a component of the central nervous system, the retina can acquire cellular abnormalities similar to those that are present in the brain (Brown and Wiesel, 1961; Chu et al., 2012; Lavoie et al., 2014; Schönfeldt-Lecuona et al., 2015; Silverstein and Rosen, 2015). Given that fERG allows the evaluation of the functional integrity of the retina, it has the potential to become a useful non-invasive tool to assess pathological abnormalities in the brain (Penn and Hagins, 1969).

The fERG response is characterized by two low-frequency waves, the a- and b-waves, (Figure 2.1) and high-frequency wave forms called oscillatory potentials (not

shown) (Robson and Frishman, 1995; Stockton and Slaughter, 1989). Both the a- and b-wave have known cellular origins (Wachtmeister, 1998; Zeidler, 1959). The first wave in the fERG is the a-wave (Faraone et al., 1994; Peterson, 1968; Vainio-Mattila, 1951), which is a corneal-negative potential that originates from photoreceptor activity (Häfner, 2003). The a-wave is followed by the b-wave, which is a corneal-positive potential originating from bipolar cells (McCulloch et al., 2015; Ochoa et al., 2012; Stockton and Slaughter, 1989). Riding on the ascending limb of the b-wave are the oscillatory potentials (OPs), which are hypothesized to originate from amacrine and retinal ganglion cells (RGC) (Wachtmeister, 1998). The clinical literature showed reduction in both the a- and b-waves in subjects with schizophrenia compared to controls; however, these studies did not fully address known gender and age differences associated with the fERG waveforms in human controls (Peterson, 1968; Vainio-Mattila, 1951; Zeidler, 1959). In healthy humans, longitudinal fERG studies demonstrated a linear decrease with age in the b-wave amplitude in men; females showed a linear decrease until ages 40-49 where there was a significant increase in the b-wave amplitude, speculated to be from hormonal changes (Bresnick and Palta, 1987; Tahara et al., 1993). Prior to age 40 in healthy females, b-wave amplitudes were significantly different from males. Not only were age and gender differences observed, but there is abundant literature on gender differences in people with schizophrenia as well. For example, symptomatic onset of schizophrenia occurs later in females and is often less severe than in males (Anis et al., 1983; Faraone et al., 1994; Woodward et al., 2007). These gender and age differences in people with schizophrenia could hypothetically be reflected in the fERGs, which highlights the importance of including age and gender in the fERG analyses.

Since age and gender differences can affect the fERG, we conducted *in vivo* fERG recordings and controlled for the mouse age and analyzed sex differences. However, we deviated from ISCEV standards (McCulloch et al., 2015) and adapted the mice under mesopic rather than dark or light conditions because it was shown to be a good indicator of pathology in diabetic retinopathy (Bresnick and Palta, 1987; Tahara et al., 1993) and schizophrenia (Demmin et al., 2018). While the differentiation between light- and mesopic-adaptation was not stated in the Demmin study (Demmin et al., 2018), the background luminance of the "Photopic 1 (P_1)" condition was insufficient to saturate rods and was technically mesopic. The mesopic adaptation reflected differences in the a- and b-wave amplitudes in people with schizophrenia in comparison to controls. We recorded from young mice to evaluate whether a reduction in the functionality of the NMDAR results in any of the fERG abnormalities observed in people with schizophrenia. Additionally, we performed a second analysis of the resulting fERG waveforms to determine if sex related differences were present.

Methods

Animals

Littermate male and female mice at 8-10 weeks of age from serine racemase null ($SR^{-/-}$) mutant mice developed as described by Basu et al. (Basu et al., 2010) and wild-type littermate controls (WT) were studied. A total of 34 mice were used, 8 and 9 per genotype for males and females respectively. All procedures followed the standards of the National Institutes of Health and the Association for Research in Vision and Ophthalmology Statement for the Use of Animals in Ophthalmic and Vision Research

and were approved by the Institutional Animal Care and Use Committee at the University of Minnesota.

Stimulation and Recording

The retina was held in a mesopic state of adaptation via a steady, white background luminance of (0.35 cd·s/m^2). Flashes (4 msec) were applied to a range of light intensities from 0.175 to 11.2 cd·s/m^2 to record flash-evoked electroretinograms (fERGs). The stimulus was a full field flash with a duration of 4 msec and a 10 sec interval between light intensities. The retinas were adapted to background light for 15 minutes prior to recording. Four traces were collected at each light intensity and averaged to attain representative traces at each light intensity for each animal. Data were collected using the D215 Espion E^2 Console (Diagnosys LLC, Lowell, MA) bandpass filter 0.3 Hz. Mice were anesthetized with 4% isoflurane gas, and anesthesia was maintained with 1.7% isoflurane. Isoflurane was selected as the anesthetic of choice because the combination of ketamine and xylazine blocks NMDAR receptor transmission, as ketamine is an NMDAR non-competitive antagonist (Anis et al., 1983). Since we measured the functionality in mice with NMDAR hypofunction, ketamine as an anesthetic would have confounded the results. Previous literature supported isoflurane as an effective anesthetic agent for maintaining normal mouse fERG (Woodward et al., 2007). After anesthesia, Tropicamide (1%) eye drops were used as a pupil dilator (Akorn, Inc., Lake Forest, IL), followed by corneal analgesic proparacaine hydrochloride eye drops (0.5%) (Akorn). A contact lens coiled wire electrode was placed on the cornea and embedded in methylcellulose (1.0%) eyedrops (Allergan, Dublin, Ireland) (Woodward et al., 2007).

Fourier Transform Analysis

A custom MATLAB program was used to determine the spectral content on fERGs via Fast Fourier Transform (FFT). Four traces collected at each light intensity were converted into power spectra using FFT and then averaged together for every animal. From these averaged power spectra, low frequency content was taken by averaging the spectra from 0-30 Hz.

Data Analysis

To remove OP contamination from the a- and b-wave measurements, each ERG response was filtered using a low-pass filter with a passband of 50 Hz and stopband of 65 Hz using a custom MATLAB program (Asi and Perlman, 1992; Benchoin et al., 2017). The four filtered traces corresponding to a given light intensity for each animal were averaged and smoothed in MATLAB. Using this filtered ERG, the a-wave amplitude was measured from the pre-flash baseline to the peak of the a-wave; while, the b-wave amplitude was measured from the peak of the a-wave (trough) to the largest peak of the b-wave. Implicit time of the a-wave and b-wave was measured from flash onset to response peak. Normality was tested using the Shapiro-Wilk's test ($p>.05$) for each group at each level of light intensity. Female $SR^{-/-}$ a-wave amplitude were not normally distributed at the dimmest light intensities, 0.175 and 0.35. Female WTs a-wave amplitude were not normally distributed at light intensity 0.35. The b-wave amplitude was not normally distributed at the dimmest light intensity (0.175) of female $SR^{-/-}$. Aside from the aforementioned data points, the remaining light intensities across groups were normally distributed. Two-factor between-subject Analysis of Variance (ANOVA) was conducted to evaluate a potential significant interaction between the independent

variables sex and genotype and simple main effects of sex (male vs female) and genotype (WT vs *SR*$^{-/-}$). Lastly, we carried a two-way mix ANOVA (light intensity * sex) and (light intensity*genotype) to account for changes in light intensity, the repeated measure for all mice, in all dependent variables. The dependent variables tested were: a-wave amplitude and implicit time; b-wave amplitude and implicit time; b/a ratio and low frequency Fourier transforms. All analyses were conducted for each light intensity. If there was a statistically significant two-way ANOVA, analysis for simple main effects of the given dependent variable was performed using a Bonferroni adjustment with statistical significance at $p<0.025$. To evaluate the effect of genotype or sex alone, main effects were analyzed through differences between the unweighted marginal means. All analyses were conducted in IBM SPSS Statistics 25.

Retinal Histology

To assess if there were significant changes in overall morphology of the retina from the *SR*$^{-/-}$ mice compared to WT, three eyes from 3 animals per genotype were removed after euthanasia, fixed in 4% phosphate-buffered paraformaldehyde (Affymetrix, Cleveland, OH), post-fixed in paraformaldehyde for several hours, followed by rinses in phosphate buffered saline (PBS), and incubation overnight in 10% sucrose in PBS and 20% sucrose in PBS. The eyes were embedded in paraffin and sectioned at 10µm on a sliding microtome. The sections were stained with hematoxylin and eosin by standard procedures. Sections through the optic nerve head and through a defined location in peripheral retina, based on the anterior appearance of the ciliary body and cornea in the sections (see Supplemental Figure 2.2), were used for measurements in order to be consistent where our measurements were taken. Using the Bioquant Imaging

System (Bioquant, Nashville, TN), the mean height of each of the layers of the retina was determined using 3 separate measurements per layer per area in the central retina and a mean of six measurements of the retinal layers in peripheral retina in two locations. These data were analyzed using unpaired t-tests for each layer and each region, with significance at <0.05.

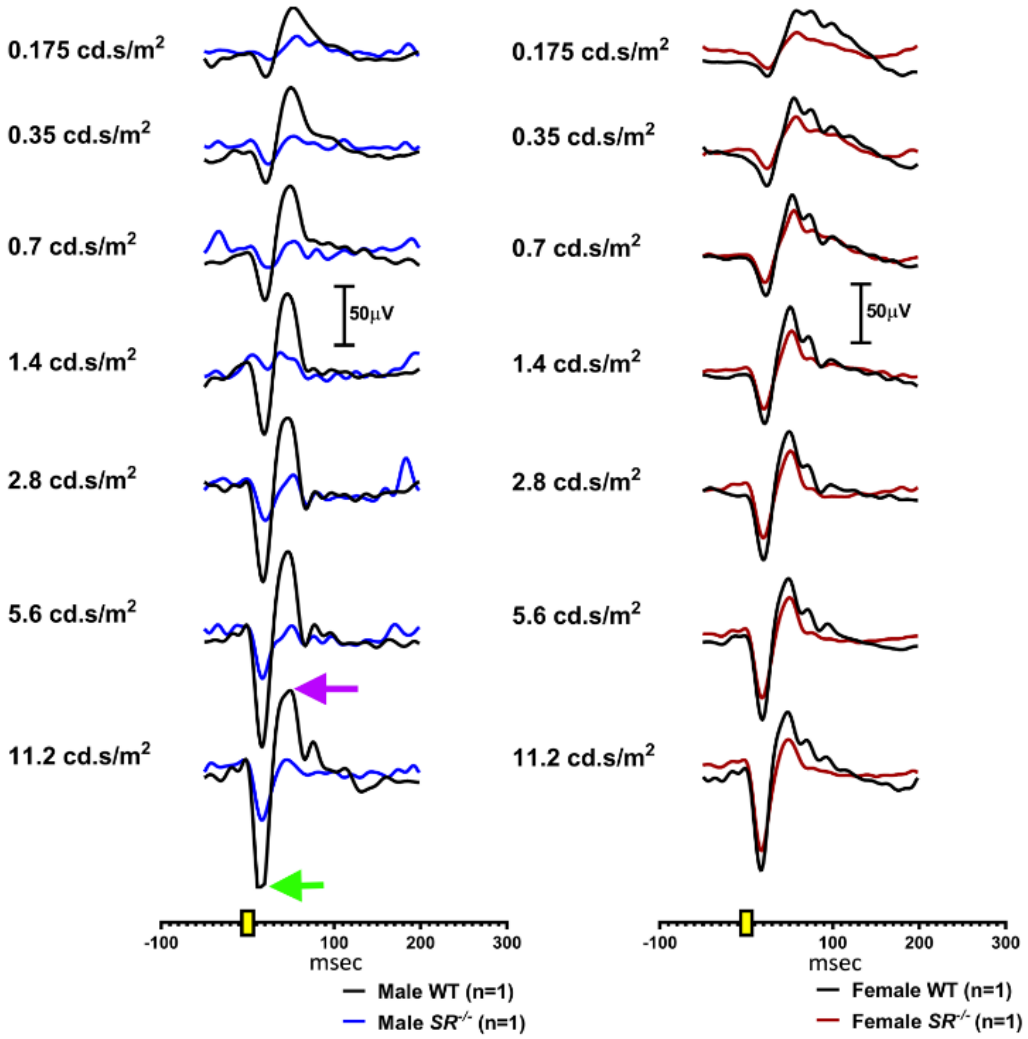

Figure 2.1 Representative fERG recordings from WT and SR$^{-/-}$. *Representative flash-ERG (fERG) recordings from WT (black), SR$^{-/-}$ male mice (blue), and SR$^{-/-}$ female mice (red) at 7 light intensities at 0-69Hz frequency. Green arrow indicates the a-wave, and purple arrow indicates the b-wave*

Results

Effect of *NMDAR* hypofunction on the mesopic a-wave amplitude

The differences in amplitude and implicit times between the fERGs in the male and female WT and *SR*$^{-/-}$ are displayed as waveforms at each light intensity (Figure 2.1). Analysis of the main effects of the mesopic a-wave amplitude showed no statistically significant difference between WT and *SR*$^{-/-}$ mice (Supplemental Figure 2.1A, Supplemental Table 2.1). Analysis of simple main effects of sex for male mice showed the a-wave amplitudes were significantly different only at the highest intensity (Figure Supplemental 2.1B, Supplemental Table 2.1), while female mice showed a significant difference at the lowest light intensity (Supplemental Figure 2.1C). Significance at the brightest intensity was similar to the ERG in a study of people with schizophrenia (Demmin et al., 2018).

Effect of NMDAR hypofunction on the mesopic a-wave implicit time

The a-wave implicit time was significantly elevated in *SR*$^{-/-}$ mice compared to WT mice at all light intensities, with the *SR*$^{-/-}$ mice significantly delayed compared to the normal WT a-wave as reflected by the main effects analysis of genotype (Figure 2.2A; Table 2.1). The simple main effect for sex revealed that *SR*$^{-/-}$ male mice had a significantly increased a-wave implicit time in comparison to male WT at all light intensities except one (Figure 2.2B, Table 2.2), while there were no differences in the a-wave implicit time between female WT and *SR*$^{-/-}$ mice (Figure 2.2C).

Table 2.1	a-wave implicit time (ms)		
Flash intensity ($cd \cdot s/m^2$)	*WT vs $SR^{-/-}$*		*Main Effects Genotype*
0.175	22 ± 6.3	26 ± 8.2	F(1,30)=4.7, ***p* =0.039**
0.35	23 ± 2.6	28 ± 6.3	F(1,30)=11.0, ***p*= 0.002**
0.7	22 ± 1.6	26 ± 4.3	F(1,30)=14.3, ***p*= 0.001**
1.4	20 ± 1.5	24 ± 4.1	F(1,30)=17.4, ***p*< 0.0005**
2.8	19 ± 1.4	22 ± 3.6	F(1,30)=14.7, ***p*= 0.001**
5.6	18 ± 1.2	20 ± 3.1	F(1,30)=9.1, ***p*= 0.005**
11.2	17 ± 1.2	19 ± 3.0	F(1,30)=7.4, ***p*= 0.011**

Table 2.1 Comparison of a-wave implicit time in WT and $SR^{-/-}$ mice: *Data represents a-wave implicit time given genotype, with data from males and females pooled. Data expressed as mean± S.D. The p-values are the results of main effects analysis.*

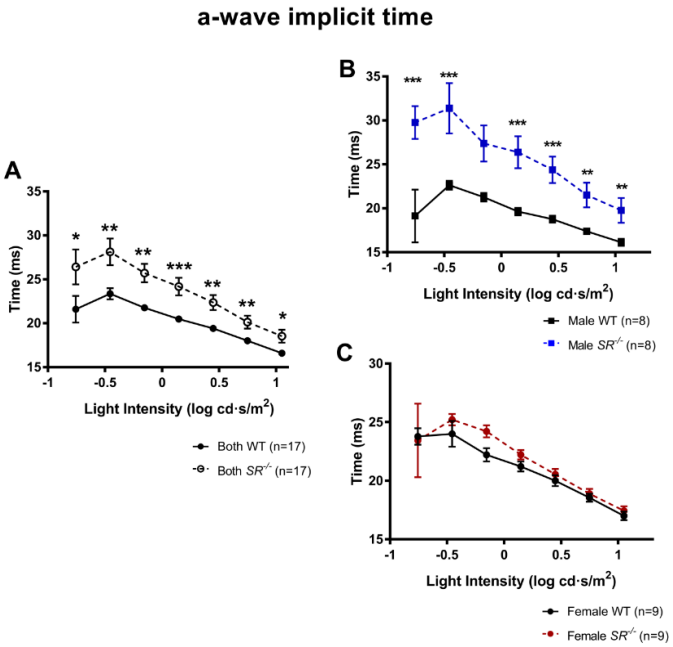

Figure 2.2 A-wave implicit time analysis: *(A) Comparison of a-wave implicit time based on genotype and evaluation of the main effects (WT=solid line & close circles, $SR^{-/-}$=dashed line & open circles). (B, C) Comparison of genotype for a specific gender evaluating the simple main effects of sex: males (B) and females (C), WT (black) and $SR^{-/-}$ mice (♂ blue line, ♀ red line) at all light intensities. Data expressed: mean (line), SEM (error bars), and significance ([*] p = 0.05-0.01**;** [**] p = 0.001-0.005**;** [***] p<0.0005).*

Table 2.2	a-wave implicit time (ms)						
	Female		Male				
Flash intensity ($cd \cdot s/m^2$)	WT	$SR^{-/-}$	WT	$SR^{-/-}$	Interaction Sex*Genotype	SME: Sex	SME: Genotype
0.175	24	23	19	30	F(1,30) = 5.3, **p = 0.029**	Male: **p <0.0005**	N.S.
0.35	24	25	23	31	F(1,30) = 6.2, **p = 0.018**	Male: **p <0.0005**	$SR^{-/-}$: **p =0.007**
0.7	22	24	21	27	F(1,30) = 3.7, p = 0.064	N.A.	N.A.
1.4	21	22	20	26	F(1,30) = 9.6, **p = 0.004**	Male: **p <0.0005**	$SR^{-/-}$: **p =0.004**
2.8	20	21	19	24	F(1,30) = 9.9, **p = 0.004**	Male: **p <0.0005**	$SR^{-/-}$: **p =0.002**
5.6	19	19	17	22	F(1,30) = 6.6, **p = 0.016**	Male: **p <0.001**	$SR^{-/-}$: **p =0.018**
11.2	17	17	16	20	F(1,30) = 4.5, **p = 0.042**	Male: **p <0.002**	$SR^{-/-}$: **p =0.038**

Table 2.2 Comparison of a-wave implicit time in WT and $SR^{-/-}$ mice depending on sex: *The first two columns represent the mean a-wave implicit time at each condition. The interaction column includes the results from the analysis examining the interaction between sex and genotype with its corresponding p-values. Simple main effects for sex (SME: Sex) and Genotype (SME: Genotype) are in the last two columns with p-values Bonferroni-adjusted within each simple main effect.*

Effect of NMDAR hypofunction on the mesopic b-wave amplitude

We compared the b-wave amplitude between WT and $SR^{-/-}$ mice (Figure 2.3). Analysis of main effects showed that the b-wave amplitudes were significantly reduced at every light intensity between the $SR^{-/-}$ and WT mice. $SR^{-/-}$ mice had a reduced b-wave amplitude ranging from 21-62 µV depending on light intensity, and interestingly did not change when light intensity was increased (Figure 2.3A, Table 2.3). Examination of the simple main effects was conducted to evaluate whether members of the same sex but opposing genotypes were different from one another. The simple main effect for sex revealed that $SR^{-/-}$ male mice had significantly smaller b-wave amplitudes in comparison to male WT at all light intensities except the highest (Figure 2.3B, Table 2.4,). Female mice showed a decrease in b-wave amplitude for three of the seven light intensities (Figure 2.3C). Simple main effects of genotype were determined to understand whether mice of the same genotype, but opposite sex, differed from one another. The simple main effects for genotype revealed that between male and female WT mice, male mice had statistically higher b-wave amplitudes in comparison to females at low light

intensities (Table 2.4), while the *SR*$^{-/-}$ female and *SR*$^{-/-}$ male mice were not statistically different from one another. A two-way mixed ANOVA was performed to understand if there was an interaction between sex with repeated changes in light intensity and between genotype and repeated changes in light intensity. No dependent variables were significant for sex and light intensity interaction; however, b-wave amplitude was the only dependent variable that showed significant differences between light intensity and genotype ($df(6,180)=4.6$, $p<0.0005$). These results suggest that SR$^{-/-}$ mice b-wave did not modulate to increasing light intensity. These results demonstrate that at all light intensities, D-serine deficiency through NMDAR hypofunction reduced the b-wave amplitude. However, this reduction in amplitude depended on whether the animal was male or female. Male *SR*$^{-/-}$ mice exhibited a statistically significant reduction in b-wave amplitude in comparison to WT males across light intensities; however, only at the middle light intensities were the *SR*$^{-/-}$ females statistically lower than the WT females. Interestingly, the b-wave amplitude between *SR*$^{-/-}$ male and *SR*$^{-/-}$ female did not differ from one another, while WT female and WT male mice differed at lower light intensities. This highlights the importance of investigating sex differences in fERG of WT animals as well as genetically modified mice.

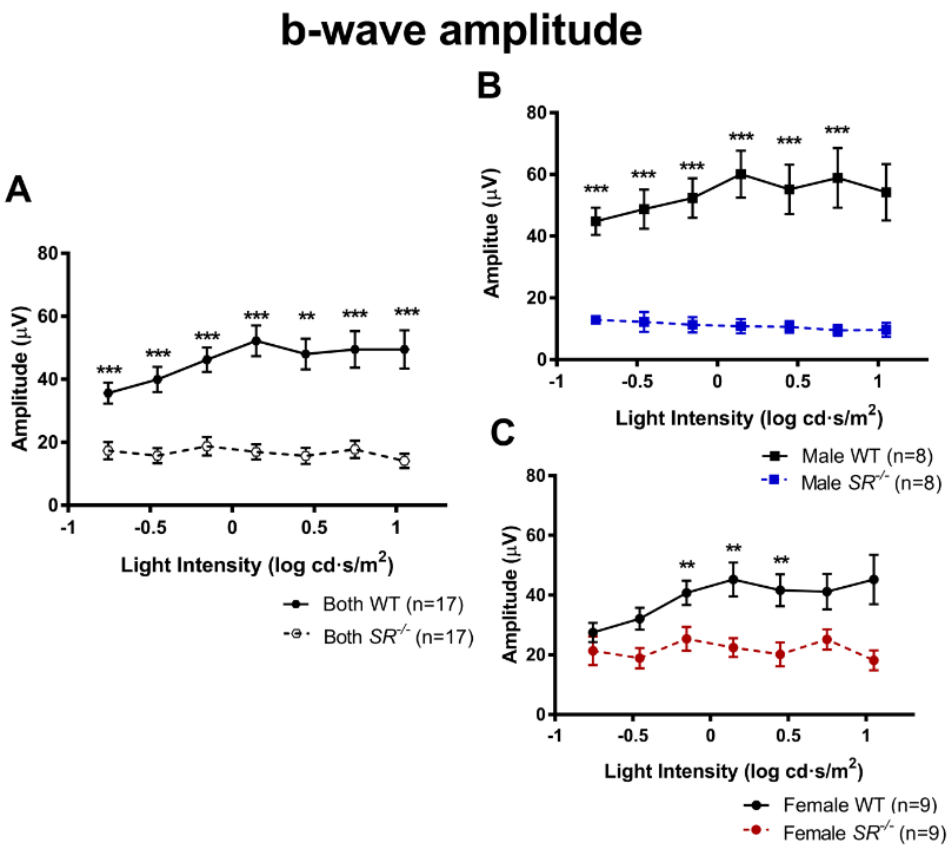

Figure 2.3 B-wave amplitude analysis: *(A) Comparison of b-wave amplitudes given genotype by evaluating the main effects (WT=solid line & close circles, $SR^{-/-}$ =dashed line & open circles). (B,C) Comparison of genotype given a specific gender by evaluating the simple main effects of sex: males (B) and females (C), WT (black) and $SR^{-/-}$ mice (♂ blue line, ♀ red line) at all light intensities. Data expressed: mean (line), SEM (error bars), and significance ([*] p = 0.05-0.01**;** [**] p = 0.001-0.005**;** [***] p<0.0005).*

Table 2.3 b-wave amplitude (μV)			
Flash intensity ($cd \cdot s/m^2$)	*WT vs $SR^{-/-}$*		*Main Effects Genotype*
0.175	36 ± 14.0	17 ± 11.3	F(1,30)=25.7, ***p*< 0.0005**
0.35	40 ± 16.7	16 ± 9.9	F(1,30)=33.6, **p<0.0005**
0.7	46 ± 16.0	19 ± 12.1	F(1,30)=40.3, ***p*< 0.0005**
1.4	52 ± 20.2	17 ±10.0	F(1,30)=49.8, ***p* <0.0005**
2.8	48 ± 20.1	16 ± 10.4	F(1,30)=39.4, ***p*< 0.0005**
5.6	50 ± 23.9	18 ± 11.3	F(1,30)=30.9, ***p* <0.0005**
11.2	49 ± 25.0	14 ± 9.4	F(1,30)=30.4, ***p* <0.0005**

Table 2.3 Comparison of b-wave amplitudes in WT and $SR^{-/-}$ mice: *Data represents b-wave amplitudes given genotype, with data from males and females pooled. Data expressed as mean± S.D. The p-values are the results of main effects analysis.*

Table 2.4 b-wave amplitude (μV)							
	Female		*Male*				
Flash intensity ($cd \cdot s/m^2$)	*WT*	*$SR^{-/-}$*	*WT*	*$SR^{-/-}$*	*Interaction Sex*Genotype*	SME: Sex	SME:Genotype
0.175	27	21	45	13	F(1,30) = 11.8, ***p* =0 .002**	Male: ***p* <0.0005** | Female: *p* =N.S.	WT: ***p* =0.003**
0.35	32	19	49	12	F(1,30) = 7.4, ***p*= 0.011**	Male: ***p* <0.0005** | Female: *p*= 0.032	WT: ***p* =0.010**
0.7	41	25	52	11	F(1,30) = 8.3, ***p* =0.007**	Male: **p<0.0005** | Female: ***p* =0.017**	WT: *p*=0.075
1.4	45	22	60	11	F(1,30) = 6.7, ***p* =0.015**	Male: **p<0.0005** | Female: ***p* =0.003**	WT: *p*=0.048
2.8	41	20	55	11	F(1,30) = 4.8, ***p* =0 .036**	Male: **p<0.0005** | Female: ***p* =0.006**	WT: *p* =0.080
5.6	41	25	59	9	F(1,30) = 8.1, **p=0.008**	Male: **p<0.0005** | Female: *p* =N.S.	WT: *p*=0.041
11.2	45	18	54	10	F(1,30) = 1.8, *p* =0 .188	N.A.	N.A.

Table 2.4 Comparison of b-wave amplitudes in WT and $SR^{-/-}$ mice depending on sex: *The first two columns represent the mean b-wave amplitude at each condition. The interaction column includes the results from the analysis examining the interaction between sex and genotype with its corresponding p-values. Simple main effects for sex (SME: Sex) and Genotype (SME: Genotype) are in the last two columns with p-values Bonferroni-adjusted within each simple main effect.*

Effect of NMDAR hypofunction on the mesopic b-wave implicit time

The b-wave implicit times for the *$SR^{-/-}$* mice were significantly delayed from those generated by WT retinas at all light intensities as shown by the main effects' analysis (Figure 2.4A, Table 2.5). However, there was an interaction effect between sex and

genotype at two of the brightest light intensities (Table 2.6). *SR*$^{-/-}$ males had a statistically significant delay in the b-wave implicit time in the brightest light intensities in comparison to WT male mice (Figure 2.4B, Table 2.6). This difference was not present in female mice (Figure 2.4C). Comparing the b-wave implicit time for members of the same genotype but opposing sex, *SR*$^{-/-}$ male and female mice differed at the brightest light intensities, with male mice having a statistically greater delay in the b-wave implicit time (Table 2.6), while WT female and WT male mice did not differ from one another. This demonstrates that the peak of the b-wave in *SR*$^{-/-}$ mice occurs later in time after flash onset compared to WT mice. However, this delay in the b-wave implicit time depended on the light intensity and sex of the animal. At brighter light intensities, *SR*$^{-/-}$ male mice had a statistically significant delay in the b-wave implicit time in comparison to: *SR*$^{-/-}$ females, WT females, and WT males (Table 2.6).

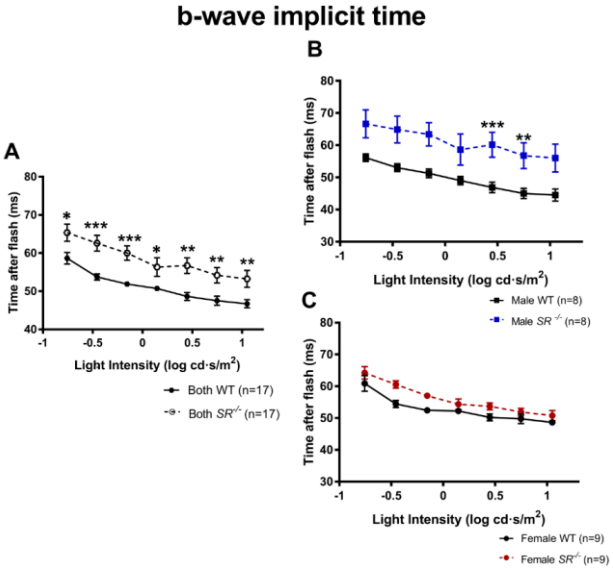

Figure 2.4 B-wave implicit time analysis: *(A) Comparison of b-wave implicit time given genotype by evaluating the main effects (WT=solid line & close circles, SR*$^{-/-}$ *=dashed line & open circles). (B,C) Comparison of genotype for a specific gender by evaluating the simple main effects of sex: males (B) and females (C). WT (black) and SR*$^{-/-}$ *mice (♂ blue line, ♀ red line) at all light intensities. Data expressed: mean (line),*

*SEM (error bars), and significance ([*] p = 0.05-0.01**;** [**] p = 0.009-0.001**;** [***] p<0.0005).*

Table 2.5	b-wave implicit time (ms)		
Flash intensity ($cd \cdot s/m^2$)	*WT vs SR $^{-/-}$*		*Main Effects Genotype*
0.175	59 ± 6.2	65 ± 9.2	F(1,30)=6.6, ***p* =0.016**
0.35	54 ± 3.4	63 ± 8.5	F(1,30)=16.3, ***p*< 0.0005**
0.7	52 ± 3.2	60 ±7.8	F(1,30)=18.6, ***p*< 0.0005**
1.4	51 ± 3.2	56 ± 10	F(1,30)=5.3, ***p* =0.028**
2.8	49 ± 4.2	57 ± 8.4	F(1,30)=15.0, ***p* =0.001**
5.6	48 ± 5.1	54 ± 8.3	F(1,30)=9.3, ***p* =0.005**
11.2	47 ± 4.4	53 ± 9.2	F(1,30)=8.0, ***p* =0.008**

Table 2.5 Comparison of b-wave implicit time in WT and SR$^{-/-}$ mice: *Data represent b-wave implicit times for each genotype; male and female were pooled. Data are expressed as mean ± S.D. The p-values are the results of main effects analysis.*

Table 2.6	b-wave implicit time (ms)						
	Female		*Male*				
Flash intensity ($cd \cdot s/m^2$)	*WT*	*SR $^{-/-}$*	*WT*	*SR $^{-/-}$*	*Interaction Sex*Genotype*	SME: Sex	SME:Genotype
0.175	61	64	56	67	F(1,30) = 1.8, *p* = N.S.	N.A.	N.A.
0.35	54	61	53	65	F(1,30) = 1.7, *p* = N.S.	N.A.	N.A.
0.7	52	57	51	63	F(1,30) = 3.8, *p* = N.S.	N.A.	N.A.
1.4	52	54	49	59	F(1,30) = 2.2, *p* = N.S.	N.A.	N.A.
2.8	50	54	47	60	F(1,30) = 5.2, ***p* = 0.030**	Male: ***p* <0.0005**	SR$^{-/-}$: ***p* = 0.043**
5.6	50	52	45	57	F(1,30) = 4.5, ***p* = 0.043**	Male: ***p* = 0.001**	N.S.
11.2	49	51	45	56	F(1,30) = 3.8, *p* = N.S.	N.A.	N.A.

Table 2.6 Comparison of b-wave implicit time in WT and SR$^{-/-}$ mice depending on sex: *The first two columns represent the mean b-wave implicit time each condition. The interaction column includes the results from the interaction between sex and genotype with its corresponding p-values. Simple main effects analysis for sex (SME: Sex) and genotype (SME: Genotype) are in the last two columns with p-values Bonferroni-adjusted within each simple main effect. (N.A.) stands for not applicable.*

Effect of NMDAR hypofunction on the mesopic b/a wave ratio

Since the amplitude of the b-wave depended on the interaction between sex and genotype at all light intensities while the a-wave amplitude did not (Supplemental Figure 2.1, Supplemental Table 2.1), we calculated the b/a wave ratio to determine whether the

relationship between the a- and b-wave differences depended on the interaction of genotype and sex. At all light intensities except the lowest, the main effects analysis revealed that the b/a wave ratio was significantly reduced in *SR*$^{-/-}$ mice in comparison to WT mice (Figure 2.5, Table 2.7). There was no interaction effect between sex and genotype (analysis not shown). In sum, the b/a wave ratio quantification demonstrated a reduction in the *SR*$^{-/-}$ mice, regardless of the sex of the animal. This is the first use of the b/a ratio in analysis of the ERG from an animal model or from humans with schizophrenia. It will be important to determine if these differences are seen in people with schizophrenia.

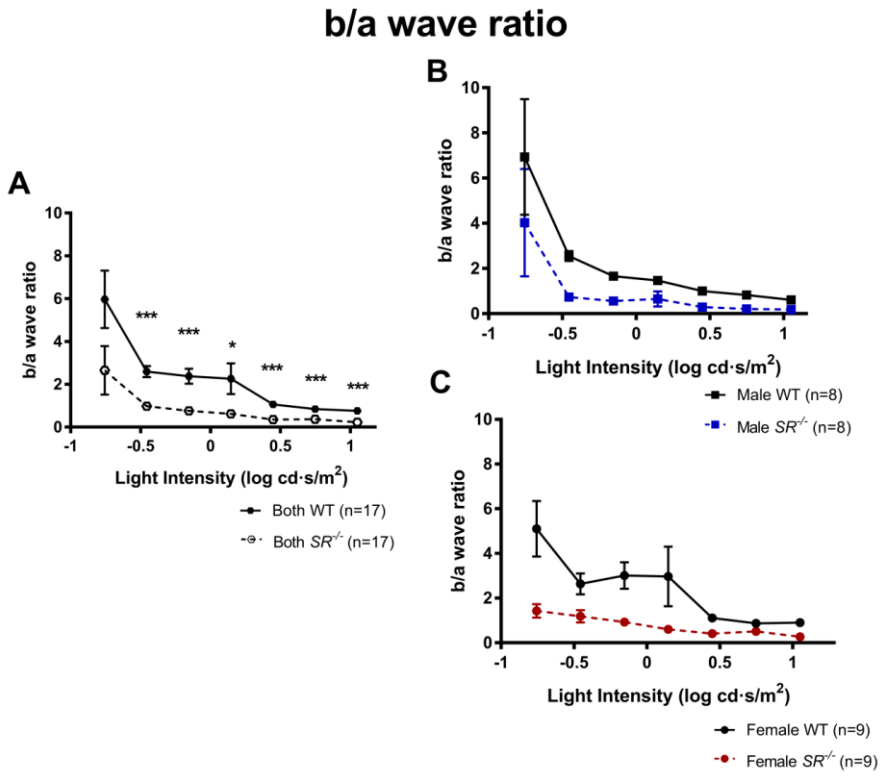

Figure 2.5 b/a wave ratio analysis: *(A) Comparison of b/a wave ratio given genotype by evaluating the main effects (WT=solid line & close circles, SR*$^{-/-}$*=dashed line & open circles). (B,C) Comparison of genotype given a specific gender by evaluating the*

*simple main effects of sex: males (B) and females (C). WT (black) and SR$^{-/-}$ mice (♂ blue line, ♀ red line) at all light intensities. Data expressed: mean (line), SEM (error bars), and significance ([*] p = 0.05-0.01**;** [**] p = 0.009-0.001**;** [***] p<0.0005).*

Table 2.7	b/a wave ratio		
Flash intensity (cd·s/m^2)	*WT vs SR$^{-/-}$*		*Main Effects Genotype*
0.175	6 ± 5.6	3 ± 4.7	F(1,30)=3.4, p=0.074
0.35	3 ± 1.1	1 ± 0.7	F(1,30)=26.5, **p< 0.0005**
0.7	2 ± 1.5	0.8 ± 0.5	F(1,30)=22.3, **p <0.0005**
1.4	2 ± 2.9	0.6 ± 0.7	F(1,30)=4.7, **p=0.038**
2.8	1 ± 0.4	0.4 ± 0.2	F(1,30)=38.2, **p <0.0005**
5.6	0.8 ± 0.2	0.4 ± 0.2	F(1,30)=37.8, **p <0.0005**
11.2	0.8 ± 0.4	0.2 ± 0.1	F(1,30)=25.6, **p< 0.0005**

Table 2.7 Comparison of b/a wave ratio given in WT and SR$^{-/-}$ mice: *Data represent the b/a wave ratio for each genotype; male and female data are pooled. Data are expressed as mean of each genotype ± S.D. The p-values are the results of main effects analysis. (N.A.) stands for not applicable and (N.S.) stands for not significant.*

Advanced Fourier transform analysis

Fourier transform analysis decomposes a signal into contributing frequency components and provides the weight (power) that each frequency contributes to the original signal. Fourier transform analysis on the low frequency components of the fERG, the a- and b-waves, showed a statistically significant reduction of *SR$^{-/-}$* mice in comparison to WT mice at all light intensities except the dimmest (Figure 2.6A, Table 2.8). There was a significant interaction between genotype and sex at the three lowest light intensities (Table 2.9). Examination of the simple main effects was conducted to evaluate whether members of the same sex but opposing genotypes were different from one another. The simple main effect for sex revealed that *SR$^{-/-}$* male mice had a significantly smaller low frequency component in comparison to male WT at all light

intensities (Figure 2.5B, C, Table 2.9). There was no statistically significant difference between *SR*$^{-/-}$ and WT females (Figure 2.5D, E). Analysis of the low frequency component demonstrated that *SR*$^{-/-}$ mice had lower power in comparison to WT mice, but this difference was greater in males at the lowest light intensities.

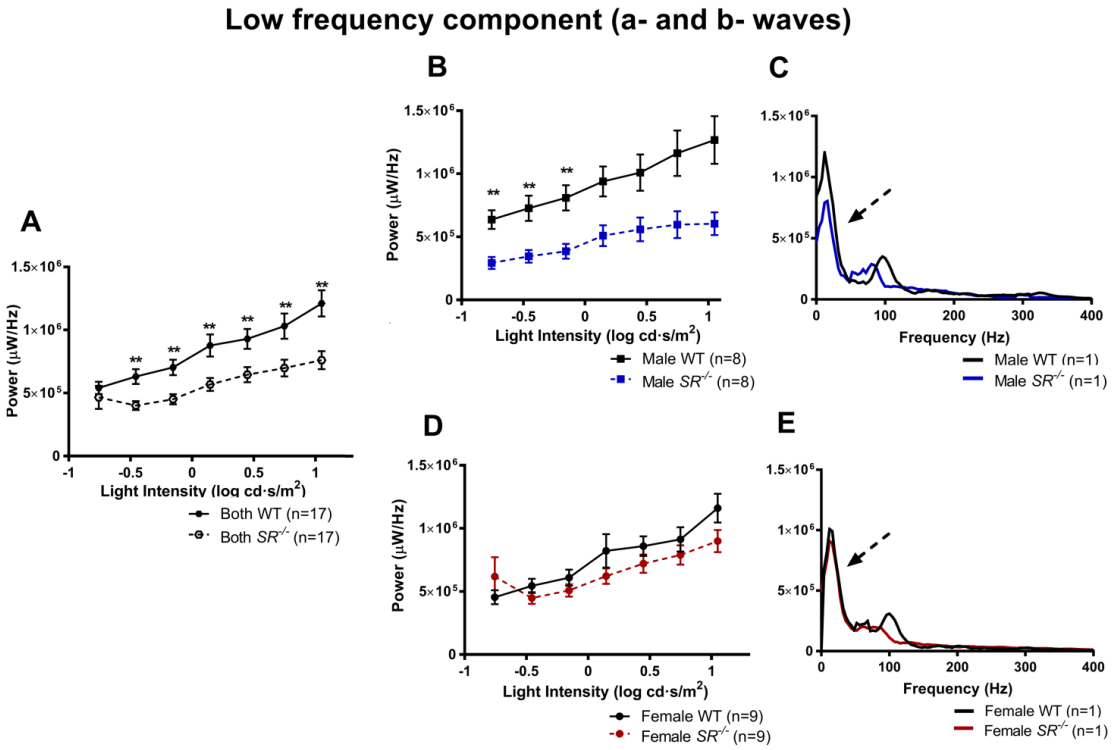

Figure 2.6 Fourier transform analysis: *Fourier transform analysis in males and females of WT (black) and SR*$^{-/-}$ *mice (♂ blue line, ♀ red line) of the a- and b-waves at all light intensities. Sample Fourier transform output of one animal per given genotype at light intensity 5.6 2 cd·s/m*^{2} *for males (C) and females (E). The black dashed arrow points to the low frequency component. (A) Comparison of the low frequency component given genotype by evaluating the main effects (WT=solid line & close circles, SR*$^{-/-}$ *=dashed line & open circles). SR*$^{-/-}$ *mice had reduced low frequency component in comparison to WT at the dimmest light intensities in the males (B) but not females (D). Data expressed: mean (line), SEM (error bars), significance ([*] p = 0.05-0.01; [**] p = 0.009-0.001; [***] p<0.0005).*

Table 2.8	Low Frequency Component		
Flash intensity (cd·s/m²)	*WT vs SR -/-*		*Main Effects Genotype*
0.175	5.4x105	4.7x105	F(1,30)=0.874, *p*=0.357
0.35	4.0x105	6.3x105	F(1,30)=13.3, ***p*= 0.001**
0.7	7.0x105	4.5x105	F(1,30)=14.1, ***p*= 0.001**
1.4	8.8x105	5.7x105	F(1,30)=9.3, ***p*= 0.005**
2.8	9.3x105	6.5x105	F(1,30)=8.9, ***p*= 0.006**
5.6	1.0x106	7.0x105	F(1,30)=8.6, ***p*= 0.006**
11.2	5.7x106	7.6x106	F(1,30)=13.7, ***p*= 0.001**

Table 2.8 Comparison of low frequency component in WT and SR$^{-/-}$ mice: *Data represent the low frequency component given genotype; male and female data are pooled. Data are expressed as mean± S.D. The p-values are the results of main effects analysis*

Table 2.9	Low frequency component						
	Female		*Male*				
Flash intensity (cd·s/m²)	*WT*	*SR -/-*	*WT*	*SR -/-*	*Interaction Sex*Genotype*	SME: Sex	SME:Genotype
0.175	$4.5x10^5$	$6.2 x 10^5$	$6.4x10^5$	$2.9x10^5$	F(1,30) = 6.9, ***p* = 0.013**	Male: ***p*= 0.02**	SR$^{-/-}$: ***p* =0.023**
0.35	$5.4x10^5$	$4.5x10^5$	$7.3x10^5$	$3.5x10^5$	F(1,30) = 4.7, ***p* = 0.038**	Male: ***p* <0.0005**	N.S.
0.7	$6.1x10^5$	$5.1x10^5$	$8.1x10^5$	$3.7x10^5$	F(1,30) = 5.3, ***p* = 0.028**	Male: ***p* <0.0005**	N.S.
1.4	$8.2x10^5$	$6.2x10^5$	$9.4x10^5$	$5.1x10^5$	F(1,30) = 1.2, *p* = 0.276	N.A.	N.A.
2.8	$8.6x10^5$	$7.2x10^5$	$1.0x10^6$	$5.6x10^5$	F(1,30) = 2.5, *p* = 0.124	N.A.	N.A.
5.6	$9.1x10^5$	$7.9x10^5$	$1.2x10^6$	$6.0x10^5$	F(1,30) = 3.5, *p* = 0.070	N.A.	N.A.
11.2	$1.2x10^6$	$9.0x10^5$	$1.3x10^6$	$6.0x10^5$	F(1,30) = 2.6, *p = 0.118*	N.A.	N.A.

Table 2.9 Comparison of low frequency component given in WT and SR$^{-/-}$ mice depending on sex: *Data represent mean power of the low frequency component for each genotype. Data are expressed as mean of each genotype. The p-values are the results of main effects analysis. Simple main effects for sex (SME: Sex) and genotype (SME: Genotype) are in the last two columns with p-values Bonferroni-adjusted within each simple main effect.*

Morphometric Analysis of Retinal Thickness in *SR$^{-/-}$* and WT mice.

The thickness of each layer of the retina in both the central and peripheral retina from *SR$^{-/-}$* and WT mice were analyzed for differences due to loss of D-serine in the *SR$^{-/-}$*

mice. No significant differences were seen in any of the layers of either the central or peripheral retina (Supplemental Figure 2.2). It should be noted that these mice were generated and validated in the Coyle laboratory, where they were shown to mimic a number of aspects of the human disease (Basu et al., 2010). The retinas of these mice were also shown to have significantly reduced D-serine concentration, as measured by capillary electrophoresis, and both significantly reduced co-agonist occupancy of the NMDAR and a significant reduction in the NMDAR component of ganglion cell light-evoked responses with retention of normal vision as measured by the optokinetic reflex (Sullivan et al., 2011).

Discussion

This study demonstrated that mesopic-adapted fERG in mice with reduced function of the NMDAR had a reduced b-wave amplitude, delayed a-wave and b-wave implicit time, smaller b/a ratio and a decreased low frequency component of the FFT. This highlights the potential of using mesopic background luminance in identifying abnormalities pertinent to schizophrenic pathology. Similar to people with schizophrenia, mice with NMDAR hypofunction have a reduced b-wave amplitude and delayed b-wave implicit time in comparison to controls. However, we emphasize that this reduction depended on whether the mouse was female or male and, therefore, suggests including sex in future fERG data analyses. Furthermore, we explored two additional dependent variables not examined by the schizophrenic-fERG literature to date, the b/a wave ratio and the low frequency component of the FFT. Our work demonstrates the b/a ratio did not depend on sex and can be used exclusively to evaluate genotypic differences. Lastly, the low-frequency component of the fERG, which reflects the a- and b- wave

combined, can inform about sex and genotype differences as well, but it can be a better measure for recording in instances with a low signal to noise ratio. Due to its sensitivity to sex and genotype, the b-wave amplitude and implicit time and the low frequency component of the FFT emerged as potential candidates for use as a schizophrenia biomarker.

Studies comparing people with schizophrenia to healthy human controls showed a reduction of the b-wave amplitude in the people with schizophrenia under different light adaptation conditions (Demmin et al., 2018; Gerbaldo et al., 1992; Hébert et al., 2010; Hébert et al., 2015). While some earlier work did not observe differences in people with schizophrenia in comparison to controls (Marmor et al., 1988; Schechter et al., 1987; Balogh, 2008), the recent studies cited above used a variety of dependent variables in broader stimulus and background luminance, which may explain the inconsistencies with the earlier studies. The reduced b-wave amplitude and delayed implicit times at all light intensities in *SR*$^{-/-}$ mice compared to WT mice agreed with similar changes in the b-wave seen in people with schizophrenia compared to healthy controls (Demmin et al., 2018). However, our work highlights the importance in examining sex differences in electroretinographic measurements from people with schizophrenia, as they are also known to be present in the normal human fERG (Zeidler, 1959).

The b/a ratio has not been examined previously in the human fERG-schizophrenic literature nor in animal models of schizophrenia. However, it was reported to be a good marker for central retinal vein occlusion and predicting neovascular glaucoma (Matsui et al., 1994; Sabates et al., 1983). Since the b-wave amplitude was significantly reduced in *SR*$^{-/-}$ mice but the a-wave amplitude was not, calculation of the b/a ratios allowed the evaluation of its usefulness in quantifying genotypic differences. In

the *SR*$^{-/-}$ NMDAR hypofunction mice, the b/a ratio was reduced at all light intensities in comparison to WT mice. This reduction was independent of the sex of the animal and therefore can be used as a tool to evaluate genotypic differences in b-wave parameters when data from both sexes are pooled together.

In addition to performing traditional quantification of the fERG a- and b-wave components, we implemented a higher order analysis on these components, the Fast Fourier transform (FFT), even though analyses of the fERG waves using this technique have not been reported in human schizophrenic subjects previously. In normal ERGs from human subjects, FFT measurements were better at reflecting differences than traditional amplitude and implicit time measurements because of their resistance to a low signal-to-noise variability (Gur & Zeevi, 1980). This finding suggests that frequency domain measurements would be essential in when examining subjects with schizophrenia, where there is a low signal to noise ratio, such as might be expected from pathology of those afflicted with schizophrenia (Association, 2013). To mitigate this difficulty, current schizophrenia-fERG investigations are utilizing portable, hand-held fERG devices (Demmin et al., 2018). We conducted frequency domain measurements due to their translational potential of reducing inherit variability brought about by the population studied (Gur and Zeevi, 1980). In our research, the low frequency component was significantly reduced in *SR*$^{-/-}$ NMDAR hypofunction mice in comparison to controls. Similar to the b-wave amplitude, the low frequency component provides information on genotype and sex differences. In contrast to the b-wave amplitude, the low frequency component can also account for inherent variability in the data resulting from studying individuals with schizophrenia (Gur and Zeevi, 1980). We suggest that an analysis of the

low frequency component be included in fERG analyses of people with schizophrenia as well.

Our findings strongly support the value of the *SR*$^{-/-}$ mouse model of schizophrenia, consistent with the NMDAR hypofunction hypothesis contributing to the pathophysiology of schizophrenia. This mouse model would facilitate investigation into potential therapeutic interventions that might ameliorate these abnormalities in the retina, and by extension, within the brain. Previously tested mouse models, with relevance to psychiatric disorders, examined fERG changes resulting from dopaminergic dysfunction (Lavoie et al., 2014). Lavoie and colleagues observed a reduction in the b-wave amplitude at all light intensities in both photopic and scotopic conditions in the dopamine D1 receptor knock-out (D1R-KO) mice, commenting on the similarity between D1R-KO results and high-risk schizophrenic off-spring. However, this reduction in b-wave was expected from knocking-out the D1 receptor, a dopamine receptor type known to be expressed in bipolar cells (Farshi et al., 2016) and essential for normal response to light adaptation from bipolar cells (Chen et al., 2017; Flood et al., 2018). We also observed a decrease in b-wave amplitude in *SR*$^{-/-}$ mouse, but it differs from the previous research in that SR expression normally changes dynamically in the retina with age (Dun et al., 2008). In addition, the ERG in the *SR*$^{-/-}$ mouse showed sex differences and interaction of sex with the waveform amplitudes, b/a ratios, and spectral frequency components that cannot be predicted from glutamatergic manipulation alone. Specifically, in comparison to infant mice (3-week old), adult mouse retina has limited D-serine and SR expression. Our study shows that the absence of D-serine expression from birth affects bipolar cell function; furthermore, it can potentially show within-subject longitudinal differences that may be relevant to changes associated with the onset of

psychosis in schizophrenia. As this is a constitutive knockout, it would affect development. The onset of schizophrenia is not linked to the onset of psychosis, which typically occurs in the late teens or early 20s in males (Hambrecht et al., 1992). Cognitive impairments and social/motivational deficits (negative symptoms), which best reflect NMDAR hypofunction, are present in childhood in most individuals who later are diagnosed with schizophrenia – after the appearance of psychosis (Loebel et al., 1992).

Importantly, our study demonstrated distinctly different patterns of the fERG in male and female mice, only showing significant changes in the male *SR*$^{-/-}$ mice compared to WT mice but not in females. While some fERG studies in people with schizophrenia demonstrated that components of the photopic a- and b-waves were reduced in people with schizophrenia in comparison to healthy controls, most studies grouped male and female subjects for their data analyses. Only one study included sex as a factor, and they did not observe a statistically significant difference in the fERG between females and males with schizophrenia (Hébert et al., 2015). However, this study measured subjects that were at high risk for schizophrenia and did not account for sex on the follow-up study examining subjects who had developed schizophrenia (Hébert et al., 2015). It is difficult to interpret these results because questions remain as to cause and effect of these relationships. Several studies showed a sex difference in the fERGs among healthy human controls, including differences in amplitude and implicit time (Peterson, 1968; Sannita et al., 1989). This is reflected in our work whereby the fERG of WT mice differed depending on sex at specific parameters. Previous studies have shown that the prevalence of schizophrenia is lower in females, who also have a later age of onset and a less severe disease course than males (Loranger, 1984;

Shepherd et al., 1989). Notably, the behavioral phenotype was less severe in female *SR*$^{-/-}$ mice than in males (Frishman and Wang, 2011).

The power of the present study is two-fold. First, we demonstrate that our current knowledge of D-serine's role in the retina requires further investigation due to the reduction of the b-wave amplitude and time delay observed in *SR*$^{-/-}$ mice. It would be essential to understand how the changes in D-serine and SR expression during development (Gustafson et al., 2007) reflect changes in the fERG at various light intensities. D-serine plays a pivotal role in the retina as the endogenous co-agonist of the NMDAR (Gustafson et al., 2015). Since it is known that NMDARs are recruited in RGCs based on light intensity demands, looking at a range of light intensities can serve as an indirect evaluation of dynamic recruitment of NMDARs that may differentiate one person with schizophrenia from another (Coyle, 2006). As a result, we recommend that examination of the differences between the fERGs in people with schizophrenia and controls needs to be performed at a range of light intensities with the same background condition, not just the standard flash intensity of 1.68 cd/m^2, in order to understand the full scope of functional alterations in the retina. Secondly, we demonstrate that signals from mesopic-adapted retina warrant further investigation regarding inner retinal involvement in the fERG, particularly how these changes can be used to as a potential diagnostic tool for identification of psychiatric disorders. The b-wave amplitude under mesopic conditions contains inner retinal contributions, likely from amacrine cells (Mojumder et al., 2008), and dopamine plays a role in switching between photopic and mesopic states (Krizaj, 2000). This suggests that the network needed for adapting to mesopic light conditions can be severely affected by neuropsychiatric diseases, like schizophrenia, because it requires both dopamine and glutamate. It is the consensus

that schizophrenia is a disorder of complex genetics and that no single molecular event can account for the pathophysiology of schizophrenia (Coyle, 2006), which implies that people with schizophrenia may be quite diverse in the underlying cause of their disorder. This may explain the inconsistent results from human fERG data from people with schizophrenia (Demmin et al., 2018; Gerbaldo et al., 1992; Hébert et al., 2015; Schechter et al., 1987; Warner et al., 1999; Bulogh, 2008), Including mesopic-adapted conditions in the human fERG literature may provide further insight. Lastly, the calculation of the b/a ratio may prove to be important in demonstrating differences between people with schizophrenia and normal individuals. This finding needs to be replicated in studies of the ERG of human subjects, as this dependent measure has not been previously evaluated in these individuals. Our results demonstrate that specific analyses of the ERG waveform may allow more accurate and sensitive measures of differences between people with schizophrenia and normal individuals. Our study suggests that subgroups within these populations are likely to be differentiated by using a wider range of light intensities and mesopic adaptation. Second, the replication of the fERG results in people with schizophrenia by this mouse model supports the potential role of NMDAR hypofunction as one of the causative mechanisms. This mouse model will allow us to assess methods that might modify the abnormal fERG that may in turn result in new therapeutic approaches for the treatment of schizophrenia.

In conclusion, even though the current diagnostic measurement using clinical interviews is effective at identifying schizophrenia once present, clinical screens prior to the appearance of psychosis are weakly predictive of schizophrenia (Weickert et al., 2013). The power of having a biomarker for schizophrenia lies on prognostics, the ability to predict who will become ill prior to symptoms. As there is a known genetic risk for the

development of schizophrenia (Baron et al., 1983; Kendler and Robinette, 1983), this may aid in the early identification of at-risk individuals with impaired NMDAR function and facilitate early intervention. The human studies demonstrate that there are anomalies in the fERG of humans with schizophrenia in comparison to normal persons; however, insights into the cellular mechanisms behind these differences are needed. Further studies in this mouse model of schizophrenia should help explain why the fERG differences are present and provide stronger support for the use of fERG as a tool to decipher the etiology of schizophrenia.

Supplemental Table:

Supplemental Table 2.1

Supp. Table 2.1	a-wave amplitude (μV)							
	Female		Male					
Flash intensity ($cd \cdot s/m^2$)	WT	$SR^{-/-}$	WT	$SR^{-/-}$	Interaction Sex*Genotype	SME: Sex	SME: Genotype	Main Effects Genotype
0.175	7	16	12	10	F(1,30) = 5.4, ***p* = 0.027**	Female:***p* =0.009**	N.S.	N.S.
0.35	16	20	20	19	F(1,30) = 0.5, *p* = 0.466	N.A.	N.A.	N.S.
0.7	16	28	26	33	F(1,30) = 5.3, ***p* = 0.029**	N.S.	WT:***p* =0.007**	N.S.
1.4	24	39	42	33	F(1,30) = 4.5, ***p* = 0.042**	N.S.	N.S.	N.S.
2.8	39	48	59	43	F(1,30) = 3.4, *p* = 0.073	N.A.	N.A.	N.S.
5.6	47	55	71	49	F(1,30) = 4.1, *p* = 0.052	N.A.	N.A.	N.S.
11.2	52	74	88	54	F(1,30) = 12.8, ***p* = 0.001**	Male:***p* =0.006**	WT:***p* =0.003**	N.S.

Supplementary Table 2.1. Comparison of a-wave amplitudes in WT and $SR^{-/-}$ mice depending on sex: *The first two columns represent the mean a-wave amplitude at each condition. The interaction column includes the results from the analysis examining the interaction between sex and genotype with its corresponding p-values. Simple main effects for sex (SME: Sex) and Genotype (SME: Genotype) are in the last two columns with p-values Bonferroni-adjusted within each simple main effect*

Supplemental Figures:

Supplemental Figure 2.1

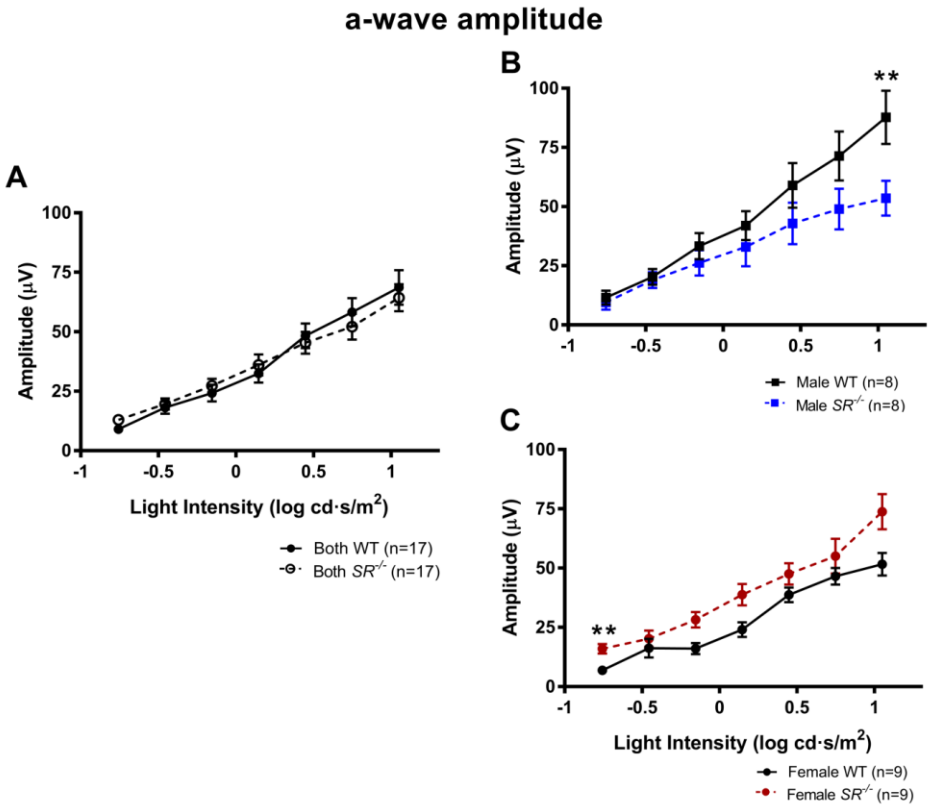

Supplementary Figure 2.1. a-wave amplitude analysis: *(A) Comparison of A-wave amplitudes given genotype by evaluating the main effects (WT=solid line & close circles, $SR^{-/-}$=dashed line & open circles). (B,C) Comparison of genotype given a specific gender by evaluating the simple main effects of sex: males (B) and females (C), WT (black) and $SR^{-/-}$ mice (♂ blue line, ♀ red line) at all light intensities. Data expressed: mean (line), SEM (error bars), and significance ([*] p = 0.05-0.01**;** [**] p = 0.001-0.005**;** [***] p<0.0005).*

Supplemental Figure

2.2

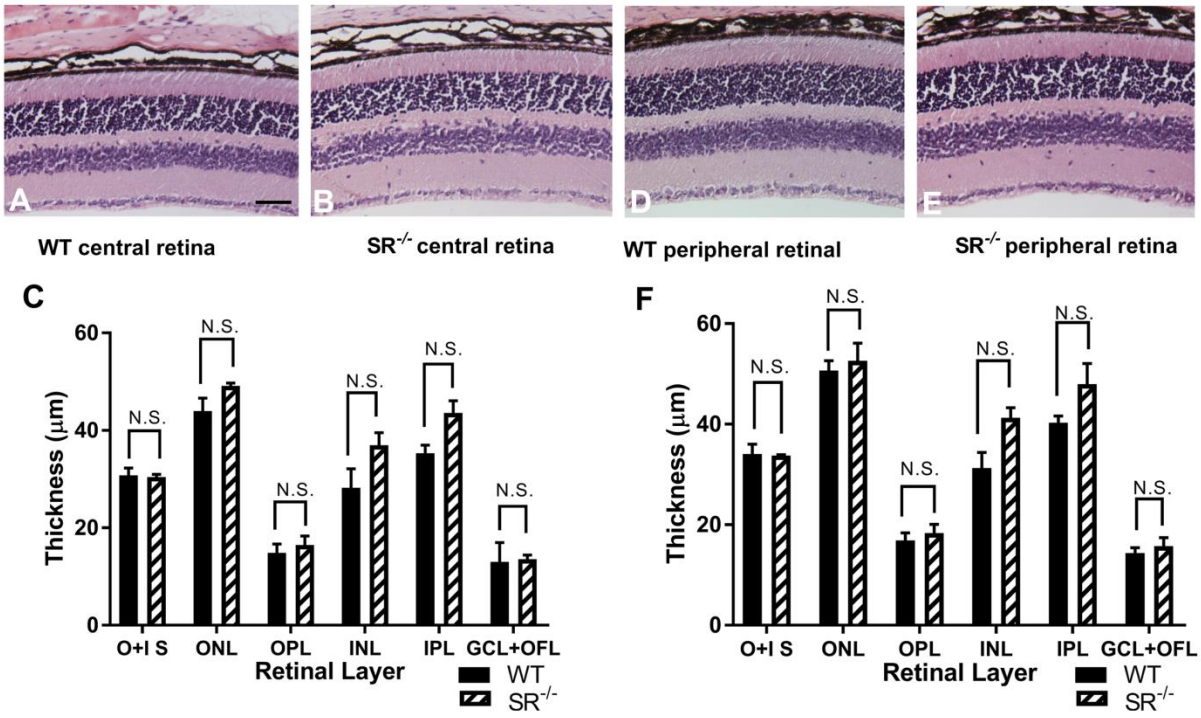

Supplementary Figure 2.2. Retinal Layer Height Calculations.
Photomicrographs of retinal sections from the central (A-C) and peripheral (D-F) regions of the retina from SR$^{-/-}$ (B and E) and littermate controls (A and D) at two months stained with hematoxylin and eosin. Retinal layers were quantified for height in µm. O+IS: outer and inner segments; ONL: outer nuclear layer; OPL: outer plexiform layer; INL: inner plexiform layer; IPL: inner plexiform layer; GCL+OFL: ganglion cell layer and outer fiber layer. N.S.: not significant. Bar is 50µm.

Chapter 3

Effects of D-Serine on Outer Retinal Function

Synopsis

The role of NMDAR in outer retina is unclear despite expression of the NMDAR-complex and its subunits in the outer retina. The flash-electroretinogram (fERG) offers a non-invasive measurement of the retinal field potentials of the outer retina that can serve to clarify NMDAR contribution on early retinal processing. I report alteration in fERG components as a result of NMDAR hypo- and hyperfunction, through the use of a genetic mouse model for NMDAR hypofunction ($SR^{-/-}$) where the absence of the enzyme serine racemase results in a significant reduction of D-serine, followed by examination of the fERG after an exogenous application of D-serine. I analyzed parameters of the fERG to determine whether pre- and post-topical delivery of D-serine would be affected in $SR^{-/-}$ mice and their littermate control WT counterparts. Amplitude and implicit time of the low-frequency components, the a- and b-wave, were conducted. A reduced functionality of the NMDAR results in a statistically significantly delayed a-wave and reduced b-wave in $SR^{-/-}$ animals. The effect of NMDAR deprivation was more prominent in male $SR^{-/-}$ mice. A hyperfunction of NMDAR, though exogenous topical delivery of 5mM D-serine, in WT mice showed a significantly delayed a-wave implicit time and reduced b-wave amplitude. These changes were not observed in female WT mice. There were temporal delays in the a-wave and amplitude and a decrease in the b-wave amplitude and implicit time because of hypo- and hyperfunction of the NMDAR in male mice. This suggests that NMDAR and D-serine are involved in the retinal field potentials of the outer retina that interact with the animal's sex. This implicates the involvement of gonadal hormones and D-serine in retinal functional integrity.

Introduction

The N-Methyl-D-Aspartate (NMDAR) receptor is an ionotropic glutamate receptor essential for synaptic plasticity and learning and memory in the brain (Malenka & Bear, 2004). One of the unique characteristics of this receptor is that it requires another ligand other than glutamate to activate the channel (Kleckner & Dingledine, 1988; Paoletti, 2011), which makes glycine and D-serine, the two co-agonists, indispensable for NMDAR functioning. In the retina, NMDARs are known to contribute to the light-evoked response of retinal ganglion cells (RGCs) (Cohen and Miller, 1994; Massey and Miller, 1990), mediate GABAergic feedback (Ferreira et al., 1994) and excitotoxicity (Vorwerk et al., 2000). Unfortunately, most of the knowledge about NMDAR functionality in the retina is focused on the retinal ganglion cell layer, even though functional NMDARs have been found in horizontal cells (O'Dell and Christensen, 1989), and NMDAR subunits have been localized in photoreceptors and cells in the inner nuclear layer (Brandstätter et al., 1994). Therefore, it is unclear if the NMDAR plays a role in early retinal processing.

The role of D-serine as an NMDAR co-agonist has illuminated our understanding of NMDAR function in the retina (Hashimoto et al., 1992a; Hashimoto et al., 1993; Kleckner and Dingledine, 1988; Mothet et al., 2000). D-serine serves as an endogenous co-agonist for the NMDAR in the retina, potentiating NMDAR currents in RGC several fold greater than glycine at the same concentration (Gustafson et al., 2007; Stevens et al., 2003). This increase of NMDAR currents by the addition of D-serine suggested that NMDARs are not saturated, and that release of D-serine would result recruitment of NMDAR (Gustafson et al., 2007; Stevens et al., 2003). However, it is as yet unclear how dynamic recruitment of NMDAR through D-serine is initiated by light, and how this

recruitment affects upstream retinal function. Studies of D-serine in the retina have been limited to its effects on RGC currents and not on retinal field potentials as a whole. Given that functional NMDARs are located earlier in the vision pathway, D-serine acting on NMDAR may affect electric potentials in the outer retina. One such electric potential is reflected in the flash-electroretinogram (fERG), a light-evoked potential from the retina in response to a flash of light (Frishman & Wang, 2010). The fERG assesses the integrity of the retina, shedding a light on the vertical signal processing. The first low-frequency component is known as the a-wave, which represents activity from photoreceptors; the second low-frequency component is known as the b-wave, which reflects activity from on-bipolar cells (Frishman & Wang, 2010; Frishman and Wang, 2011). These components represent retinal field potentials that can be used to investigate the role of NMDAR and D-serine in the outer retina. The electroretinogram offers a quantitative, non-invasive method to examine neural activity under hypo- and hyper-functionality of the NMDAR in the outer retina.

Methods

Animals

Serine racemase knock out ($SR^{-/-}$) mice were obtained from Dr. Joseph Coyle (Balu & Coyle, 2015) and the colony was maintained by Resource Animal Resources at the University of Minnesota. Littermate controls and $SR^{-/-}$ mice were used at ages 8-16 weeks and included both males and females. A total of 34 mice were used for all experiments, seventeen for each genotype. All procedures were in accordance with the standards provided by the National Institutes of Health for use of animals in research and the animal care and use standards set by the Association for Research in Vision

and Ophthalmology and approved by the Institutional Animal Care and Use Committee at the University of Minnesota.

Experimental design and D-serine delivery

In vivo fERGs were conducted in all mice pre- and post-topical delivery of D-serine at a concentration of 5 mM diluted in 0.05% carboxymethylcellulose Refresh Plus Lubricant Eye Drops (Allergan, Inc., Irvine, CA). One day prior to recording, normal Refresh Plus eye drops (0.05%) were topically delivered. On the day of recording, either normal eye drops were administered or eye drops containing 5mM D-serine were used.

Stimulation and recording

Pupils were dilated with tropicamide (1%) eye drops (Akorn, Inc., Lake Forest, IL), followed by proparacaine hydrochloride eye drops (0.5%) (Akorn, Inc.). Mice were anesthetized for the fERG recordings with 4% isoflurane, an anesthetic known to leave the fERG recordings unchanged (Anis et al., 1983). A contact lens with a coiled wire electrode was placed on the cornea, and methylcellulose eyedrops (1.0%) (Allergan) were used to hold the contact in place and protect the cornea from drying out. The stimulus duration was 4 msec, and retinas were adapted to a steady white background luminance of 0.35 $cd \cdot s/m^2$ for 15 minutes prior to recording. A D215 Espion E^2 Console (Diagnosys LLC, Lowell, MA) was used for data collection under a bandpass filter of 0.3-300 Hz. At each light intensity, four traces were collected, which were averaged to determine the representative response at each light intensity for each mouse tested.

After data collection, a customized MATLAB program was used to remove oscillatory potentials from the a- and b-wave recordings. Once filtered, the a-wave amplitude was measured from the pre-flash baseline to the peak of the a-wave, the b-

wave amplitude was measured from the peak of the a-wave (trough) to the largest peak of the b-wave, and implicit times of the a-waves and b-waves were measured from flash onset to the peak of the response.

Statistical analysis

A three-way (2x2x2) mixed Analysis of Variance (ANOVA), with two between-subject (Genotype and Sex) and one within-subject factor (Treatment), was conducted at each flash strength to evaluate the interaction between treatment, genotype, and sex. We tested all possible simple two-way interactions that were adjusted with Bonferroni correction at statistical significance set at $p<0.025$. If simple two-way interactions were significant, simple main effects were analyzed. The dependent variables tested were a-wave amplitude and implicit time and b-wave amplitude and implicit time. All analyses were conducted for each light intensity. An IBM SPSS Statistics 26 program was used to conduct all statistical analyses.

Results

Effect of D-serine on the a-wave amplitude

When the a-wave amplitude data from the pre- and post-treatment were analyzed, only the a-wave amplitude from the male WT mice was significantly different from the other cohorts and only at the brightest flash strength. Statistical significance was based on demonstration of a three-way interaction between treatment, genotype, and sex using ANOVA (Table 1). Analysis of simple two-way interactions revealed that at the brightest flash strength, there was an interaction between sex and genotype (Table 1, Figure 1A). Surprisingly, this significant difference for the male WT at the

brightest flash strength disappeared with the application of exogenous D-serine (Table 1, Figure 1B). Simple main effects analyses examining the four distinct groups did not show statistically significant differences in the a-wave amplitude with exogenous application of D-serine (Table 2). However, the a-wave amplitude of male WT mice showed trends to a reduction in a-wave amplitude with increasing flash strength (Table 2). Also noteworthy is that the a-wave amplitudes of male WT and $SR^{-/-}$ mice became even more similar after D-serine treatment. Female $SR^{-/-}$ mice showed no significant changes at any flash strength. These results suggest that the a-wave amplitude in all groups was unaffected by exogenous addition of D-serine but rather tended to result in the WT and $SR^{-/-}$ responses being more similar to other than pre-treatment.

Table 3.1		a-wave amplitude	
		Treatment · Sex · Genotype	
Three-way interaction at each level of flash strength	**0.18**	F(1,30)=0.66 *p* =0.424	
	0.35	F(1,30)=0.17, *p* =0.683	
	0.7	F(1,30)=2.2, *p* =0.144	
	1.4	F(1,30)=3.0, *p* =0.095	
	2.8	F(1,30)=2.4, *p* =0.133	
	5.6	F(1,30)=2.4, *p* =0.136	
	11.2	F(1,30)=6.7, ***p* =0.015**	
		Treatment · Genotype	**Treatment · Sex**
Simple two-way interactions at each level of flash strength	**0.18**	F(1,30)=0.048, *p* =N.S.	F(1,30)=0.069, *p* = N.S.
	0.35	F(1,30)=0.576, *p* = N.S.	F(1,30)=0.0, *p* = N.S
	0.7	F(1,30)=0.643, *p* = N.S.	F(1,30)=3.4, *p* = N.S
	1.4	F(1,30)=0.602, *p* = N.S.	F(1,30)=2.3, *p* = N.S
	2.8	F(1,30)=1.7, *p* = N.S.	F(1,30)=2.0, *p* = N.S
	5.6	F(1,30)=1.8, *p*= N.S.	F(1,30)=0.7, *p* = N.S
	11.2	F(1,30)=9.4, *p* = N.S.	F(1,30)=0.296, *p*= N.S
		pre-Dser (Genotype · Sex)	**post-Dser (Genotype · Sex)**
	0.18	F(1,30)=5.43, *p* =0.027	F(1,30)=1.04, *p* = N.S.
	0.35	F(1,30)=0.55, *p* = N.S.	F(1,30)=0.05, *p* = N.S.
	0.7	F(1,30)=5.26, *p* =0.029	F(1,30)=0.08, *p* = N.S.
	1.4	F(1,30)=4.51, *p* =0.042	F(1,30)=0.02, *p* = N.S.
	2.8	F(1,30)=3.44, *p* = 0.073	F(1,30)=0.04, *p* = N.S.
	5.6	F(1,30)=4.10, *p* =0.052	F(1,30)=0.09, *p* = N.S.
	11.2	F(1,30)=12.88, ***p* = 0.001**	F(1,30)=0.32, *p* = N.S.

Table 3.1: Statistical analysis of the a-wave amplitude*. The top section shows the results of a three-way analysis for genotype, sex, and treatment. The bottom panel shows the results of an analysis of two-way interactions between treatment and genotype, treatment and sex, and pre- and post-treatment genotype and sex interactions. Red indicates statistical significance.*

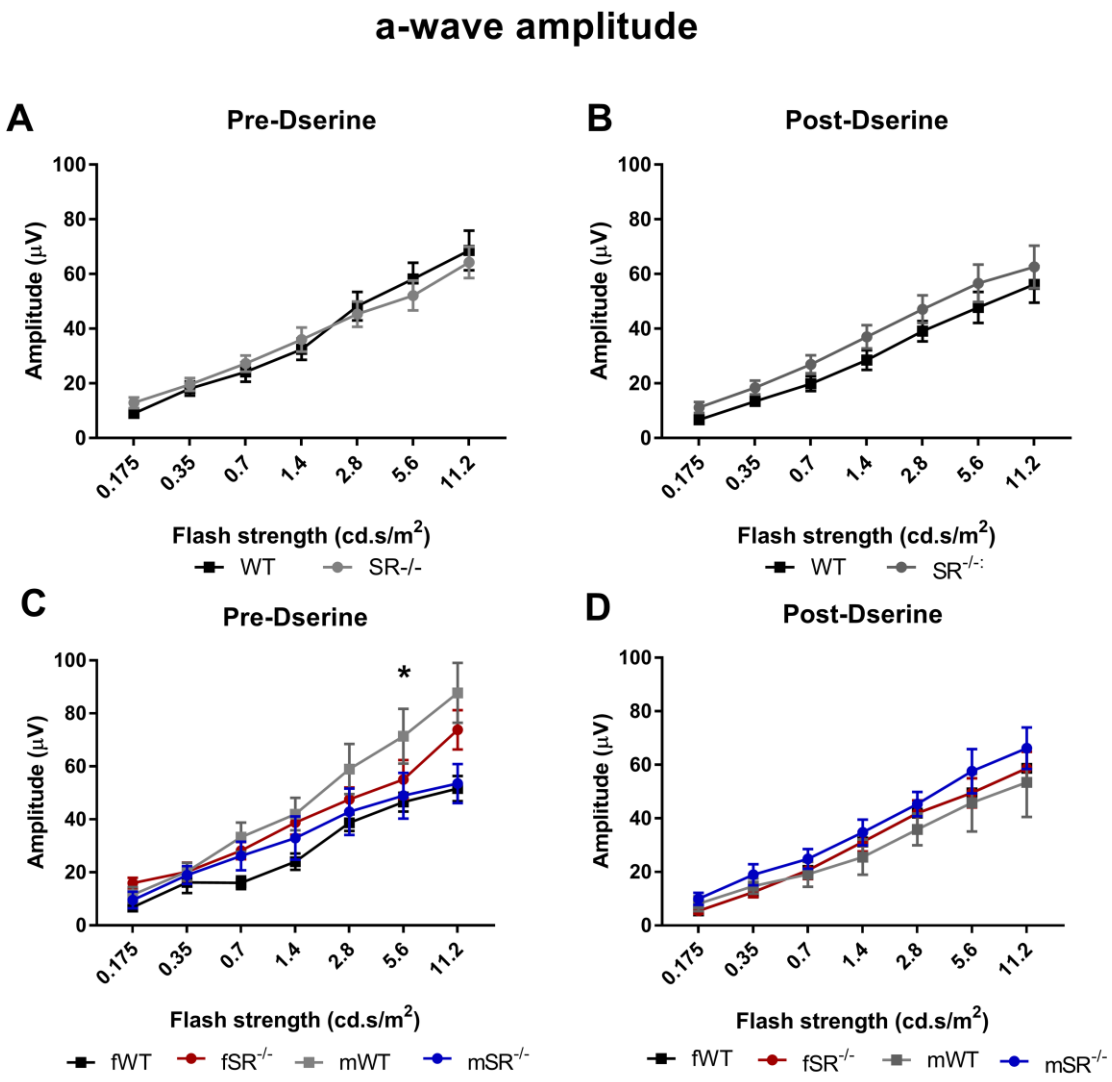

Figure 3.1. Effects of D-serine of the-wave amplitude: *(A) The a-wave amplitudes prior to treatment of all cohorts: female wild type (fWT), female serine racemase knockout (fSR$^{-/-}$), male wild type (mWT), and male serine racemase knockout (mSR$^{-/-}$). (B) The a-wave amplitudes after D-serine treatment for all cohorts. Data are expressed as mean +/- SEM. Asterisks indicate statistical significance.*

Table 3.2	Male a-wave amplitude							
	WT				$SR^{-/-}$			
Flash strength ($cd \cdot s/m^2$)	Pre-Dserine	Post-Dserine	Mean Difference	p	Pre-Dserine	Post-Dserine	Mean Difference	p
0.175	20 ± 3.7	8.1 ± 2.5	-3.4	N.S.	10 ± 2.4	9.9 ± 2.5	0.4	N.S.
0.35	49 ± 6.4	15 ± 3.2	-5.6	N.S.	19 ± 3.7	19 ± 3.2	0.0	N.S.
0.7	33 ± 4.3	19 ± 4.5	-14.2	N.S.	26 ± 4.3	25 ± 4.5	-1.3	N.S.
1.4	42 ± 5.8	26 ± 5.8	-16.5	N.S.	33 ± 5.8	35 ± 5.8	1.8	N.S.
2.8	59 ± 6.9	36 ± 6.6	-23.1	N.S.	43 ± 6.9	45 ± 6.6	2.5	N.S.
5.6	71 ± 7.9	46 ± 9.3	-25.5	N.S.	49 ± 7.9	57 ± 9.4	8.7	N.S.
11.2	**88 ± 8.1**	**53 ± 10.8**	-34.3	N.S.	54 ± 8.1	66 ± 10.2	12.7	N.S.
	Female a-wave amplitude							
	WT				$SR^{-/-}$			
0.175	7 ± 2.3	5.5 ± 2.4	0.6	N.S.	16 ± 2.3	12 ± 2.4	-3.6	N.S.
0.35	16 ± 3.5	12 ± 3.0	-0.3	N.S.	20 ± 3.5	18 ± 3.0	-2.1	N.S.
0.7	16 ± 4.1	21 ± 4.3	0.3	N.S.	28 ± 4.1	29 ± 4.3	0.6	N.S.
1.4	24 ± 5.4	31 ± 5.5	0.3	N.S.	39 ± 5.4	39 ± 5.3	6.0	N.S.
2.8	39 ± 6.5	42 ± 6.2	-0.3	N.S.	48 ± 6.5	49 ± 6.2	1.2	N.S.
5.6	47 ± 7.4	50 ± 8.9	0.0	N.S.	55 ± 7.4	56 ± 8.9	0.7	N.S.
11.2	52 ± 7.6	59 ± 10.2	-0.1	N.S.	74 ± 7.6	59 ± 10.2	-14.3	N.S.

Table 3.2: Analysis of a-wave amplitude pre- and post-D-serine for each cohort. *No significant differences were seen between any of the parameters analyzed.*

Effect of D-serine on the a-wave implicit time

In the $SR^{-/-}$ mice, there was a statistically significant delay in the a-wave implicit time compared to WT mice at all but the brightest flash strengths, based on the three-way interaction in the ANOVA (Table 3, Figure 2A). Four of those flash strengths had a statistically significant two-way interaction between treatment and genotype (Table 3; Figure 2 A, B). Pre-D-serine delivery, there was a delay in the a-wave implicit time in the male $SR^{-/-}$ mice compared to the other genotypes (Figure 2C). Post-D-serine application, there was no difference in the implicit time of the a-wave in $SR^{-/-}$ mice in comparison to WT mice (Table 3, Figure 2D). Separating the animals into four distinct groups, as revealed by the simple main effect analyses, demonstrates that the delay in a-wave implicit time observed when both male and female $SR^{-/-}$ were combined, prior to topical

delivery of D-serine, was driven by the male $SR^{-/-}$ (Table 3, Figure 3E). At the middle flash strengths, only male $SR^{-/-}$ had a statistically significant reduction in the a-wave implicit time when D-serine was added exogenously. These results suggest that adding D-serine eliminated the temporal delay in the a-wave implicit time in male $SR^{-/-}$ that was observed in the pre-D-serine condition (Table 4). In contrast, while not statistically significant, male WT mice trended to have a delay in the a-wave implicit time with exogenous D-serine treatment (Figure 3B). Female WT (Figure 3C) and female $SR^{-/-}$ (Figure 3F) had no temporal changes in the a-wave implicit time when exogenous D-serine was administered (Table 4). These results imply that changes in exogenous D-serine can affect the temporal dynamics of the a-wave in male WT mice, accelerating it in male $SR^{-/-}$ and delaying, though not significantly, in male WT. In summary, exogenous application of D-serine eliminates the genotype and sex differences observed in the normal pre-treatment retina, making the a-wave implicit time of all four groups essentially the same.

Table 3.3		a-wave implicit time	
Treatment · Sex · Genotype			
Three-way interaction at each level of flash strength	**0.18**	F(1,30)=6.75, ***p* = 0.014**	
	0.35	F(1,30)=6.28, ***p* =0.018**	
	0.7	F(1,30)=5.93, ***p* = 0.021**	
	1.4	F(1,30)=6.39, ***p* = 0.017**	
	2.8	F(1,30)=8.38, ***p* = 0.007**	
	5.6	F(1,30)=0.294, *p* = N.S.	
	11.2	F(1,30)=0.940, *p* = N.S.	
	Treatment · Genotype		**Treatment · Sex**
Simple two-way interactions at each level of flash strength	**0.18**	F(1,30)=1.39, *p* = N.S.	F(1,30)=0.36, *p* = N.S.
	0.35	F(1,30)=6.56, ***p* = 0.016**	F(1,30)=0.74, *p* = N.S.
	0.7	F(1,30)=9.62, ***p* = 0.004**	F(1,30)=0.65, *p* = N.S.
	1.4	F(1,30)=7.63, ***p* = 0.010**	F(1,30)=0.83, *p* = N.S.
	2.8	F(1,30)=7.86, ***p* = 0.009**	F(1,30)=0.35, *p* = N.S.
	5.6	F(1,30)=0.489, *p* =N.S.	F(1,30)=2.04, *p* = N.S.
	11.2	F(1,30)=0.074, *p* =N.S.	F(1,30)=2.07, *p* = N.S.
	pre-Dser (Genotype · Sex)		**post-Dser (Genotype · Sex)**
	0.18	F(1,30)=5.28, *p* =0.029	F(1,30)=0.3, p= N.S.
	0.35	F(1,30)=6.2, ***p* =0.018**	F(1,30)=0.7, p= N.S.
	0.7	F(1,30)=3.70, *p* = N.S.	F(1,30)=1.1, p= N.S.
	1.4	F(1,30)=9.60, ***p* =0.004**	F(1,30)=0.4, p= N.S.
	2.8	F(1,30)=9.86, ***p* =0.004**	F(1,30)=0.9, p= N.S.
	5.6	F(1,30)=6.57, ***p* =0.016**	F(1,30)=0.7, p= N.S.
	11.2	F(1,30)=4.4, *p* =0.042	F(1,30)=0.6, p= N.S.

***Table 3.3: Statistical analysis of a-wave implicit time**. There was a significant difference in a-wave implicit times between the $SR^{-/-}$ mouse and WT control mice, with the $SR^{-/-}$ showing a significant delay in the a-wave component. When analyzed for two-way interactions, there was a significant difference in a-wave implicit time for the majority of flash strengths, with the male $SR^{-/-}$ mice showing a significantly delayed implicit time compared to all other genotypes and between males and females. This difference was reduced by the D-serine treatment, causing a less delayed a-wave. Asterisks indicate significant difference.*

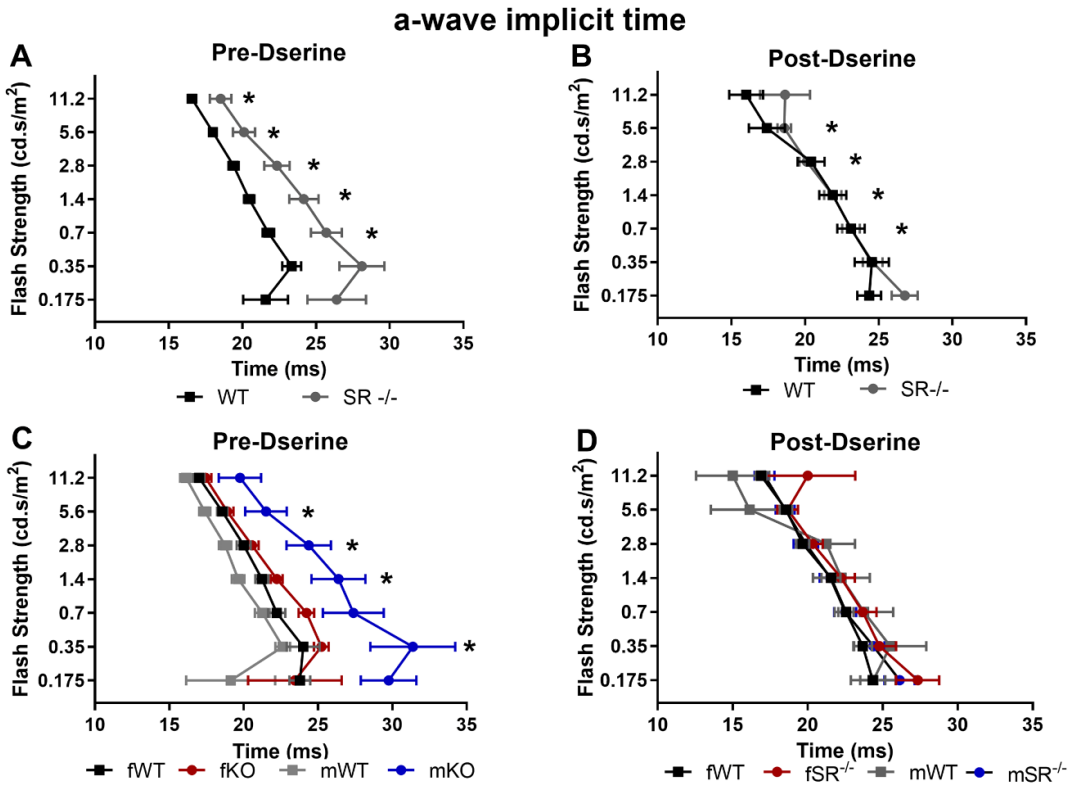

Figure 3.2. Effects of D-serine on the a-wave implicit time:
Comparison of the a-wave implicit time in WT and SR$^{-/-}$ mice before (A) and after (B) topical delivery of D-serine onto the cornea. There was a significant difference between the SR$^{-/-}$ mice and WT mice prior to D-serine treatment and a significant difference in the altered implicit time between the two genotypes. Significance in both A and B represents the interaction between treatment and genotype. Comparison between all groups, female wild type (fWT), female serine racemase knockout (fSR$^{-/-}$), male wild type (mWT), and male serine racemase knockout (mSR$^{-/-}$) before (C) or after (D) topical delivery of D-serine. Significance represents interaction between genotype and sex before D -serine (C) and after D-serine. Data are expressed as mean +/- SEM. Asterisks represent significant difference.

Table 3.4	Male a-wave implicit time							
	WT				$SR^{-/-}$			
Flash strength ($cd \cdot s/m^2$)	Pre-Dserine	Post-Dserine	Mean Difference	p	Pre-Dserine	Post-Dserine	Mean Difference	p
0.175	19 ± 2.5	24 ± 1.3	5.3	N.S.	30 ± 2.5	26 ± 1.3	-3.6	N.S.
0.35	23 ± 1.5	26 ± 1.4	2.3	N.S.	31 ± 1.5	25 ± 1.4	-7.0	0.036
0.7	21 ± 1.1	24 ± 1.2	2.5	N.S.	27 ± 1.1	23 ± 1.2	-4.9	**0.011**
1.4	20 ± 1.0	22 ± 1.2	2.6	N.S.	26 ± 1.0	22 ± 1.2	-4.9	**0.023**
2.8	19 ± 0.8	21 ± 1.1	2.5	N.S.	24 ± 0.8	20 ± 1.1	-4.5	**0.013**
5.6	17 ± 0.8	16 ± 1.4	1.3	N.S.	22 ± 0.8	19 ± 1.4	-3.0	N.S.
11.2	16 ± 0.8	15 ± 2.4	1.1	N.S.	20 ± 0.8	17 ± 2.1	-2.6	N.S.
	Female a-wave implicit time							
	WT				$SR^{-/-}$			
0.175	24 ± 2.3	24 ± 1.2	0.6	N.S.	23 ± 2.3	27 ± 1.2	3.9	N.S.
0.35	24 ± 1.5	24 ± 1.3	-0.3	N.S.	25 ± 1.5	25 ± 1.3	-0.4	N.S.
0.7	22 ± 1.0	23 ± 1.1	0.3	N.S.	24 ± 1.0	24 ± 1.1	-0.6	N.S.
1.4	21 ± 1.0	22 ± 1.1	0.3	N.S.	22 ± 1.0	22 ± 1.1	0.0	N.S.
2.8	20 ± 0.8	20 ± 1.0	-0.3	N.S.	21 ± 0.8	20 ± 1.0	-0.2	N.S.
5.6	19 ± 0.7	19 ± 1.3	0.0	N.S.	19 ± 0.7	19 ± 1.3	-0.2	N.S.
11.2	17 ± 0.7	17 ± 2.0	-1.1	N.S.	17 ± 0.7	20 ± 2.0	-2.6	N.S.

Table 3.4 Effect of D-serine on the a-wave implicit time for each cohort. *Analysis of a-wave implicit time shows significant differences based on D-serine treatment in the male SR-/- mice, but only at the middle range of flash strengths. No significant differences were seen as a result of treatment in either the male or female WT mice. Similarly, there were no significant differences in a-wave implicit time in the female SR-/- mice at any of the flash strengths.*

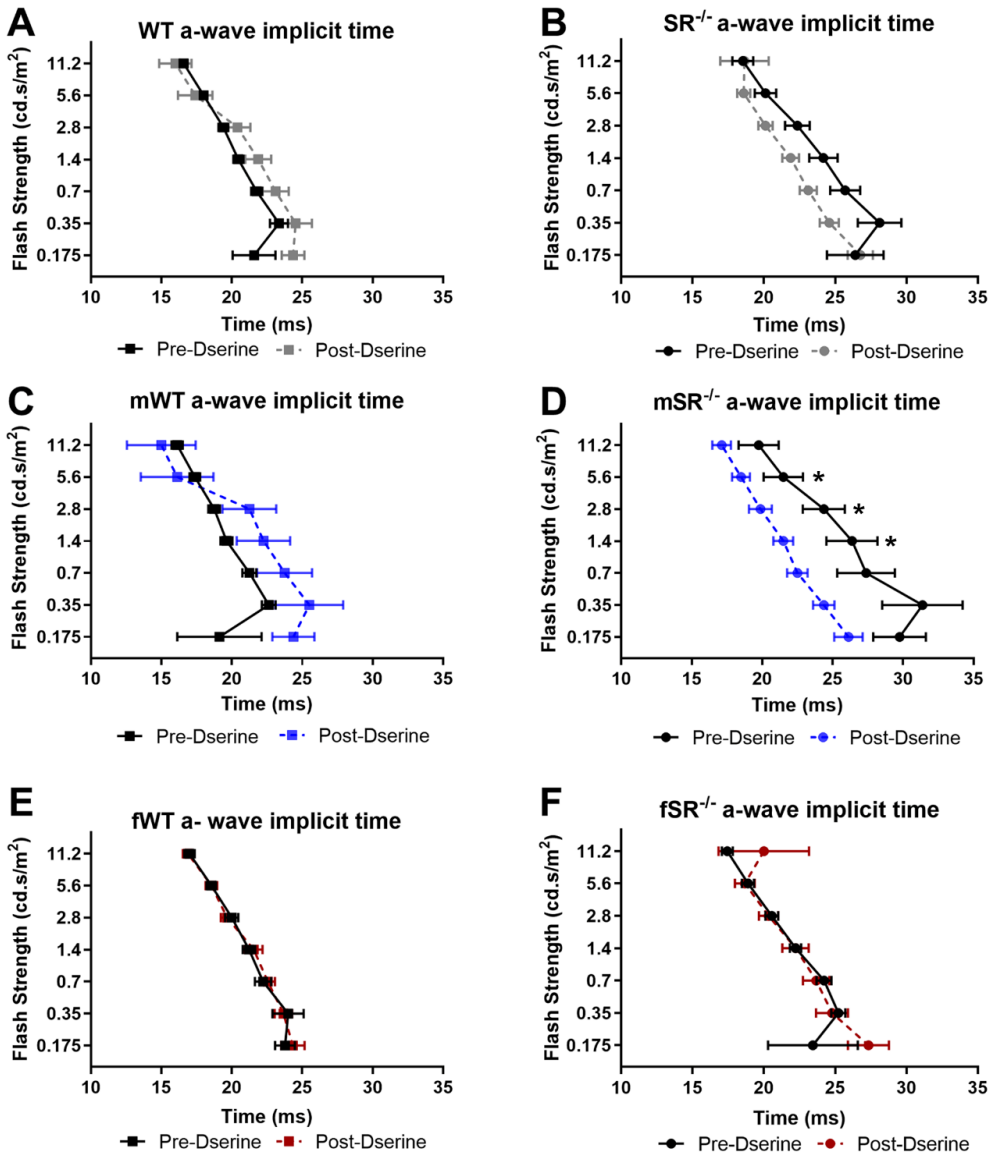

Figure 3.3. Effects of D-serine on a-wave implicit time: sex, genotype, and treatment. *The a-wave implicit time was not significantly different pre- and post-D-serine treatment. However, there was a significant delay in the a-wave implicit time in the male WT ERGs compared to the SR$^{-/-}$ controls. No differences were seen between female mice regardless of genotype or treatment. Asterisks indicate significant differences. Female wild type (fWT), female serine racemase knockout (fSR$^{-/-}$), male wild type (mWT), and male serine racemase knockout (mSR$^{-/-}$). Data are expressed as mean +/- SEM.*

Effect of D-serine on the b-wave amplitude

Unlike the a-wave amplitude, there was a highly significant difference between the b-wave amplitude between WT and $SR^{-/-}$ mice based on an ANOVA for three-way interaction between treatment, sex, and genotype at all flash strengths (Table 5, Figure 4A), as well as two-way interactions between treatment and genotype. In addition, at all flash strengths, there was a statistically significant decrease in b-wave amplitude in the untreated male $SR^{-/-}$ mice (Table 5, Figure 4C) based on the analysis of two-way interactions between genotype and sex (Table 5, Figure 4C). Interestingly, with exogenous application of D-serine, the differences in the b-wave amplitude that depended on the animal's genotype and sex disappeared, resulting in a b-wave amplitude that was similar between all cohorts (Table 5, Figure 4D). This result suggests that exogenous D-serine eliminated the difference in the b-wave amplitude that depended on the animal's genotype and sex. Our simple main effect analysis, which separates the animals into four distinct groups, revealed that exogenous D-serine significantly reduced the b-wave amplitude of male WT compared to the male $SR^{-/-}$ (Table 6, Figure 5C, D). In male WT, exogenous D-serine decreased the b-wave amplitude; this decrease was statistically significant at four dimmest flash strengths (Table 6, Figure 5C). In male $SR^{-/-}$ mice, exogenous D-serine increased the b-wave amplitude; this increase was statistically significant at 3 of the brighter flash strengths (Table 6, Figure 5D). There were no statistically significant differences in the b-wave amplitude in either female WT or female $SR^{-/-}$ with exogenous application of D-serine (Table 6, Figure 5 E, F). These results demonstrate that the exogenous addition of D-serine affected the b-wave amplitude of only male mice, and the effect was opposite

depending on the genotype of the male mice. In male WT, exogenous D-serine reduced the amplitude of the b-wave; while, in male $SR^{-/-}$ exogenous D-serine increased the amplitude of the b-wave. This effect was more prominent at some flash strengths than at others.

Table 3.5		b-wave amplitude	
		Treatment · Sex · Genotype	
Three-way interaction at each level of flash strength	**0.18**	F(1,30)=9.31, ***p* =0.005**	
	0.35	F(1,30)=4.55, ***p* =0.041**	
	0.7	F(1,30)=11.05, ***p* =0.002**	
	1.4	F(1,30)=11.05, ***p* =0.002**	
	2.8	F(1,30)=4.77, ***p* =0.037**	
	5.6	F(1,30)=10.88, ***p* =0.003**	
	11.2	F(1,30)=4.93, ***p* =0.034**	
		Treatment · Genotype	**Treatment · Sex**
Simple two-way interactions at each level of flash strength	**0.18**	F(1,30)=9.73, ***p* =0.004**	F(1,30)=0.41, *p* = N.S.
	0.35	F(1,30)=10.26, ***p* =0.003**	F(1,30)=0.74, *p* = N.S.
	0.7	F(1,30)=13.08, ***p* =0.001**	F(1,30)=0.22, *p* = N.S.
	1.4	F(1,30)=22.64, ***p*< 0.0005**	F(1,30)=0.05, *p* = N.S.
	2.8	F(1,30)=9.07, ***p* =0.005**	F(1,30)=0.71, *p* = N.S.
	5.6	F(1,30)=16.74, ***p*< 0.0005**	F(1,30)=0.02, *p* = N.S.
	11.2	F(1,30)=14.53, ***p* =0.001**	F(1,30)=0.14, *p* = N.S.
		pre-Dser (Genotype · Sex)	**post-Dser (Genotype · Sex)**
	0.18	F(1,30)=11.8, ***p* =0.002**	F(1,30)=1.1 *p* = N.S.
	0.35	F(1,30)=7.4, ***p* =0.011**	F(1,30)=0.26, *p* = N.S.
	0.7	F(1,30)=8.3, ***p* =0.007**	F(1,30)=2.1, *p* = N.S.
	1.4	F(1,30)=6.7, ***p* =0.015**	F(1,30)=0.20, *p* = N.S.
	2.8	F(1,30)=4.8, *p* = 0.036	F(1,30)=0.46, *p* = N.S.
	5.6	F(1,30)=8.1, ***p* =0.008**	F(1,30)=0.19, *p* = N.S.
	11.2	F(1,30)=1.8, *p* = N.S.	F(1,30)=1.2, *p* = N.S.

Table 3.5 Statistical analysis of the b-wave amplitude .*There was a statistically significant reduction in b-wave amplitude of the $SR^{-/-}$ mice compared to WT controls at all flash strengths. When examined for interactions of sex and genotype, there again was a significant difference between male WT and male $SR^{-/-}$ mice, with the male SR-/- mice showing a significant reduction in b-wave amplitude compared to the male WT controls. After D-serine treatment, there were no significant differences in b-wave amplitude between any of the cohorts. Asterisks indicate significant difference. Female wild type (fWT), female serine*

racemase knockout ($fSR^{-/-}$), male wild type (mWT), and male serine racemase knockout ($mSR^{-/-}$).

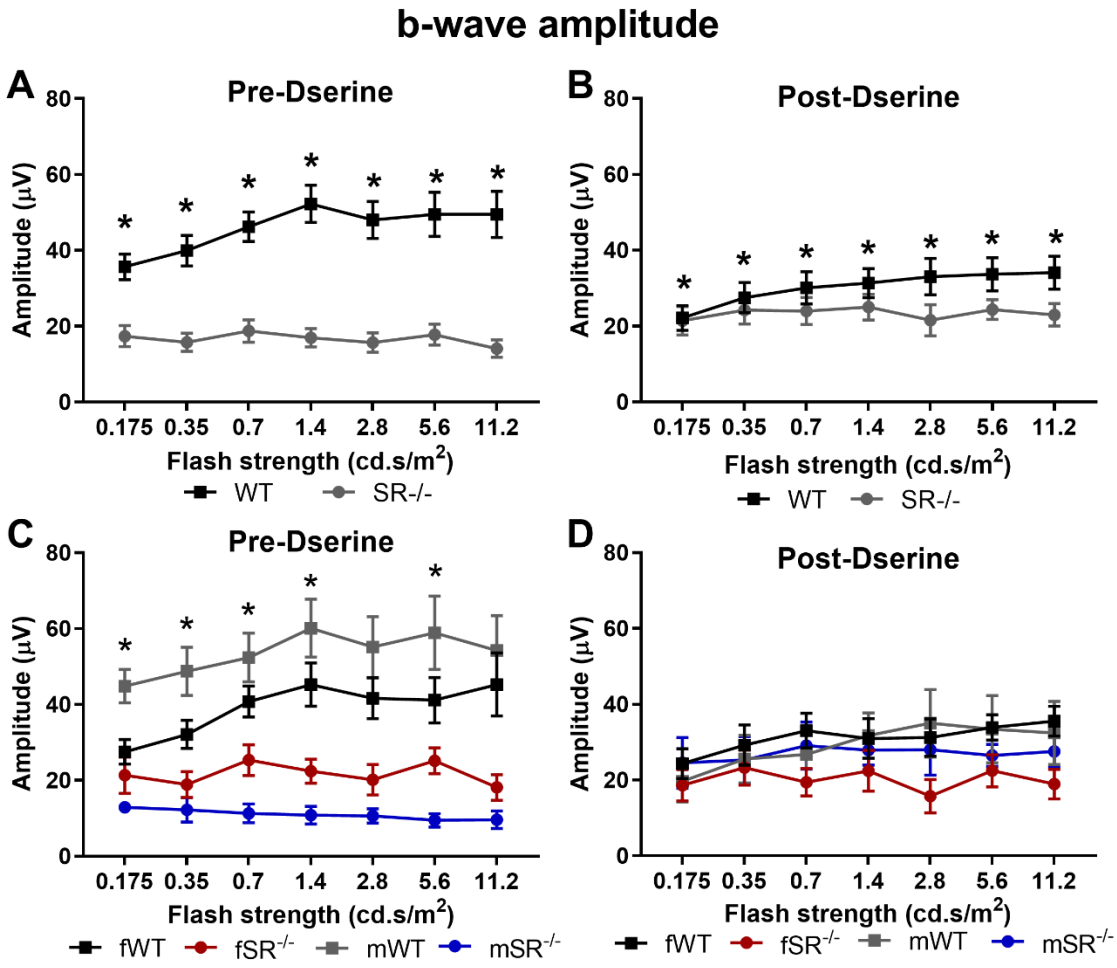

Figure 3.4 Effects of D-serine on b-wave amplitude: *Comparison of WT and $SR^{-/-}$ mice b-wave amplitude before (A) and after (B) topical delivery of D-serine. Significance in both A and B represent the interaction between treatment and genotype. Comparison between all groups, female WT (fWT), female $SR^{-/-}$ ($fSR^{-/-}$), male WT (mWT), and male $SR^{-/-}$ ($mSR^{-/-}$), before (C) or after (D) topical delivery of D-serine. Significance represents interaction between genotype and sex before D -serine (C) and after D-serine. Data are expressed as mean +/- SEM. Asterisks indicate statistical significance.*

Table 3.6	Male b-wave amplitude							
	WT				$SR^{-/-}$			
Flash intensity ($cd \cdot s/m^2$)	Pre-Dserine	Post-Dserine	Mean Difference	p	Pre-Dserine	Post-Dserine	Mean Difference	p
0.175	45 ± 4.4	20 ± 5.4	-25.4	**0.002**	13 ± 1.2	24 ± 5.4	11.6	0.152
0.35	49 ± 6.4	26 ± 6.3	-23.2	**0.008**	12 ± 3.2	25 ± 6.1	13.1	0.102
0.7	52 ± 6.4	27 ± 7.6	-25.6	**0.009**	11 ± 2.5	29 ± 6.2	17.8	0.302
1.4	60 ± 7.6	32 ± 6.0	-28.4	**0.003**	11 ± 2.3	28 ± 3.9	17.1	**0.021**
2.8	55 ± 8.0	35 ± 8.9	-20.1	0.085	11 ± 1.9	28 ± 6.8	17.5	0.043
5.6	59 ± 9.7	33 ± 8.9	-25.5	0.036	9 ± 1.8	27 ± 2.9	17.0	**0.004**
11.2	54 ± 9.2	32 ± 8.3	-21.8	0.035	10 ± 2.3	28 ± 4.1	17.9	**0.020**
	Female b-wave amplitude							
	WT				$SR^{-/-}$			
0.175	28 ± 3.2	24 ± 3.9	-3.2	0.564	21 ± 4.8	19 ± 4.2	-2.8	0.661
0.35	32 ± 3.7	29 ± 5.2	-2.9	0.664	19 ± 3.4	23 ± 4.6	4.4	0.508
0.7	41 ± 4.1	33 ± 4.6	-7.7	0.134	25 ± 4.0	19 ± 3.6	-8.9	0.377
1.4	45 ± 5.7	31 ± 5.3	-14.3	0.031	22 ± 3.2	22 ± 5.3	0.1	0.994
2.8	42 ± 5.4	31 ± 4.9	-10.4	0.037	20 ± 4.0	16 ± 4.4	-4.3	0.546
5.6	41 ± 6.0	34 ± 3.3	-7.3	0.079	25 ± 3.4	22 ± 4.2	-2.7	0.513
11.2	45 ± 8.3	36 ± 3.9	-9.7	0.195	18 ± 3.3	19 ± 3.9	0.8	0.876

Table 3.6 Effect of D-serine on b-wave amplitude for each group. *Analysis of the b-wave amplitude for male and female mice. Only the male mice showed significant changes in b-wave amplitude, both pre-D-serine treatment and post-D-serine treatment. Red indicates significance.*

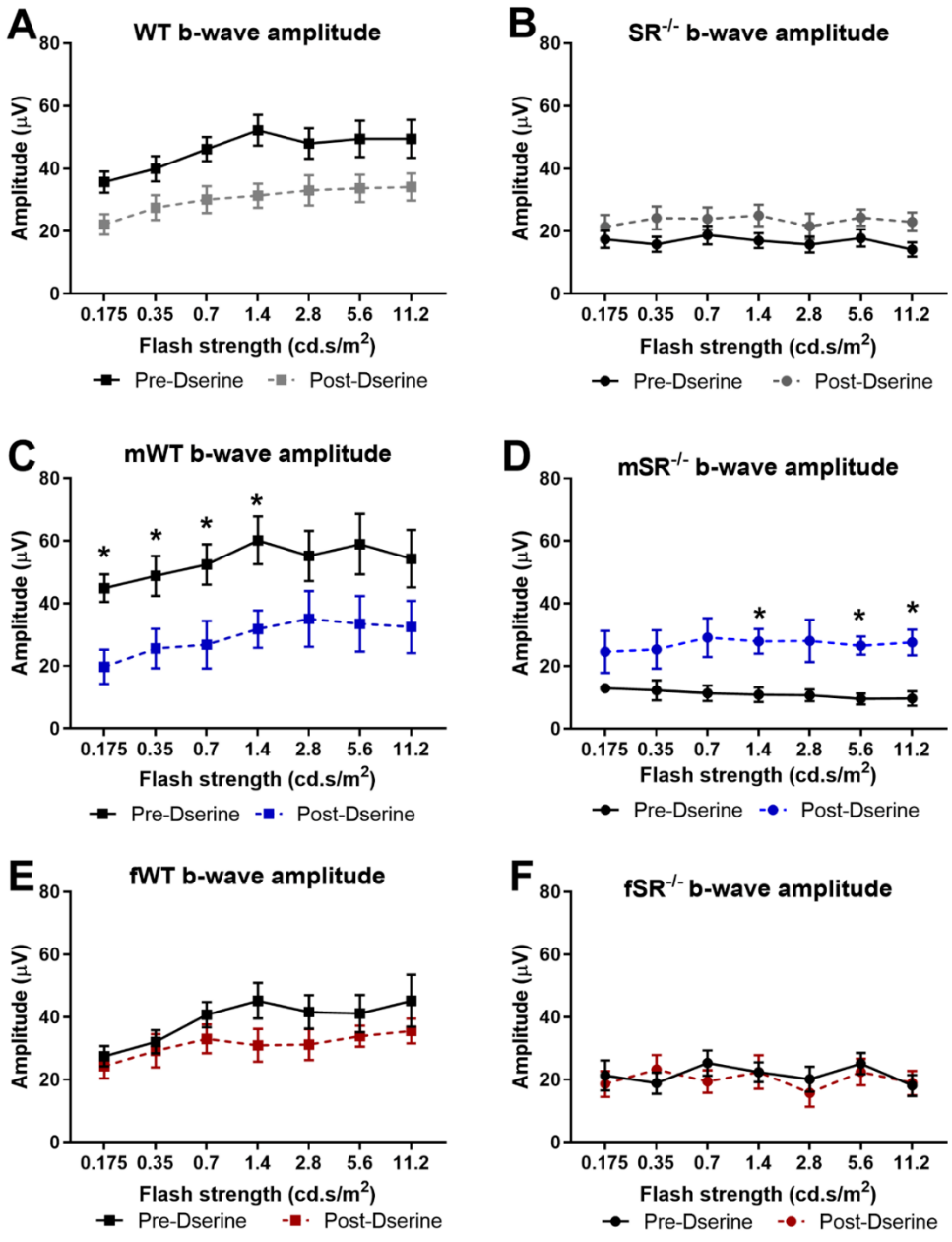

Figure 3.5 Effects of D-serine on the b-wave amplitude: sex, genotype, treatment. *In the male WT prior to treatment, the b-wave amplitude was significantly decreased compared to the WT controls, but only at the 4 lowest flash strengths. In the male SR$^{-/-}$ mice, D-serine treatment resulted in a significant increase in b-wave amplitude. No significant differences were seen in the female mice for either genotype or treatment. Data are expressed as mean +/- SEM. Asterisks indicate statistical significance.*

Effect of D-serine on the b-wave implicit time

The b-wave implicit time was significantly delayed in the $SR^{-/-}$ mice before treatment based on the ANOVA showing a significant three-way interaction at all flash strengths (Table 7, Figure 6A). At all the flash strengths there was a statistically significant difference between b-wave implicit times before and after D-serine treatment, based on a simple two-way interactions between treatment and genotype (Table 7; Figure 6A, B). Exogenous D-serine reduced the temporal delay in the b-wave implicit time for the $SR^{-/-}$ mice (Table 7, Figure 6B).

At all flash strengths but one, there were significant differences in the b-wave implicit time based on genotype and sex interaction across all groups either before D-serine treatment (Table 7, Figure 6C) or after D-serine delivery. In fact, the differences between the b-wave implicit time for all groups became relatively the same post D-serine treatment (Figure 6D). Simple main effect analyses revealed that the b-wave implicit time of the $SR^{-/-}$ decreased after stimulus onset with the addition of exogenous D-serine (Table 8). However, this effect was only statistically significant in two flash strengths in male $SR^{-/-}$ and in one flash strength in female $SR^{-/-}$ (Table 8). B-wave implicit time was not statistically significantly different in any of the WT mice. This result suggests that the significant differences seen in the b-wave implicit times at all light intensities in the grouped data were not dependent on genotype and sex. It appears that D-serine may

only affect the temporal dynamics of the $SR^{-/-}$ mice at selected flash strengths (Figure 7).

Table 3.7		b-wave implicit time	
		Treatment · Sex · Genotype	
Three-way interaction at each level of flash strength	**0.18**	F(1,30)=9.31, ***p* =0.005**	
	0.35	F(1,30)=6.28, ***p* =0.018**	
	0.7	F(1,30)=11.05, ***p* =0.002**	
	1.4	F(1,30)=11.05, ***p* =0.002**	
	2.8	F(1,30)=4.77, ***p* =0.037**	
	5.6	F(1,30)=10.88, ***p* =0.003**	
	11.2	F(1,30)=4.93, ***p* =0.034**	
		Treatment · Genotype	**Treatment · Sex**
Simple two-way interactions at each level of flash strength	**0.18**	F(1,30)=9.73, ***p* =0.004**	F(1,30)=0.41, *p* = N.S.
	0.35	F(1,30)=10.26, ***p* =0.003**	F(1,30)=0.74, *p* = N.S.
	0.7	F(1,30)=13.08, ***p* =0.001**	F(1,30)=0.22, *p* = N.S.
	1.4	F(1,30)=22.64, ***p*< 0.0005**	F(1,30)=0.05, *p* = N.S.
	2.8	F(1,30)=9.07, ***p* =0.005**	F(1,30)=0.71, *p* = N.S.
	5.6	F(1,30)=16.74, ***p*< 0.0005**	F(1,30)=0.02, *p* = N.S.
	11.2	F(1,30)=14.53, ***p* =0.001**	F(1,30)=0.14, *p* = N.S.
		pre-Dser (Genotype · Sex)	**post-Dser (Genotype · Sex)**
	0.18	F(1,30)=2.5, *p* = N.S.	F(1,30)=0.1, p= N.S.
	0.35	F(1,30)=1.7, *p* = N.S.	F(1,30)=0.0, p= N.S.
	0.7	F(1,30)=3.8, *p* = N.S.	F(1,30)=0.6, p= N.S.
	1.4	F(1,30)=2.2, *p* = N.S.	F(1,30)=0.6, p= N.S.
	2.8	F(1,30)=5.2, ***p* = 0.03**	F(1,30)=0.2, p= N.S.
	5.6	F(1,30)=4.5, *p* = N.S.	F(1,30)=2.1, p= N.S.
	11.2	F(1,30)=3.8, *p* = N.S.	F(1,30)=0.3, p= N.S.

Table 3.7 Statistical analysis of b-wave implicit time. *An analysis for a three-way interaction for treatment, sex, and genotype showed that there was a significant difference between the groups. A two-way interaction analysis showed that for treatment and genotype, the male mice showed a significantly increased b-wave implicit time*

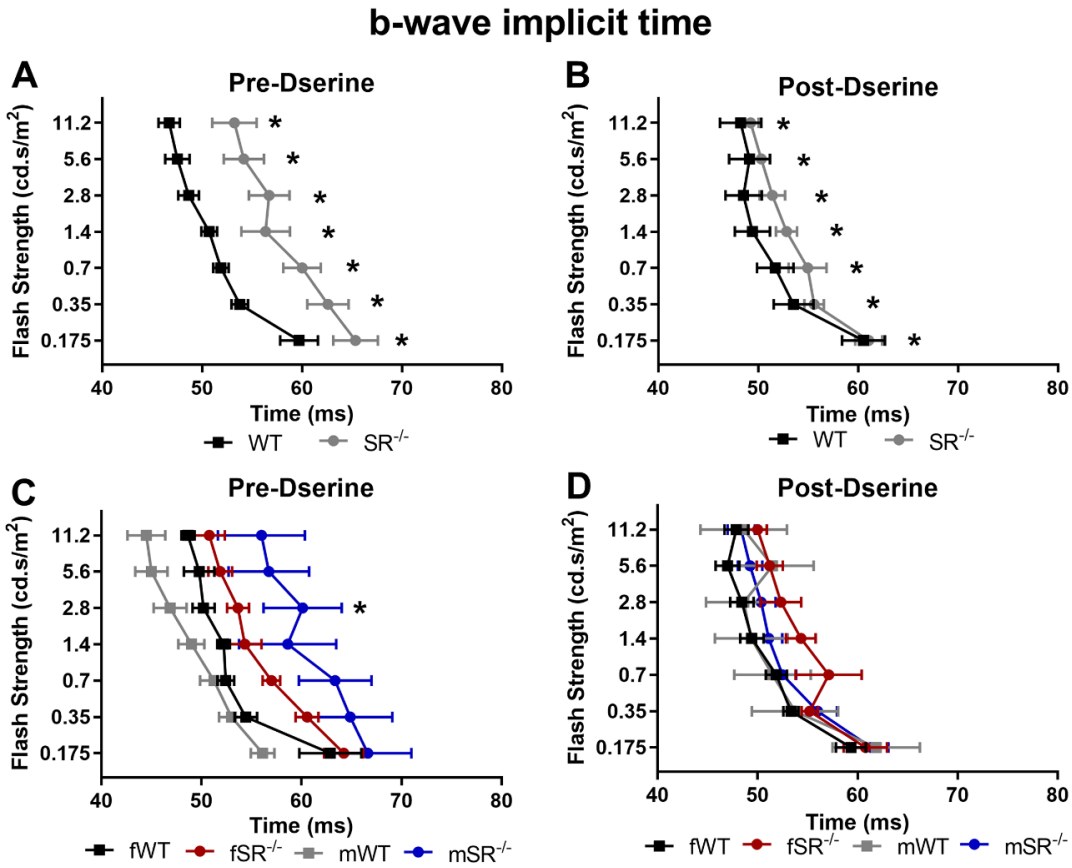

Figure 3.6 Effects of D-serine on b-wave implicit time: *Comparison of WT and SR$^{-/-}$ mice b-wave implicit time before (A) and after (B) topical delivery of D-serine. Significance in both A and B represent the interaction between treatment and genotype. Comparison between all groups, female WT (fWT), female SR$^{-/-}$ (fSR$^{-/-}$), male WT (mWT), and male SR$^{-/-}$ (mSR$^{-/-}$), before (C) or after (D) topical delivery of D-serine. Significance represents interaction between genotype and sex before D-serine (C) and after D-serine. Data are expressed as mean +/- SEM. Asterisks indicate statistical significance.*

Table 3.8	Male b-wave implicit time							
	WT				*SR -/-*			
Flash strength (cd·s/m²)	*Pre-Dserine*	*Post-Dserine*	*Mean Difference*	*p*	*Pre-Dserine*	*Post-Dserine*	*Mean Difference*	*p*
0.175	56 ± 3.0	62 ± 2.7	5.8	N.S.	67 ± 3.0	61 ± 2.7	-5.3	N.S.
0.35	53 ± 2.3	54 ± 2.4	0.8	N.S.	65 ± 2.3	56 ± 2.4	-8.9	N.S.
0.7	51 ± 2.0	52 ± 2.8	0.3	N.S.	63 ± 2.0	53 ± 2.8	-10.9	**0.018**
1.4	49 ± 2.6	49 ± 2.1	0.4	N.S.	59 ± 2.6	51 ± 2.1	-7.5	N.S.
2.8	47 ± 2.2	49 ± 2.3	1.8	N.S.	60 ± 2.2	50 ± 2.3	-9.8	**0.021**
5.6	45 ± 2.3	52 ± 2.3	6.5	N.S.	57 ± 2.3	49 ± 2.3	-7.5	N.S.
11.2	45 ± 2.5	49 ± 2.3	4.1	N.S.	56 ± 2.5	48 ± 2.3	-7.6	N.S.
	Female b-wave implicit time							
	WT				*SR -/-*			
0.175	63 ± 2.8	59 ± 2.5	-3.6	N.S.	64 ± 2.8	61 ± 2.5	-3.4	N.S.
0.35	54 ± 2.2	53 ± 2.2	-1.1	N.S.	61 ± 2.2	55 ± 2.2	-5.3	**0.005**
0.7	52 ± 1.9	52 ± 2.6	-0.6	N.S.	57 ± 1.9	57 ± 2.6	0.1	N.S.
1.4	52 ± 2.5	49 ± 2.0	-2.8	N.S.	54 ± 2.5	54 ± 2.0	0.0	N.S.
2.8	50 ± 2.1	48 ± 2.2	-1.8	N.S.	54 ± 2.1	52 ± 2.2	-1.3	N.S.
5.6	50 ± 2.2	47 ± 2.2	-2.8	N.S.	52 ± 2.2	51 ± 2.2	-0.7	N.S.
11.2	49 ± 2.3	48 ± 2.2	-0.8	N.S.	51 ± 2.3	50 ± 2.2	-0.8	N.S.

Table 3.6 Effect of D-serine on the b-wave implicit time for each group. *Relative to genotype and treatment, there were relatively few significant differences in the b-wave implicit time before or after D-serine, with only significant differences seen at two flash strengths based genotype in the male mice and one based on genotype in the female mice. Red indicates statistical significance.*

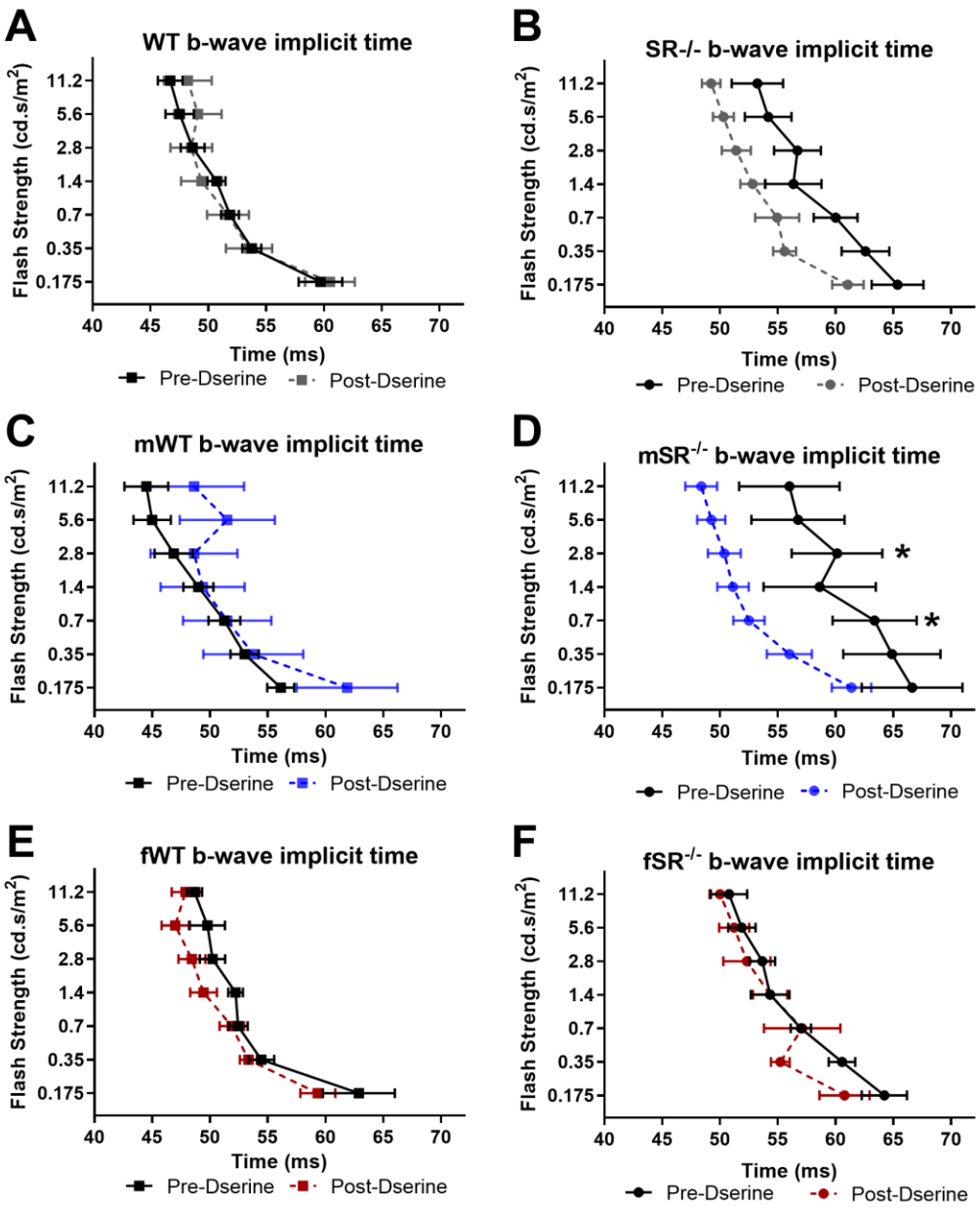

Figure 3.7 Effects of D-serine on b-wave implicit time: sex, genotype, and treatment. *Based on genotype or sex, very few significant differences were seen in the b-wave implicit times. There were several significant differences in the SR$^{-/-}$ mice, but overall there was a shift in the male SR$^{-/-}$ mice to a faster implicit time than in the absence of exogenously added D-serine.*

Discussion

Our work demonstrates that D-serine affects the amplitude and timing of the field potentials of the outer retina, reflected in the a- and b-wave. Furthermore, this work illuminates an interaction between hypo- or hyper-availability of D-serine and sex that has never been reported.

D-serine is the endogenous co-agonist for the glycine site of the NMDAR (Gustafson et al., 2007). D-serine has been demonstrated to potentiate NMDAR currents constantly upon exogenous delivery of D-serine (Stevens et al., 2003). This suggest that NMDAR co-agonist site are not saturated, and more D-serine can serve to recruit more NMDAR to light intensity demands (Sullivan and Miller, 2012). This dynamic role of D-serine is possible due to the sodium-dependent glycine transporter type 1 (GlyT1) uptake system that serve to reduce available glycine, preventing competition between the two co-agonists of the NMDAR (Reed et al., 2009). This places D-serine in a critical role for responding various light demands. A study investigating the role of D-serine at different light conditions, demonstrated that D-serine enhanced retinal ganglion cell currents at low contrast values, where stimulus is lower than the blow background light (Gustafson et al., 2015). This was further supported by extracellular recording of the proximal negative potential (PNFP), which revealed that at increasing flash strengths, sensitivity of D-serine decrease (Gustafson et al., 2015). This work demonstrated that at low contrast, the co-agonist site of the NMDAR is not saturated, but with increasing light, D-serine occupies the NMDAR co-agonist site at the retinal ganglion cell layer. Given that there are NMDAR in the outer retina, it is possible that D-serine mediation of the light response occurs earlier in retinal processing. Our work showed a delayed of the temporal property of the a-wave rather than magnitude differences. This delayed in the

a-wave was a result of excess or deficiency of D-serine that was sex dependent.

Lastly, our work showed a reduction in the b-wave amplitude in both hypo- and hyperfunctional conditions that was also sex dependent. One possible hypothesis for D-serine administration effects on only male mice can be attributed to known effects of testosterone on D-amino acid oxidase (DAAO) (Clark et al., 1943; Konno and Yasumura, 1983). In the kidney, higher DAAO enzyme is found in male mice across all six different mouse strains in comparison to their female counterparts (Konno and Yasumura, 1983). In addition, castration reduced the amount of pyruvic acid, a DAAO by product, by 70% in comparison to controls (Clark et al., 1943). On the other hand, adding nutritional supplements of testosterone propionate increased the amount of pyruvic acid by 55% in normal mice, and restored the amount of pyruvic acid by 64% in castrated mice (Clark et al., 1943). This shows that increasing DAAO would consequently decrease the amount of D-serine, which implies sex-related differences in D-serine and, in turn, in NMDAR function where D-serine is the endogenous co-agonist. While the presence of DAAO has been detected in the retina (Romero et al., 2014), sex specific analysis has not been conducted to our knowledge.

The main limitations to our work are that the exact concentration of D-serine in the retina is unknown. Our decision to have a topical delivery of D-serine was to avoid puncturing the eye and activating signaling cascades involved NMDAR excitotoxicity, as it is well established that NMDAR is involved in the neurotoxicity of the retina (Bai et al., 2013). However, we also show that topical delivery of D-serine to the cornea reaches the retina at levels that affect change in neuronal function, and this has never been documented before. Our future studies will use intravitreal injections of D-serine at different concentrations, and we will assess a- and b-wave amplitude and implicit time

differences that may result from a more nuanced and localized exogenous delivery of D-serine. An in depth-analysis of the temporal properties of the a-wave in states of hypo and hyper-functionality of NMDAR is warranted. It is also apparent from this study that the fERG responses to stimuli need to encompass a wide range of temporal frequencies (temporal response function).

Chapter 4

Electroretinographic Evidence of Retinal Ganglion Cell-Dependent Function in Schizophrenia

Pantea Moghimi,* Nathalia Torres Jimenez,*Linda K. McLoon, Theoden I. Netoff,[1,3,5] Michael S. Lee, Angus MacDonald III, Robert F. Miller
*co-first authors.

Synopsis

Schizophrenia is a complex disorder that is diagnosed mainly with clinical observation and evaluation. Recent studies suggest that many people with schizophrenia have abnormalities in the function of the N-methyl-D-aspartate receptor (NMDAR). The retina is part of the central nervous system and expresses the NMDAR, raising the possibility of the early detection of NMDAR-related schizophrenia by detecting differences in retinal function. As a first-step, we used two non-invasive outpatient tests of retinal function, the photopic negative response (PhNR) of the light-adapted flash electroretinogram (PhNR-fERG) and the pattern ERG (PERG), to test individuals with schizophrenia and controls to determine if there were measurable differences between the two populations. The PhNR-fERG showed that males with schizophrenia had a significant increase in the variability of the overall response, which was not seen in the females with schizophrenia. Additionally, at the brightest flash strength, there were significant increases in the PhNR and N72 amplitude in people with schizophrenia that were maximal in controls. Our results show measurable

dysfunction of retinal ganglion cells (RGCs) in schizophrenia using the PhNR-fERG, with a good deal of variability in the retinal responses of people with schizophrenia. The PhNR-fERG holds promise as a method to identify individuals more at risk for developing schizophrenia, and may help understand heterogeneity in etiology and response to treatment.

Introduction

Schizophrenia is a complex disorder with variable onset of symptoms and progression. One strong association is the link to altered excitation and inhibition in cortical circuitry related to N-methyl-D-aspartate receptor (NMDAR) hypofunction (Balu and Coyle, 2015). While other potential underlying biochemical mechanisms have been hypothesized to cause schizophrenia, proteomic and genomic evidence suggests that a relatively large number of individuals diagnosed with schizophrenia have abnormalities in NMDAR-interacting molecules at the synapse (Föcking et al., 2015). Antagonists to the NMDAR, such as phencyclidine or ketamine, produce schizophrenia-like symptoms in healthy subjects and provide evidence for the receptor's involvement in the disease (Driesen et al., 2013; Javitt and Zukin, 1991a). These studies collectively provide significant support for the NMDAR hypofunction hypothesis, also known as glutamate dysfunction hypothesis, in the onset and progression of schizophrenia (Coyle, 1996; Gao and Snyder, 2013; Moghaddam and Javitt, 2012; Olney and Farber, 1995).

A direct prediction of the NMDAR hypothesis is that the activity of neurons that express NMDAR is altered in people with schizophrenia. Since NMDARs are expressed by many neuronal types, including those in the retina (Shen, Liu, & Yang, 2006), retinal electrophysiology may indicate abnormal physiological responses among individuals with schizophrenia. This study tested the hypothesis that NMDAR dysfunction could be measured directly and non-invasively by monitoring retinal neuronal responses to visual stimulation in people with schizophrenia. One measure of retinal neuron activity in response to

visual stimulation is electroretinography (ERG). The ERG is a non-invasive, low-cost test that records the electrical potentials evoked by visual stimuli and is widely used in clinical settings (McCulloch et al., 2015). ERG data are collected under different protocols with variable visual stimuli in order to capture activity of different retinal neurons. The two ERG tests we used in the present study were the full-field or flash ERG (fERG) and the pattern ERG (PERG). The fERG measures the retinal response to a uniform flash of light, while the PERG stimulates the retina using an alternating, contrast-reversing black and white pattern, usually a checkerboard. These two tests complement each other because they target different neuronal populations in the retina. This should allow visualization of significant functional changes in people with schizophrenia when compared to normal controls.

Various protocols of the fERG, such as dark- and light- adapted fERGs, have been used to compare retinal activity of people with schizophrenia and controls. In one study people with schizophrenia demonstrated altered retinal activity when compared to bipolar disorder (Balogh et al., 2008), but only in the “acute stage” of schizophrenia. Other studies showed decreased ERG a- or b-wave amplitudes in people with schizophrenia compared to healthy subjects. (Adams and Nasrallah, 2018; Demmin et al., 2018; Lavoie et al., 2014; Silverstein and Rosen, 2015) These studies used fERG protocols that capture activity of the outer retinal layer, specifically the photoreceptors and bipolar cells. Only one study to date measured the activity of the inner retinal layers, the RGCs and amacrine cells, in their assessment of people with schizophrenia compared to controls (Demmin et al., 2018). They used a light-adapted fERG that evokes a

photopic negative response, the PhNR protocol of the fERG (PhNR-fERG). Evaluating the activity of the inner retinal layers in schizophrenia aids understanding of signal transmission to the brain.

It is well established that RGCs express functional NMDARs (Aizenman et al., 1988; Lukasiewicz and McReynolds, 1985; Massey and Miller, 1990) that contribute 12% to light-evoked responses from RGCs in non-human primates (Cohen & Miller, 1994). The NMDAR is also present on photoreceptors, amacrine cells, and bipolar cells, which play a modulatory role in neuronal excitation and inhibition (Dixon and Copenhagen, 1992; Harsanyi et al., 1996). These studies support the hypothesis that changes in neuronal function should be visible in both the fERG and the PERG. To examine RGC function specifically, we used fERG to measure the PhNR (Frishman et al., 2018) and the PERG (Bach et al., 2013). The PERG has the added benefit of recording the electrical activity of RGCs in addition to photoreceptor and bipolar neurons. This is accomplished by modifying the traditional fERG from a white to a red flash on a blue background luminance (Frishman et al., 2018; Viswanatha et al., 1999). The resultant waveform consists of four components: 1) the a-wave, a corneal-negative deflection that captures activity of cone photoreceptors; 2) the b-wave, a subsequent corneal-positive deflection that captures activity of retinal bipolar cells; 3) the oscillatory potentials, high-frequency oscillations that are superimposed on the b-wave, capturing activity from the inner nuclear layer (Wachtmeister, 1998); and 4) the photopic negative response (PhNR), a corneal-negative deflection following the b-wave that captures activity of the RGCs.(Machida, 2012) While earlier studies attributed the b-wave response to

both bipolar and Müller cells, examination of mice whose Müller cells were functionally inactivated showed that the b-wave was unchanged, supporting the view that Müller cells are not involved in b-wave activity (Kofuji et al., 2000). The changes in amplitude and latency of each of these components may serve as biomarkers for disease state. Previous PhNR-fERG testing in people with schizophrenia revealed a significant difference in a-wave amplitude at brighter flash strengths, but borderline significance for PhNR amplitude (Demmin et al., 2018). An important question left unanswered was whether there were any functional changes to RGCs in these retinas. Despite no significant difference in the PhNR amplitude, the same study reported a significant correlation between the PhNR amplitude and patient symptom severity (Demmin et al., 2018). It may be that the flash strength used to evoke the PhNR in their study was insufficient for demonstrating RGC deficits in people with schizophrenia. Since PhNR amplitude positively correlates with flash strength (Frishman et al., 2018), recording at higher flash strengths might increase sensitivity to more subtle NMDAR dysfunction expressed in the retina. In the present study, we recorded PhNR-fERG test at three flash strengths in order to evaluate whether functional changes to RGCs are present in people with schizophrenia.

We also analyzed a component present in the fERG test rarely considered for evaluating differences in people with schizophrenia - the oscillatory potentials (OPs). The OPs ride on the ascending b-wave, but their cellular origin is more distributed within the inner retina rather than specifically due to photoreceptor or bipolar cells (Wachtmeister, 1998). The first study reporting differences in the OPs between people with schizophrenia and controls

demonstrated greater amplitude variance in males with schizophrenia (Raese et al., 1982); however, that work was not replicated (G Schechter et al., 1987). Since then, evaluation of the OPs in people with schizophrenia has not been reported, although new methods of extracting the OPs from the b-wave are now readily achievable (Gauvin et al., 2014) through the use of 75Hz and 300Hz bandpass filters (McCulloch et al., 2015). These studies evaluating OPs in schizophrenia only measured amplitude and time domain but did not perform a frequency-domain analysis. Given that OPs are collected during most fERG protocols - scotopic, photopic, and PhNR protocols - and provide information regarding RGC activity, we analyzed the OPs in our study. Time-frequency analysis in non-human primates showed that OPs can be deconstructed into two frequency bands, slow and fast, that distinguish between activity in retinal neuron layers (Zhou et al., 2007). Pharmacological studies revealed that the low-frequency OPs, from 75Hz to 100Hz, originate from non-spiking activity of amacrine cells and retinal neurons with non-sodium spiking mechanisms; high-frequency OPs, from 100Hz to 300Hz, originate from spiking retinal ganglion cells and partially from amacrine cells. Analysis of the OPs holds promise for investigating inner retinal function in schizophrenia because they reflect different populations of retinal neurons, making the fERG an all-in-one test with information from all retinal layers.

In addition to the PhNR-fERG test, we evaluated PERG responses as a second measure of RGC function. To our knowledge, no studies have reported PERG differences in people with schizophrenia, although it is well established that RGCs contribute to generation of the PERG response (Holder, 2001). The

PERG response is composed of three components that are named for the negative and positive neuronal responses and the expected times (ms) at which each peaks - N35, P50, and N95 (Holder, 2001). While the specific neuronal origins of each of these components are not fully understood (Porciatti, 2015), direct attribution to inner retinal neurons has been validated across species including humans (Aldebasi et al.,2004; Ventura and Porciatti, 2006), monkeys (Maffei et al., 1985; Viswanathan et al., 1999), and rodents.(Miura et al., 2009). The PERG response is sensitive to retinal pathology, such as in glaucoma (Preiser et al., 2013) and diabetic retinopathy (Prager, Garcia, Mincher, Mishra, & Chu, 1990). As a well-established ophthalmological tool for assessing RGC function, PERG is arguably superior for assessing RGC dysfunction in schizophrenia.

One complicating factor is the role of sex in NMDAR activity. Rodent studies demonstrated differences in NMDAR activity in the brain between male and female rats (Cyr et al., 2001; McEwen, 2002; McRoberts et al., 2007; Woolley, 1998). Our recent study examining fERG in a control and mouse model of schizophrenia, a serine racemase knock-out which results in NMDAR hypofunction, reported significant differences between a- and b- wave amplitudes in male and female mice regardless of genotype or flash strength (Torres Jimenez et al., 2019). In the present study, we also included sex as a variable. A sex-dependent difference in NMDAR activity and fERG variables may relate to the numerous sex differences in schizophrenia, such as age of onset, symptom expression, and treatment response (Loranger, 1984; Peterson, 1968).

We compared retinal responses using PERG and PhNR-fERG protocols from a cohort of people with chronic schizophrenia and normal controls. For the PERG test, we analyzed N35, P50, and N95 amplitudes and latencies. For the PhNR-fERG test, we evaluated three different flash strengths and measured the a-wave, b-wave, and PhNR amplitude and implicit times. We also analyzed high- and low- frequency OPs to determine whether differences in the activity of inner retinal neurons were present in people with schizophrenia. All analyses included sex as a factor to investigate whether sex-related ERG abnormalities were present in people with schizophrenia.

Methods

Participants

We recruited 30 people with schizophrenia and 34 demographically similar healthy controls, aged 18 to 65, within a large metropolitan area as reported in Table 4.1. Patient diagnosis was confirmed using the SCID-IV (First, Regier, & Kupfer, 2002). The severity of psychotic symptoms was rated using the Brief Psychiatric Rating Scale (BPRS) (J. Ventura et al., 1993). The BPRS values for each of the people with schizophrenia was graphed based on age (Supplemental Figure 4.1; Table 4.1). The BPRS showed that all subjects had a significant number of symptoms associated with schizophrenia, with a range of score from 26 - 93. Most subjects were on an array of anti-psychotic medications; only 3 people with schizophrenia were on no medications at the time of ERG recording. Using multiple linear regression analyses, there were no significant differences between disease severity between males and females with

schizophrenia nor was age a significant predictor for BPRS score. All participants gave informed consent. For 6 controls and 5 people with schizophrenia, minority data were unavailable. All procedures were done in accordance with a University of Minnesota IRB approved protocol and adhered to the principles of the Declaration of Helsinki.

Table 4.1 Clinical and demographic characteristics of the participants. *Data are mean (standard deviation). Two of the 30 subjects with schizophrenia did not have a BPRS score and were omitted from this analysis. This table was produced by Nathalia Torres Jimenez.*

Table 4.1 Subject Information			
	Scz (N=30)	HC(N=35)	Difference
Sex (% Female)	46.70%	48.60%	3.90%
Age (M ± S.D.)	40.27 ± 11.53	39.97 ± 13.01	0.75%
Minority (%)	24%	23%	4.26%
BPRS score (M ±S.D.)	58.7 ± 15.99	0	-
Unmedicated	6	-	-

Data collection

Participants came to three sessions, which included a clinical psychiatric evaluation and an ophthalmologic examination to evaluate for any eye diseases that could affect ERG outcomes. In the control group, 73.5% were either 20/20 or better and in the group with schizophrenia, 80% were 20/20. The rest of the subjects were 20/20 with correction and otherwise had completely normal vision and no history of eye disease that would affect the ERG data. ERG data were collected in the third session using the Diagnosys LLC (Boston, MA) system at a sampling frequency of 1.2kHz. DTL fiber electrodes manufactured by Diagnosys

LLC (Boston, MA) were utilized for all tests. Two types of ERG responses were collected: responses to a full-flash red light on a blue background (PhNR-fERG test) and responses to contrast-reversing checkerboard or bars (PERG test). The time of the PhNR-fERG and the PERG tests for each subject are shown in Supplemental Figure 4.2. The majority were between 9:30 a.m. and 6:30 p.m., with only two subjects at 7:30 p.m. However, it should be noted that a number of recent studies looking at the ERG responses compared to time of day showed no changes in ERG amplitudes or implicit times due to time of day the recordings were taken(Heinemann-Vernaleken, Palmowski, & Allgayer, 2000; Marcus, Cabael, & Marmor, 2004) unless performed at very late evening times (e.g. 11 p.m.).(J Lavoie et al., 2010; Rufiange, Dumont, & Lachapelle, 2002) All of our recordings were within the time window shown not to be affected by time of day.

PhNR-fERG test. The pupils were dilated with Tropicamide (1%) (Sandoz, Princeton, NJ), and 50 red light flashes were presented against a blue background at a frequency of 4Hz. Three different light intensity levels were used as stimuli. Table 4.2 summarizes both luminance and retinal illuminance of the visual stimuli. We used constant luminance level visual stimuli. Retinal illuminance was calculated as the constant luminance multiplied by the mean pupil area across subjects.

***Table 4.2. Parameters of the visual stimuli used for data collection**. The average retinal luminance for each stimulus are calculated by multiplying luminance by average pupillary area across subjects and reported within brackets [ ]. This table was produced by Nathalia Torres Jimenez.*

Table 4.2	PhNR-fERG Stimulus Conditions		
Red Flash Strength	**Flash Duration**	**Blue Background Luminance**	**Interstimulus Duration**
1 cd·s/m^2 [60 Td·s]	4 ms	10 cd/m^2 [600 Td·s]	250 ms
5 cd·s/m^2 [300 Td·s]	4 ms	10 cd/m^2 [600 Td·s]	250 ms
7 cd·s/m^2 [420 Td·s]	4 ms	10 cd/m^2 [600 Td·s]	250 ms
Transient PERG Stimulus Conditions			
Visual Stimulus Display	**Stimulus Pattern**	**Mean Luminance**	**Reversal Rate**
CRT	Checkerboard	999 cd/m^2	2.1 rps
LED	Bar	999 cd/m^2	8 rps

PERG test. We collected two datasets under the PERG protocol where pupil dilation was not used. For the first dataset, PERG responses were collected in response to a contrast reversing black and white checkerboard pattern at 0.8 degrees spatial frequency, with a luminance of 999 cd.s/m^2. Contrast was reversed at a rate of 2.1 reversals per second (1.05Hz). Visual stimuli were presented on a CRT display at 1000mm distance and at 100% contrast. The response to 150-contrast reversal for each stimulus was recorded for each subject.

Partway through the study, an LED display was implemented, which allowed for faster stimulation of the retina (Monsalve et al., 2017). Twenty-four controls (11 males and 13 females) and 25 people with schizophrenia (13 males and 12 females) returned for additional PERG recording with the LED display.

The LED PERG data were collected using reverse contrasting black and white bars at a luminance of 999 cd.s/m^2 (Table 4.2). All stimuli had a spatial frequency of 0.5 degrees and were presented at 100% contrast. The subjects viewed the monitor at a distance of 57 cm. Contrast of each bar was reversed at a rate of 8 reversals per second (4Hz). The response to 150-contrast reversal for each stimulus was recorded for each subject.

Data Analysis

PhNR-fERG test. For each subject, single ERG traces in response to each light flash were averaged. Prior to averaging, noisy traces were identified and excluded. A trace was excluded if it deviated more than one standard deviation from the average in more than 50% of time points. Visual inspection of the traces showed that this criterion robustly identified noise.

The average waveform for each subject was used to measure amplitude and latency of the a-wave, b-wave, and PhNR components. Prior to measuring any of the indices, each waveform was visually inspected. Subjects with noisy waveforms where at least one of the indices could not be identified with certainty were excluded (4 subjects with schizophrenia, 2 females; and 6 control subjects, 3 females). Each waveform was low-pass filtered using a digital 5th order Butterworth filter with cut-off frequency at 50Hz to filter out and avoid contamination from oscillatory potentials (Weymouth and Vingrys, 2008). Amplitude of the a-wave component was measured as the trough of the first negative deflection after visual stimulus onset with respect to the baseline. Latency or implicit time of the a-wave component was measured as the

occurrence time of the trough post stimulus. Amplitude of the b-wave component was calculated as the difference between the peak of the positive deflection and the a-wave trough. Implicit time of the b-wave component was calculated as occurrence time of the peak post-stimulus. We measured amplitude of the PhNR deflection using two indices previously used to report PhNR amplitude. The first index measured the negativity of the PhNR deflection with respect to baseline 72ms after the onset of the visual stimulus (Demmin et al., 2018; Kundra et al., 2016). The PhNR reaches its maximum reflection on average around 72ms post-stimulus (Kundra et al., 2016), and the amplitude of the waveform at this time point is commonly used as an index for PhNR amplitude. Previous studies reported altered latencies in the photoreceptor responses of people with schizophrenia (Hébert et al., 2015). Consequently, we could not assume that the PhNR latency would occur at 72ms in the subjects. To compensate for this, we used an index that measures the trough of the PhNR component with respect to the baseline (Demmin et al., 2018; Kundra et al., 2016). Implicit time of PhNR was measured as time of the trough post-stimulus (Figure 4.1). As a control, we repeated all statistical analyses with the a-wave and b-wave amplitudes measured using unfiltered waveforms and obtained qualitatively similar results.

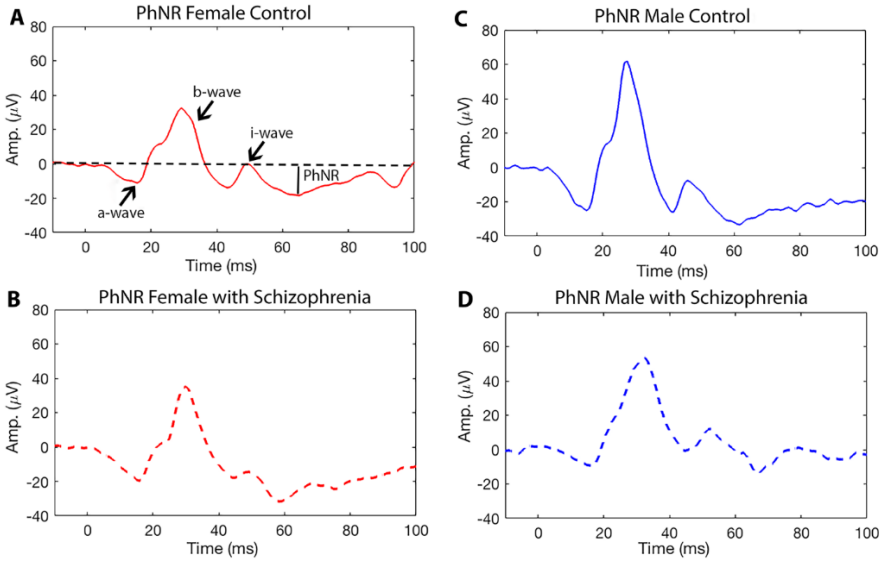

Figure 4.1 Individual PhNR-fERG waveform for a single at subject at a single flash strength. *Individual PhNR-fERG wave form for a single subject at a single flash (1 cd.s/m^2) intensity from a A) female control, (B) female with schizophrenia, (C) male control, and (D) male with schizophrenia with time in milliseconds (ms) on the x-axis and amplitude (Amp.) in microvolts (μV) on the y-axis. Arrows indicate the a-wave, b-wave, i-wave, and PhNR components of the PhNR-fERG. This figure was co-developed by Pantea and I, and produced by Pantea Moghimi]*

To measure the strength of fast and slow OPs, total power in the 75-100Hz and 100-300Hz frequency bands were calculated (Zhou et al., 2007). OPs typically appear shortly after the stimulus onset and continue until 65ms post-stimulus (Zhou et al., 2007). We calculated total power in each frequency band from the power spectral density of the waveform from 0 to 70ms post-stimulus. We chose 70ms instead of 65ms to make sure the entire duration of OPs was included. Although strength of the OPs was quantified within a time window where other post-b-wave components lie, OPs were isolated from other components in the frequency-domain rather than the time-domain. I-wave and

PhNR correspond to frequency bins around 11 Hz (Kundra et al., 2016); while OPs were post-75Hz. Values from the two eyes were averaged for each subject.

PERG test. Single traces from each contrast reversal were averaged for each subject after exclusion of outliers. A trace was excluded if it deviated more than one standard deviation from the average in more than 60% of time points. Visual inspection of the traces proved this criterion to be robust. Average traces were subsequently filtered using a digital 5th order Butterworth bandpass filter with cut-off frequencies at 6 and 72Hz to filter out low frequency drifts in the signal as well as high frequency noise. Amplitude and implicit times of each component were measured from the average trace from each subject. Subjects with noisy waveforms were identified through visual inspection of each waveform and excluded from further analysis. One female subject with schizophrenia was excluded from the data collected using CRT. Four control subjects (two female) were excluded from the data collected using LED. N35 amplitude was measured as the trough of the first negative deflection occurring 30-35ms post-stimulus with respect to baseline. Occurrence time of the trough post-stimulus was measured as N35 implicit time. P50 amplitude was measured as the peak of the positive deflection following the N35 component with respect to baseline. P50 implicit time was measured as time of the peak post-stimulus. N95 was measured as trough of the negative deflection following the P50 deflection with respect to baseline. Occurrence time of the trough post-stimulus was used as the N95 implicit time. Amplitude and implicit times from the right and left eyes were averaged. When data from only one eye were available, values from the single eye were used.

Statistical Analysis

For the statistical analyses collected from the PhNR-fERG response; we analyzed 11 dependent variables: a-wave, b-wave, and PhNR amplitude and implicit time; b/a ratio; low-frequency OPs (75-100 Hz), high-frequency OPs (100-300 Hz), and combined frequency OPs (75-300 Hz). For each of these dependent variables, we conducted a 3-way mixed ANOVA with two between-subject factors, disease state and sex, and one within-subject factor, flash strength. We performed Levene's test for equal variances for each group of the between-subjects factor at each flash strength. To comply with the assumption of sphericity, Greenhouse-Geisser corrected statistics were reported. We tested simple two-way interactions (disease state · sex) at each level of flash strength and flash strength against one of the between-subject factors, (flash strength and sex) and (flash strength and disease state). We analyzed the main effects at each flash strength. Main effects from the two-way interactions were reported for all dependent variables attained at each flash strength. The variances for the a-wave, N72, and PhNR amplitudes were not equal, necessitating the use of Welch independent sample t-tests to evaluate differences in disease state at each level of flash strength. The Pearson correlation coefficient between the variable and disease severity symptoms for subjects with schizophrenia was also reported.

For the statistical analyses collected from the PERG protocol, we analyzed 6 dependent variables: N37, P50, and N95 amplitude and implicit time. We performed a two-way between-subject ANOVA to examine the effects of disease state and sex on each dependent variable. Since interaction effects were not significant, analysis of main effect was conducted from pairwise-comparisons

of unweighted marginal means. Analysis of the PERG recorded from CRT and LED visual display were conducted separately. Statistics were performed using SPSS Statistics 25 program (IBM, Armonk, NY).

Results

PhNR-fERG Analyses

When the PhNR-fERG waveforms from all the tested subjects were graphed (Figure 4.2), several generalizations could be made. First, variability in the strength of the neuronal responses were evident in the ERG waveforms at each flash strength. There were few overt changes in the ERG between females with schizophrenia and female controls (Figure 4.2 A,B). However, there was a huge variability in the waveforms in the male controls, and an even greater variability in the males with schizophrenia compared to male controls (Figure 4.2 C,D), as highlighted by the variance and standard deviation of each group of various dependent variables (Supplemental Table 4.1). We analyzed the a- and b-wave amplitudes and b/a ratio (Supplemental Figure 4.3, Table 4.3) and implicit times (Supplemental Table 4.2) for all subjects. There was no statistically significant difference in a-wave amplitude between people with schizophrenia and controls at any flash strength (Table 4.3). For b-wave and b/a ratio, there were no significant 3-way nor 2-way interactions; however, there was a borderline b-wave main effect of disease state at the middle flash strength (Supplemental Table 4.2). While there were no statistically significant differences, b-waves trended toward reduced amplitude and delay in time at all flash strengths in people with schizophrenia in comparison to controls. Since this effect

was seen among males, females, and combined datasets, it warrants further investigation with a larger sample size. While not significant in this study, this trend toward increased a-wave amplitude in male subjects with schizophrenia mirrored that seen in another study where sex was not used as a factor for analysis (Demmin et al., 2018). These data correlate with our study in the NMDAR hypofunction mouse, where significant differences were seen between male and female mice (Torres Jimenez, 2019). At the highest flash strengths for the a-wave amplitude, disease state differed significantly in male versus females. These trends suggest that a clearer differentiation of these waveforms would be more likely at the higher flash strengths; our future study will use brighter flash strengths as well as increased sample size.

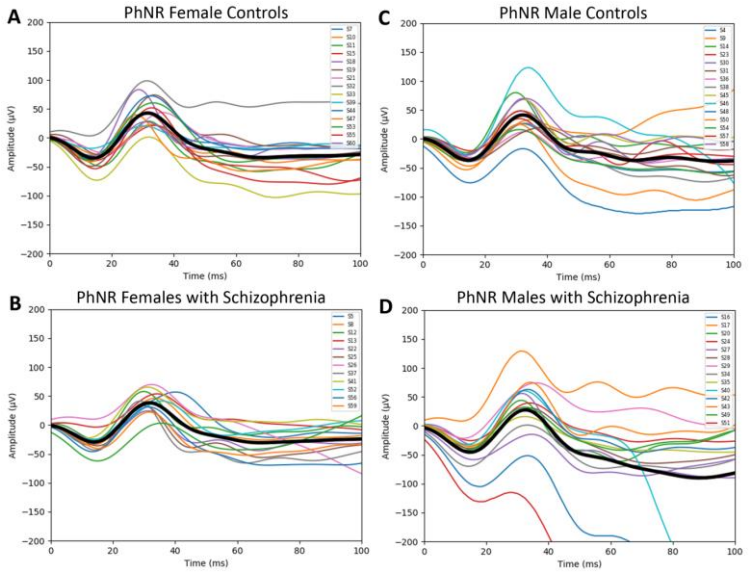

Figure 4.2 Filtered PhNR-fERG for every subject at the brightest flash strength. *PhNR-fERGs at the brightest flash strength of 10 cd·s/m^2 from (A) female controls, (B) females with schizophrenia, (C) male controls, and (D) males with schizophrenia. Each color represents the PhNR-fERG from a single individual and black line represents the mean of each group. Time in milliseconds (ms) is on the x-axis and amplitude (Amp.) in microvolts (μV) on the y-axis.*

Arrows indicate the a-wave, b-wave, i-wave, and PhNR components of the PhNR-fERG. This figure was produced by Nathalia Torres Jimenez.

***Table 4.3**: **Statistical analysis of the PhNR-fERG**, examining the amplitude of the a-wave, PhNR and PhNR at negative 72 ms (N72). Red indicates significance. Blue indicates approaching significance. Statistical analyses and creation of the table were done by Nathalia Torres Jimenez.*

Table 4.3		a-wave amplitude	PhNR amplitude	N72
		Independent t-test		
Disease State at each level of flash strength	1 cd·s/m2	t(53)=-0.456, p=0.650, *d* =.12	t(53)=--1.050, *p* =0.298, *d* =.28	t(53)=-0.565, p=0.575, *d* =.15
	5 cd·s/m2	t(53)=-0.859, p=0.394, *d* =.23	t(53)=-1.615, *p* =0.112, *d* =.44	t(53)=-1.445, p=0.154, *d* =.39
	7 cd·s/m2	t(33)=--1.650, p=0.108, *d* =.46	t(27)=-2.110, ***p* =0.046**, *d* =.59	t(28)=-2.110, ***p* =0.044**, *d* =.60

NMDARs are highly expressed on RGCs (Aizenman et al., 1988; Massey and Miller, 1990). Any functional change in people with schizophrenia would be evident in the PhNR amplitude and N72 amplitude, which are specifically associated with RGC function (Barnes and Holt, 2005; Viswanathan et al., 1999). At the brightest flash strength, the Welch's t-test showed disease state differences in both the PhNR amplitude and N72 (Table 4.3). The mean PhNR amplitude was statistically significantly different between people with schizophrenia and healthy controls t(27.265)=-2.092, *p*= 0.046 at the brightest flash strength (Figure 4.3, Table 4.3). Mean PhNR amplitude was 40.6 µV higher (95%CI, -80.34 to -0.79) in people with schizophrenia than controls. Mean N72 amplitude was statistically significantly different between people with schizophrenia and healthy controls t(28.148)=2.110, *p*= 0.044 at the brightest flash strength (Figure 4.3, Table 4.3). Mean N72 amplitude was 15.6 µV higher (95%CI, -6.4 to 37.5) in people with schizophrenia compared to controls (Figure 4.3). The brightest flash strength was chosen because it was below the level of response saturation in humans (Binns et al., 2011) resulting in a PhNR amplitude

that should not change at the brightest flash strength in healthy controls. The response saturation threshold appeared to be different in people with schizophrenia, as there was no change in the PhNR amplitude relative to flash strength in healthy controls but showed a continued increase in people with schizophrenia (Figure 4.3, Table 4.3). As this flash strength was not tested by other investigators, it would be important to validate this stimulus condition and report variability (Supplemental Table 4.3). This suggests that use of brighter flash strengths should improve visualization of differences between people with schizophrenia and controls. Furthermore, to evaluate whether changes in the PhNR amplitude were due to changes in retinal ganglion cells or from more distal retina (i.e. photoreceptors, bipolar cells), a one-way Welch's *F* test was conducted to analyze differences in PhNR/b-wave ratio across the 4 groups (Supplemental Table 4.4). The PhNR/b-wave ratio was statistically different across groups ($F(3, 82.4)=3.23$, $p=0.027$), with male schizophrenics having a larger PhNR/b-wave ratio. However, none of the pairwise comparisons using the Games-Howell post-hoc test were significant. We show that in males with schizophrenia, the PhNR amplitude was enhanced but not due to a decreased response from bipolar cells, as would be reflected in the b-wave amplitude.

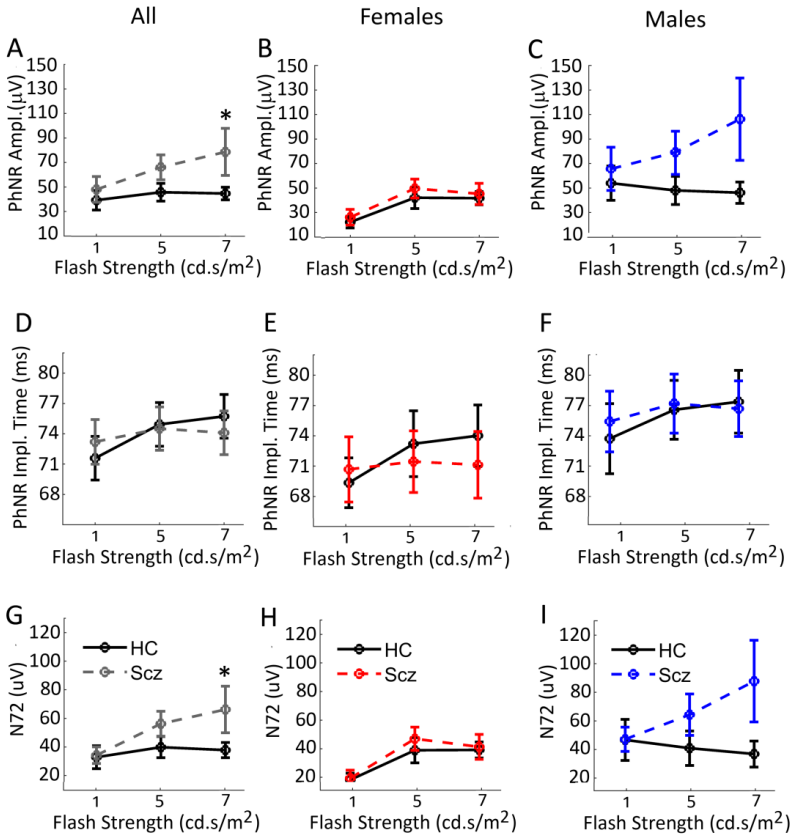

Figure 4.3 PhNR-fERG N72 and PhNR component: amplitude and time. *Graphs represent the (A) PhNR trough amplitude, (B) PhNR implicit time, and (C) negativity of the PhNR deflection at 72 ms (N72) amplitude averaged for all subjects at each flash strength. Black represents the controls, dotted lines represent the people with schizophrenia, gray dotted lines represent all people with schizophrenia, blue represents the male people with schizophrenia, and red represents the females with schizophrenia. Amp is amplitude. Impl. is implicit time. Cd.s/m2 represents candelas per second per meters squared, a measure of constant luminance. Bars indicate standard error. HC is healthy controls; Scz is people with schizophrenia. This figure was co-developed by Nathalia and Pantea, and produced by Pantea Moghimi.*

Oscillatory potentials (OP) were analyzed based on the frequency band split in three ways: between the frequencies of 75-100 Hz (low frequency OPs), between the frequencies of 100-300Hz (high frequency OPs), and combination of

the first two, between 75-300Hz (Supplemental Figure 4.4, Table 4.4, Figure 4.4). While there were no significant differences in the 3-way or 2-way interactions in any of the OP bandwidths (Table 4.4), the 75-100Hz bandwidth had a probability of 0.095, with effect of size ($\eta_p^{2=}$ 0.39). While the two-way interactions were not significant, it likely due to sample size and variability in the disease state. Main effects analyses showed significant differences for sex regardless of disease state in high-frequency OPs and the combined OP data (Table 4.4). This suggests that OP analysis might identify males with schizophrenia, and future analyses should be cautious when pooling male and female ERG data.

Table 4.4 Statistical analysis of the oscillatory potentials *(OPs) derived from the PhNR-fERG for the low-frequency OPs, between 75-100Hz, the high-frequency OPs between 100-300Hz, and the total combined OPs between 75-300 Hz. Red indicates significance. Blue indicates approaching significance. Statistical analyses and creation of the table was done by Nathalia Torres Jimenez.*

Table 4.4	Low Frequency OPs (75-100 Hz)			High Frequency OPs (100-300 Hz)			Combined (75-300 Hz)		
Flash Strength · Sex · Disease State	$F(2.0,119)=0.3$, $p=0.73$, $\eta_p^2=0.005$			$F(1.7,102)=0.02$, $p=0.97$, $\eta_p^2=0.000$			$F(1.8,110)=0.1$, $p=0.86$, $\eta_p^2=0.002$		
Simple two-way interactions									
Flash Strength · Disease State	$F(2.0,119)=2.4$, $p=0.095$			$F(1.7,102)=1.4$, $p=0.249$			$F(1.8,110)=1.9$, $p=0.161$		
Flash Strength · Sex	$F(2.0,119)=0.1$, $p=0.874$			$F(1.7,102)=1.3$, $p=0.286$			$F(1.8,110)=0.9$, $p=0.39$		
Disease State · Sex at each level of flash strength	**1 cd·s/m2**	$F(1,60)=1.6$, $p=0.204$		**1 cd·s/m2**	$F(1,60)=0.2$, $p=0.663$		**1 cd·s/m2**	$F(1, 60)=0.92$, p=0.34	
	5 cd·s/m2	$F(1,60)=0.1$, $p=0.762$		**5 cd·s/m2**	$F(1,60)=0.03$, $p=0.872$		**5 cd·s/m2**	$F(1, 60)=0.09$, p=0.76	
	7 cd·s/m2	$F(1,60)=0.4$, $p=0.538$		**7 cd·s/m2**	$F(1,60)=0.1$, $p=0.767$		**7 cd·s/m2**	$F(1, 60)=0.2$, p=0.66	
Main Effects									
Main Effects of the two-way interaction at each level of flash strength		Disease State	Sex		Disease State	Sex		Disease State	Sex
	1 cd·s/m2	0.445	0.052	**1 cd·s/m2**	0.808	0.008	**1 cd·s/m2**	0.59	0.01
	5 cd·s/m2	0.809	0.069	**5 cd·s/m2**	0.688	0.237	**5 cd·s/m2**	0.78	0.13
	7 cd·s/m2	0.057	0.278	**7 cd·s/m2**	0.160	0.556	**7 cd·s/m2**	0.09	0.41

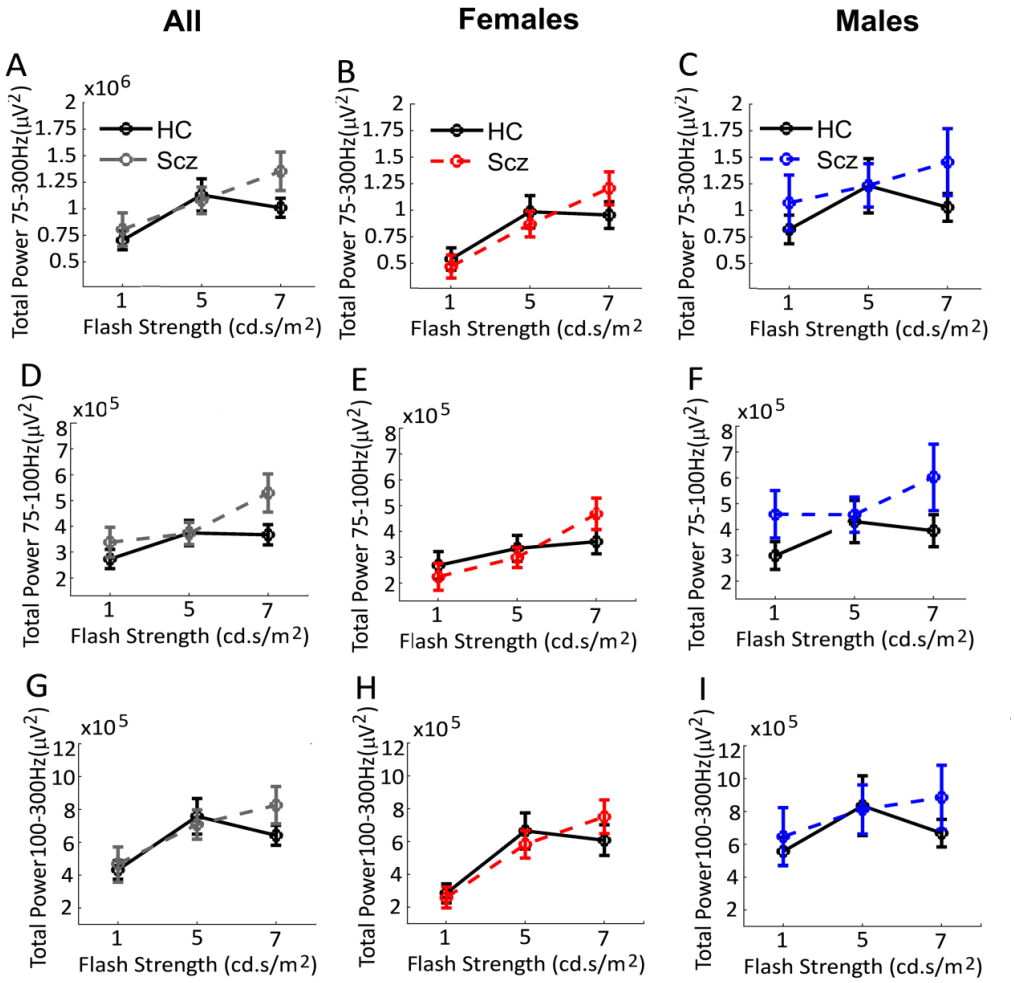

Figure 4.4 Oscillatory potentials. *Graphs summarize the power analysis of the oscillatory potentials. (A-C) Mean total power of all oscillatory potentials between 75 and 300Hz in microVolts (μV), (D-F) mean total power of oscillatory potentials between 75-100Hz in μV, and (G-I) mean total power of oscillatory potentials between 100-300Hz in μV. Cd.s/m2 represents candelas per second per meters squared, a measure of constant luminance. Bars represent standard error. HC is healthy controls; Scz is people with schizophrenia. This figure was co-developed by Nathalia and Pantea, and produced by Pantea Moghimi.*

PERG Analyses

PERG measurements were analyzed for both the CRT and the LED-generated data sets (Tables 4.5, 4.6; Figures 4.5, 4.6) and showed a trend, but not significant, for differences between people with schizophrenia and controls. There were no significant differences between N35, P50, or N95 amplitude or implicit time with the evoked PERG using either the LED or CRT visual displays. The data trended toward significance for an interaction between disease state and sex for the N95 implicit time (p=0.07) and a main effect of disease state for the N35 amplitude (p=0.06) for the LED-derived data (Table 4.6). The CRT-derived data showed a borderline main effect of disease state (p=0.054) for the N95 implicit time. Sex appears to be an important variable relative to disease state relative to the N95 implicit, but LED-display may be necessary to detect that interaction. Our CRT-derived data trended towards differences between people with schizophrenia and controls in the N95 implicit time regardless of sex. The LED-derived data trended towards an interaction between sex and disease state in the N95 implicit time. The LED-derived data may reflect disease state differences in the N35 amplitude, while the CRT-derived data did not. Due to the large and unexpected significant variance in the ERGs of people with schizophrenia (Figure 4.2), a larger cohort of subjects would likely have generated statistical significance. These data, in combination with the PhNR results, suggest that differences in ganglion cell function are likely in people with schizophrenia compared to controls.

Table 4.5 Statistical analysis for the PERG evoked using the CRT display*, examining the N35 amplitude, P50 amplitude, and N95 amplitude. Statistical analyses and creation of the table were done by Nathalia Torres Jimenez.*

.

Table 4.5	PERG evoked using CRT visual display		
	N35 amplitude	**P50 amplitude**	**N95 amplitude**
Simple two-way interactions			
Disease State · Sex	$F(1,60)=2.0$, $p=0.164$, $\eta_p^2=.032$	$F(1,60)=0.003$, $p=0.955$, $\eta_p^2=.000$	$F(1,60)=1.0$, $p=0.331$, $\eta_p^2=.016$
Main Effects of Disease	$F(1,60)=2.1$, $p=0.151$	$F(1,60)=0.2$, $p=0.625$	$F(1,60)=0.1$, $p=0.780$
Main Effects of Sex	$F(1,60)=0.4$, $p=0.527$	$F(1,60)=2.1$, $p=0.157$	$F(1,60)=1.2$, $p=0.279$
	N35 implicit time	**P50 implicit time**	**N95 implicit time**
Disease State · Sex	$F(1,60)=0.6$, $p=0.430$, $\eta_p^2=.010$	$F(1,60)=2.6$, $p=0.113$, $\eta_p^2=.041$	$F(1,60)=1.1$, $p=0.302$, $\eta_p^2=.018$
Main Effects of Disease	$F(1,60)=0.2$, $p=0.664$	$F(1,60)=0.03$, $p=0.875$	$F(1,60)=3.9$, **$p=0.054$**
Main Effects of Sex	$F(1,60)=0.004$, $p=0.948$	$F(1,60)=0.03$, $p=0.874$	$F(1,60)=0.1$, $p=0.800$

Table 4.6*: **Statistical analysis for the PERG evoked using the LED display****, examining the N35 amplitude, P50 amplitude, and N95 amplitude. Blue indicates approaching significance. Statistical analyses and creation of the table were done by Nathalia Torres Jimenez.*

Table 4.6	PERG evoked using LED visual display		
	N35 amplitude	**P50 amplitude**	**N95 amplitude**
Simple two-way interactions			
Disease State · Sex	$F(1,45)=0.1$, $p=0.763$, $\eta_p^2=.002$	$F(1,45)=0.3$, $p=0.579$, $\eta_p^2=.007$	$F(1,45)=1.6$, $p=0.218$, $\eta_p^2=.034$
Main Effects of Disease State	$F(1,45)=3.7$, **$p=0.062$**	$F(1,45)=0.2$, $p=0.682$	$F(1,45)=2.7$, $p=0.108$
Main Effects of Sex	$F(1,45)=2.0$, $p=0.167$	$F(1,45)=2.4$, $p=0.126$	$F(1,45)=0.1$, $p=0.795$
	N35 implicit time	**P50 implicit time**	**N95 implicit time**
Disease State · Sex	$F(1,45)=2.8$, $p=0.099$, $\eta_p^2=.059$	$F(1,45)=0.5$, $p=0.490$, $\eta_p^2=.011$	$F(1,45)=3.4$, **$p=0.070$,** $\eta_p^2=.071$
Main Effects of Disease State	$F(1,45)=0.2$, $p=0.673$	$F(1,45)=2.5$, $p=0.124$	$F(1,45)=0.2$, $p=0.638$
Main Effects of Sex	$F(1,45)=0.0$, $p=0.991$	$F(1,45)=0.03$, $p=0.865$	$F(1,45)=0.2$, $p=0.638$

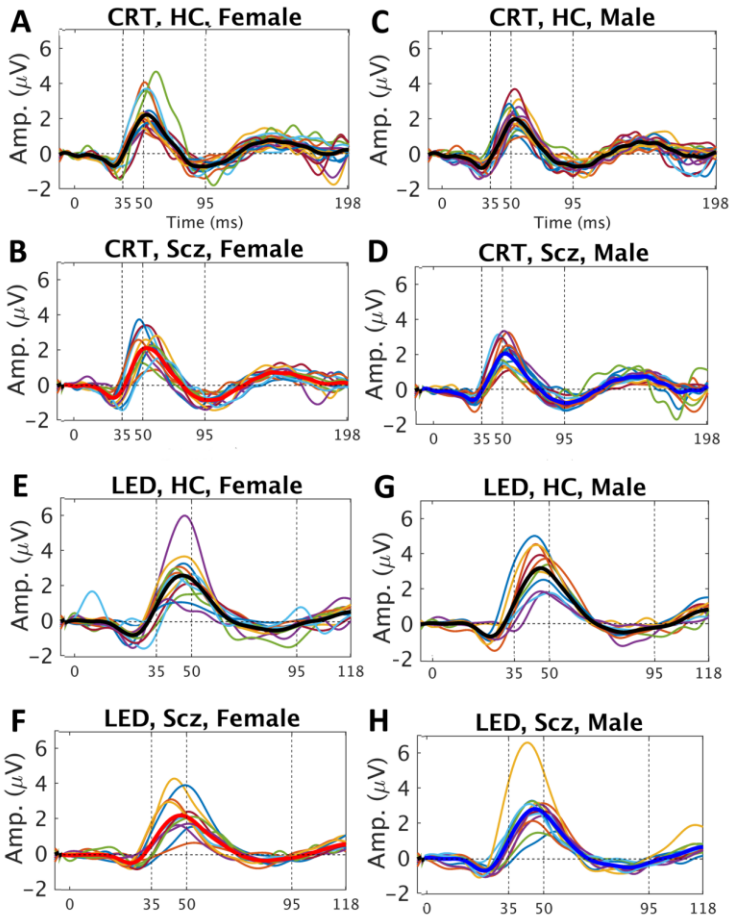

Figure 4.5 Filtered PERG traces for every subject. *Graphs of all PERG traces from the (A) healthy control female subjects examined with the CRT display (HC); (B) females with schizophrenia (Scz) examined with the CRT display; (C) control male subjects (HC) examined with the CRT display; (D) males with schizophrenia (Scz) examined with the CRT display; (E) control female subjects examined with the LED display (HC); (F) females with schizophrenia (Scz) examined with the LED display; (G) control male subjects (HC) examined with the LRD display; (H) males with schizophrenia (Scz) examined with the LED display. Black lines depict the mean of the PERG response, thick red lines depict the mean of the PERG response for female subjects, and thick blue lines represent the mean of the PERG response for male subjects. Amp is amplitude in microVolts (μV). Figure was co-developed, produced by Pantea Moghimi*

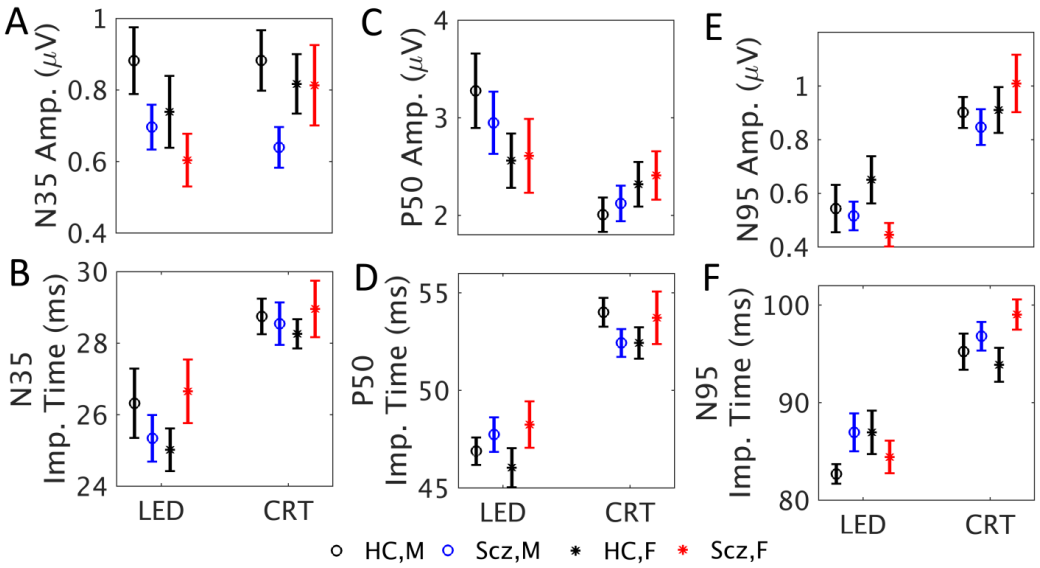

Figure 4.6 N35 component of the PERG: amplitude and time. *Analysis of the PERG using the LED and CRT displays. (A) N35 amplitude (Amp.) and (B) N35 implicit (Imp.) time; (C) P50 amplitude (Amp.) and (D) implicit (Imp.) time; and (E) N95 amplitude (Amp.) and (F) implicit (Imp.) time. Black open circles are control (HC) male subjects and blue open circles are males with schizophrenia (Scz). Black asterisks are control (HC) females and red asterisks are females with schizophrenia (Scz). Bars indicate standard error. Amplitude is in microVolts (μV) and implicit time is in milliseconds (ms).* Figure was co-developed, produced by Pantea Moghimi

Discussion

The PhNR-fERG and PERG allow visualization of the function of different retinal neurons, with the PhNR-fERG showing a large amount of variability in men with schizophrenia specifically. The PhNR-fERG and PERG both assess activity of RGCs. Analysis of the PhNR-fERG showed a significant increase of PhNR and N72 amplitude at only the highest flash strength in people with schizophrenia, suggesting a shift in the saturation threshold of RGCs in people with schizophrenia compared to controls. Similar results were seen for the low-frequency OP analyses, where there was borderline significance of disease state, suggesting changes in amacrine cell function regardless of sex. The analysis of the data from the PERG-evoked responses were largely dependent on the visual display, with LED-derived data having a greater potential than CRT to reflect interactions between sex and disease state. This was evident in the N95 implicit time and the N35 amplitude relative to disease state. A larger sample is needed to show these observed trends had statistical significance.

The large variability in the PhNR-fERG responses in people with schizophrenia is likely a reflection of the complexity of the underlying biological causes of schizophrenia. Recent genetic and proteomic studies suggested that a large proportion of people with schizophrenia have abnormalities in postsynaptic signaling complexes (Föcking et al., 2015; Kirov et al., 2012), and in particular differential expression of NMDA-interacting proteins, such as CYFIP2, SYNPO, SHANK3, ESYT and MAPK3. Receptor heterogeneity would be expected to result in differences in the manifestation of schizophrenia in different individuals. These data collectively suggest that developing a method for identifying subsets

of people with significant changes to their PhNR-fERG may provide a means for a more personalized medicine approach to their treatment.

The PhNR-fERG provides insight into the function of various neuronal populations in the retina, including RGC function from the PhNR. While one study comparing PhNR amplitude and implicit time did not observe any differences in people with schizophrenia in comparison to control (Demmin et al., 2018), our data showed a significant difference. One explanation for the former lack of significance of the PhNR is that the tested flash strength of 58 Td·s may have been too weak to distinguish differences between people with schizophrenia and controls. We hypothesize that evaluating a wider range of light intensities would shed light on dynamic modulation of NMDARs based on light intensity demands and would reveal NMDAR dysfunction. It is well established that at increasing light intensities there is a decline in the b-wave amplitude, a phenomenon referred to as the Photopic Hill (Kondo et al., 2000; Wali and Leguire, 1992). We evaluated whether changes in the PhNR amplitude were due to changes from distal retina, as reflected by the a- and b-waves amplitude. Like the b-wave amplitude, the Naka-Rushton equation provides a good fit for intensity-response data in order to determine if there was a relationship between different light intensities and the response (Binns et al., 2011; Rufiange et al., 2003). Flash strengths greater than 2.5 cd·s/m^2 would result in response saturation, and thus no increase in PhNR amplitude of controls would occur (Binns et al., 2011). Prior to our study, it was uncertain whether response saturation would occur in people with schizophrenia. We showed that increasing flash strength resulted in increased PhNR amplitude in the people with schizophrenia, with a statistically

significant increase in the PhNR amplitude in people with schizophrenia compared to controls at the brightest flash strength of 7 cd·s/m^2 (420 Td·s). Our N72 amplitude results were consistent with the PhNR results. We demonstrate that at brighter flash strengths, when the PhNR response should be saturated, there was an increase in the light-evoked potentials in the RGCs in people with schizophrenia, the same increase is not seen earlier in retinal processing (bipolar cells) because our a-wave and b-wave amplitude measurements from people with schizophrenia were not statistically significantly different from controls. However, Demmin et al. showed a statistically significant reduction in the a-wave amplitude in people with schizophrenia (Demmin et al., 2018), and we saw a trend of decreasing b-wave amplitude in people with schizophrenia. Greater sample sizes are necessary in under to understand distal retinal involvement in retinal ganglion cell changes as reflected by the PhNR. Our work suggests that people with schizophrenia have a different threshold of saturation. This is the first report of RGC layer dysregulation in schizophrenia. Even though most ganglion cells are responsive to NMDA (Shen et al., 2006), dopamine acts on almost all retinal ganglion cells (Zhang et al., 2008), more work is needed to understand the how an imbalance in both NMDAR and dopamine can affect the ERG response. Furthermore, future studies would need to explore whether dysregulation of the retinal ganglion cells in schizophrenia is present in both the ON and OFF pathway, as retinal ganglion cells are characterized by their on-center vs. off-center surround. This can be investigated by measuring the PhNR at offset period during long flash stimulation (Horn et al., 2011).

The OPs, like the PhNR, shed light into inner retinal activity. We analyzed the frequencies of the OPs in three groups to allow distinction of two cell types in the inner retina, RGCs and amacrine cells (Zhou et al., 2007). While findings did not have statistical 3-way nor 2-way interactions, it may in part due to our wide range of ages. OPs were reported to be sensitive to age (Dimopoulos et al., 2014), which would confound disease state-induced changes. However, OP analyses have potential to reflect early, age-related changes related to disease state that may not be reflected in other ERG variables, and our future studies will be directed at these analyses with a larger cohort of subjects. We saw a significant interaction between the disease state and sex for the high frequency and combined OP measurement. While the results only trended toward significant main effects of disease state at the highest flash strength only in the low-frequency OPs, this would suggest potential disruption of amacrine non-spiking activity (Zhou et al., 2007). Amacrine cells are the primary inhibitory input onto RGCs. As the NMDAR is involved in the transient response of on-off amacrine cells (Dixon and Copenhagen, 1992), investigation of their involvement is important. The two PERG data sets used different monitor types and visual stimuli.

The latencies of all three PERG components were longer in the data collected using the CRT compared to the LED display. The CRT monitor generates images using an electron gun that sweeps across the screen, and at any given point in time, only parts of the contrast-reversed image were presented to the eye. In contrast, the LED monitor synchronously reverses contrast over the entire screen, resulting in decreased latencies (Monsalve et al., 2017). Amplitude

of the PERG components were different across the two datasets, with PERG responses recorded with the CRT monitor having higher N95 amplitudes and lower P50 amplitudes than those with the LED monitor. PERG responses collected with an LED monitor were reported to have higher amplitudes than CRT monitors (Monsalve et al., 2017), which may explain the higher P50 amplitudes in the data collected using the LED monitor. N95 amplitude was lower in the LED dataset, which was recorded at a higher reversal rate. N95 amplitude was shown to decrease as reversal rate increased (Özdamar et al., 2014). PERG responses recorded with the CRT monitor showed a tendency towards significantly increased N95 implicit times in subjects with schizophrenia compared to controls. N95 implicit time of PERG responses recorded with the LED monitor had a borderline significant interaction between sex and disease state, where N95 implicit time was higher in males with schizophrenia than control males, with no differences in female subjects. PERG responses recorded using the LED monitor and not the CRT monitor showed a borderline significant attenuation of N35 amplitude in people with schizophrenia compared to controls. In the absence of a better understanding of the exact origin of the PERG components (Porciatti, 2015), interpreting these results is not straightforward. Previous studies showed that the amplitude, but not implicit time, of PERG components was reduced in diseases with damage to RGCs such as glaucoma (Preiser et al., 2013) and diabetes (Prager et al., 1990). In addition, pharmacological blocking of spiking activity of the RGCs in primates reduced the amplitude of the N95 component (Luo and Frishman, 2011; Viswanathan et al., 1999). However, diseases such as glaucoma and diabetes are associated with the death of RGCs rather than

dysfunction specifically, as we hypothesize occurs in schizophrenia. Moreover, dysfunction of NMDARs would alter the activity of other neuronal populations in the retina whose activity modulates activity of RGCs. In glaucoma, selective death of RGCs occurs while activity of photoreceptors or bipolar cells remains intact (Viswanathan et al., 1999). Our ERG results might reflect overall changes in different parts of the retinal circuitry that resulted in altered activity of RGCs as captured by the PERG response. The difference we observed between the CRT and LED data could relate to the higher temporal precision of the LED monitor, which could reveal more subtle differences among the neuronal populations under study. The difference in reversal rate or pattern of the visual stimulus may alter the dynamics of NMDAR under one stimulation condition and not the other. Our results demonstrate the potential for the PERG to visualize functional differences underlying schizophrenia when larger sample sizes are used and show the complex effects elicited by choice of visual stimulus or display type on the results. It would be valuable in the future to subdivide subjects by duration of schizophrenia as well as treatment differences.

There are several limitations of this study. The data would be significantly strengthened with a larger study population and a wider range of flash strengths. When our data using the NMDA receptor hypofunction mouse model of schizophrenia showed significant differences based on sex, we disaggregated the ERG data in the present study; this, however, lowered the overall number of subjects based on sex. In addition, only a subset of the subjects had a PERG using the LED display; comparisons would have been more easily made had we been able to obtain this data from all the subjects originally tested using the CRT

method of PERG acquisition. Finally, as will all studies using populations of individuals with schizophrenia, the medications varied between subjects. With a larger cohort of subjects, future studies should be able to analyze groups of subjects with schizophrenia on similar medications. In addition, some details, such as phase of menstrual cycle, could not be assessed, as when the data were collected, it was unknown that sex a variable. We cannot rule out a small variation in the ERG when morning recordings were compared to recordings made in the late afternoon, early evening (Lavoie et al., 2010; Marcus et al., 2004; Rufiange et al., 2003). The current study used three flash intensities that were in the lower and middle limb of the intensity-response data that fits the Naka-Rushton equation for photopic hill calculation, thus were below the levels when the phototopic hill would occur. Other studies used significantly greater ranges in light intensities, when this type of effect would certainly be present (Binns et al., 2011; Joshi, Ly, and Viswanathan, 2017). It would be beneficial to study the intensity-response function of both the b-wave amplitude and PhNR in people with schizophrenia by analyzing a wider range of flash-strengths. Future studies will more tightly control the time of ERG recordings to eliminate this potential variable. Similarly, with a larger cohort, it would be possible to control for differential disease severity (see Supplemental Figure 4.1). Collectively, the current study identified key variables for defining how the ERG could be used reliably as a biomarker for schizophrenia.

The ERG as a biomarker for schizophrenia holds promise, albeit with differential impairments across sex. It is important to note that the retina has several neurons that express NMDAR, and future work will focus on which

protocols will be best at differentiating between normal function and dysfunction as it relates to identification of individuals with different underlying causes of their schizophrenia.

Supplemental Material

Supplemental Table 4.1 Variability measurements. *Variability measurements of the a-wave, b-wave, PhNR, and PhNR at negative 72 statistics (N72). Values in S.D. [variance]. Assumption of equal variance tested with Levene's tests p-values provided. HC: healthy controls; Scz: people with schizophrenia. Statistical analyses and creation of the table were done by Nathalia Torres Jimenez.*

Supp. Table 4.1		Female		Male	
Flash Strengh	Levene's Test	HC vs Scz		HC vs Scz	
a-wave amplitude					
1 cd·s/m^2	0.432	8 [67]	9 [77]	13 [156]	13 [177]
5 cd·s/m^2	0.173	14 [195]	16 [263]	14 [207]	17 [293]
10 cd·s/m^2	0.027	13 [180]	18 [317]	8 [63]	29 [866]
b-wave amplitude					
1 cd·s/m^2	0.522	29 [865]	29 [861]	25 [606]	22 [485]
5 cd·s/m^2	0.573	23 [521]	18 [307]	28 [807]	19 [355]
10 cd·s/m^2	0.700	22 [503]	16[260]	27 [745]	23 [543]
PhNR amplitude					
1 cd·s/m^2	0.007	16 [272]	19 [351]	34 [1149]	66 [4343]
5 cd·s/m^2	0.016	33 [1058]	24 [583]	37 [1383]	62 [4127]
10 cd·s/m^2	0.000	18 [320]	29 [846]	25 [629]	124 [15270]
Neg72 amplitude					
1 cd·s/m^2	0.003	17 [276]	16 [250]	36 [1266]	31 [956]
5 cd·s/m^2	0.112	33 [1058]	25 [645]	39 [1524]	55 [3017]
10 cd·s/m^2	0.009	19 [343]	30 [873]	25 [626]	105 [11018]

Supplemental Table 4.2 Statistical for b-wave amplitude and the b/a ratio *for the PhNR-fERG. Statistical analyses and creation of the table were done by Nathalia Torres Jimenez.*

Supp. Table 4.2	b-wave amplitude		b/a ratio	
Flash Strength · Sex · Disease State	F (1.4,73)=0.5, p =0.57, η_p^2=0.009		F (1.5,78)=0.9, p =0.39, η_p^2=0.017	
Simple two-way interactions				
Flash Strength · Disease State	F(1.4,73)= 0.9, p =0.395		F(1.5,78)=0.5, p =0.54	
Flash Strength · Sex	F(1.4,73)= 1.3, p =0.275		F(1.5,78)=0.8 , p =0.41	
Disease State · Sex at each level of flash strength	**1 cd·s/m2**	F(1,51)=0.3, p =0.61	**1 cd·s/m2**	F(1,51)=0.03, p =0.86
	5 cd·s/m2	F(1,51)=0.3, p =0.57	**5 cd·s/m2**	F(1,51)=0.1, p =0.82
	7 cd·s/m2	F(1,51)=0.03, p =0.86	**7 cd·s/m2**	F(1,51)=0.9, p =0.34
Main Effects				
Main Effects of the two-way interaction at each level of flash strength		Disease State / Sex		Disease State / Sex
	1 cd·s/m2	0.576 / 0.417	**1 cd·s/m2**	0.662 / 0.767
	5 cd·s/m2	0.088 / 0.339	**5 cd·s/m2**	0.625 / 0.617
	7 cd·s/m2	0.110 / 0.760	**7 cd·s/m2**	0.687 / 0.542

Supplemental Table 4.3: Statistical analysis for a-wave, b-wave, and PhNR implicit time *from the PhNR-fERG. . [Statistical analyses and creation of the table was done by Nathalia Torres Jimenez]*

Supp. Table 4.3	a-wave implicit time		b-wave implicit time		PhNR implicit time	
Flash Strength · Sex · Disease State	F(1.5,76)= 1.8 p =0.19, η_p^2=0.033		F(1.2,62)= 0.4, p =0.59, η_p^2=0.007		F(1.5,78)= 0.1, p =0.82, η_p^2=0.003	
Simple Two-way interactions						
Flash Strength · Disease State	F(1.5,76)= 1.4 p =0.254		F(1.2,62)= 0.1, p =0.841		F(1.5,78)= 0.8 p =0.434	
Flash Strength · Sex	F(1.5,76)= 0.7 p =0.471		F(1.2,62)= 0.2, p =0.714		F(1.5,78)= 0.01 p =0.975	
Disease State · Sex at each level of flash strength	**1 cd·s/m2**	F(1,51)=0.3, p =0.573	**1 cd·s/m2**	F(1,51)=0.8, p =0.367	F(1,51)=0.01, p=0.933	
	5 cd·s/m2	F(1,51)=0.00, p =0.983	**5 cd·s/m2**	F(1,51)=0.03, p =0.872	F(1,51)=0.1, p=0.779	
	7 cd·s/m2	F(1,51)=0.7, p =0.399	**7 cd·s/m2**	F(1,51)=0.3, p =0.592	F(1,51)=0.1, p=0.764	
Main Effects						
Main Effects of the two-way interaction at each level of flash strength		Disease State / Sex		Disease State / Sex		Disease State / Sex
	1 cd·s/m2	0.247 / 0.737	**1 cd·s/m2**	0.267 / 0.649	**1 cd·s/m2**	0.520 / 0.198
	5 cd·s/m2	0.429 / 0.205	**5 cd·s/m2**	0.266 / 0.417	**5 cd·s/m2**	0.962 / 0.216
	7 cd·s/m2	0.975 / 0.244	**7 cd·s/m2**	0.299 / 0.546	**7 cd·s/m2**	0.681 / 0.184

Supplemental Table 4.4*: Analysis of the PhNR/b-wave ratio relative to light intensity for male and female people with schizophrenia compared to controls. The males with schizophrenia are the only cohort where the PhNR was increased compared to the b-wave (red). . [Descriptive statistics and creation of the table was done by Nathalia Torres Jimenez]*

Supp. Table 4.4

	Sex	Light Intensity	b-wave amplitude	PhNR amplitude	PhNR/b-wave ratio
HC	Male	1	56 ± 24.6	46 ± 33.9	0.94
		5	76 ± 28.4	49 ± 37.2	0.75
		7	80 ± 27.3	44 ± 25.1	0.64
	Female	1	54 ± 29.4	23 ± 16.5	0.54
		5	74 ± 22.8	39 ± 32.5	0.58
		7	81 ± 22.4	38 ± 17.9	0.49
Scz	Male	1	56 ± 22.0	65 ± 65.9	**1.51**
		5	69 ± 18.8	77 ± 64.2	**1.32**
		7	69 ± 23.3	111 ± 123.6	**3.28**
	Female	1	46 ± 29.3	26 ± 18.7	0.80
		5	60 ± 17.5	47 ± 24.1	0.86
		7	72 ± 16.1	48 ± 29.1	0.71

Supplemental Figures

Supplemental Figure 4.1

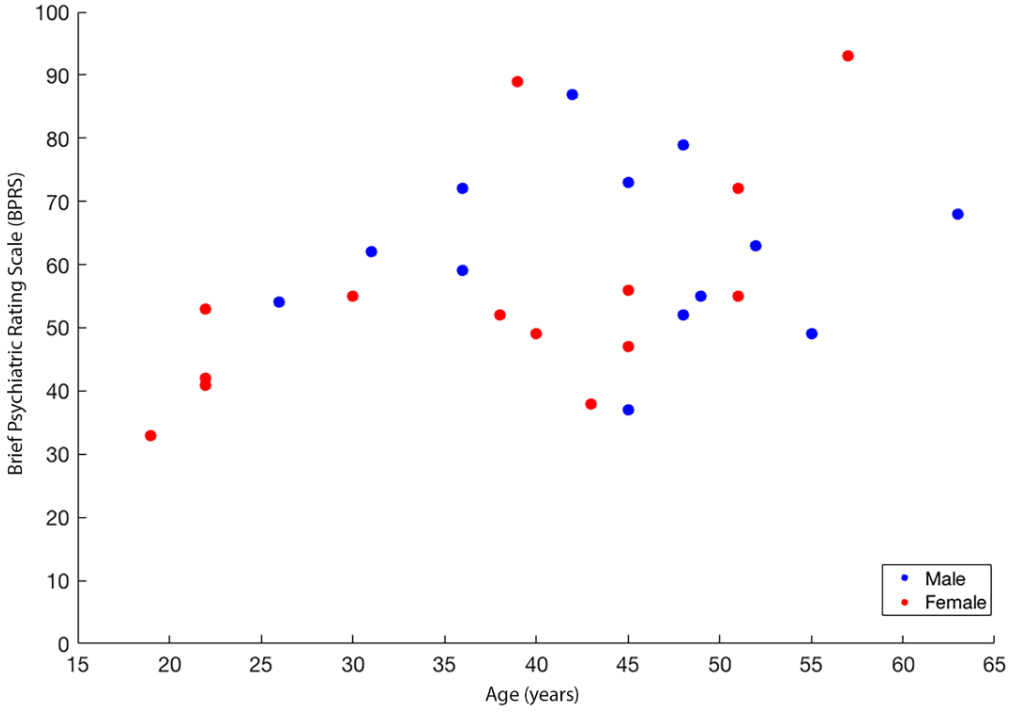

Supplemental Figure 4.1 Scatterplot of BPRS as a function of age. *Analysis of the Brief Psychiatric Rating Scale (BPRS) with age on the x-axis and BPRS score on the y-axes. Blue circles indicate males with schizophrenia and red circles indicate females with schizophrenia. Linear regression analysis showed a significant difference between disease severity of the males and females in our study despite similar age ranges. [This figure was co-developed by Nathalia and Pantea, and produced by Pantea Moghimi]*

Supplemental Figure 4.2

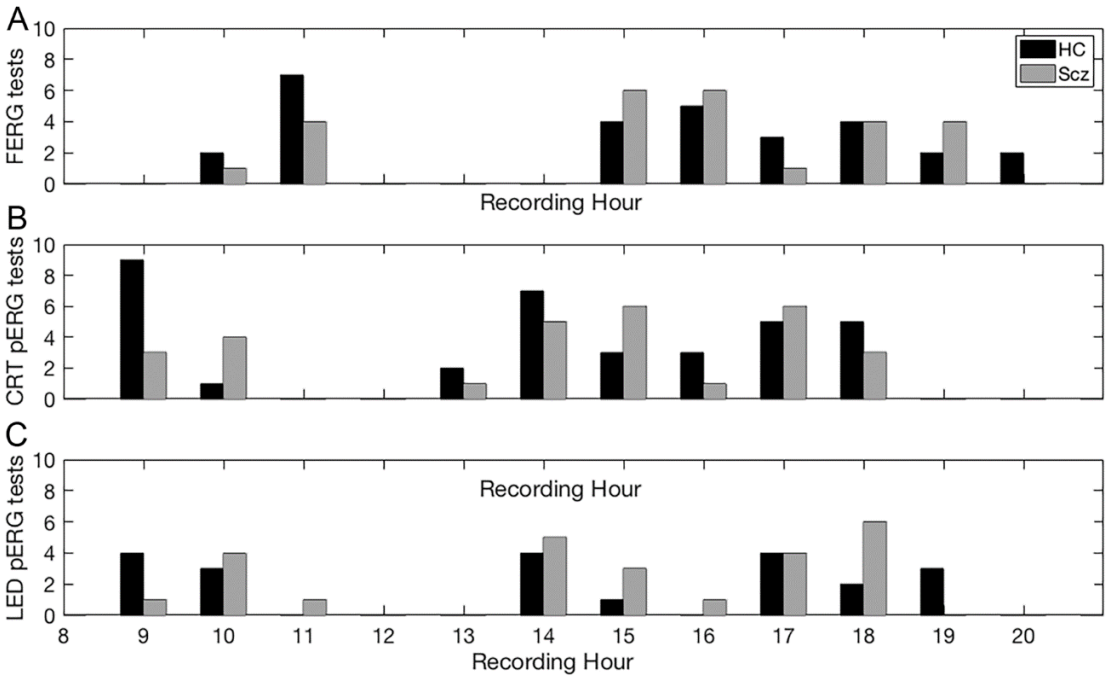

Supplemental Figure 4.2 Histograms representing time of recording. Analysis *of the time of the ERG recording for all subjects for all three tests performed. X-axis indicated time using the 24-hour clock. Black indicates control subjects and gray indicates people with schizophrenia.*

Supplemental Figure 4.3

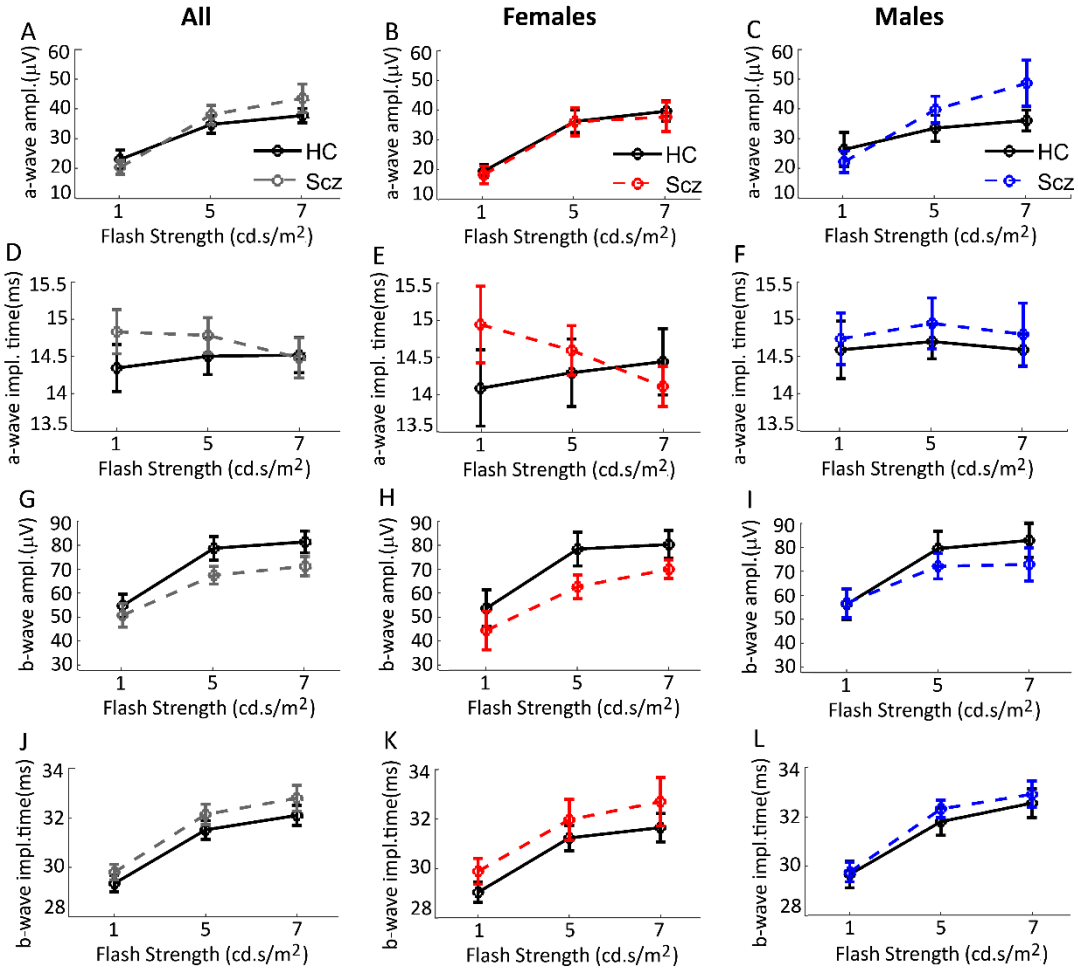

Supplemental Figure 4.3*: Analyses of the PhNR-fERG for (A,B,C) a-wave amplitude (Ampl), (D, E, F) a-wave implicit time (Impl.), (G,H, I) b-wave amplitude, and (J,K,L) b-wave implicit time for all subjects (black), for female controls (black) and females with schizophrenia (red), and male controls (black) and males with schizophrenia (blue). Solid lines are control subjects (HC) and dotted lines are people with schizophrenia (Scz). Bars indicate standard deviation. Flash strength is in candelas per second per meters squared (Cd.s/m2), a measure of luminance levels. [This figure was co-developed by Nathalia and Pantea, and produced by Pantea Moghimi.]*

Supplemental Figure 4.4

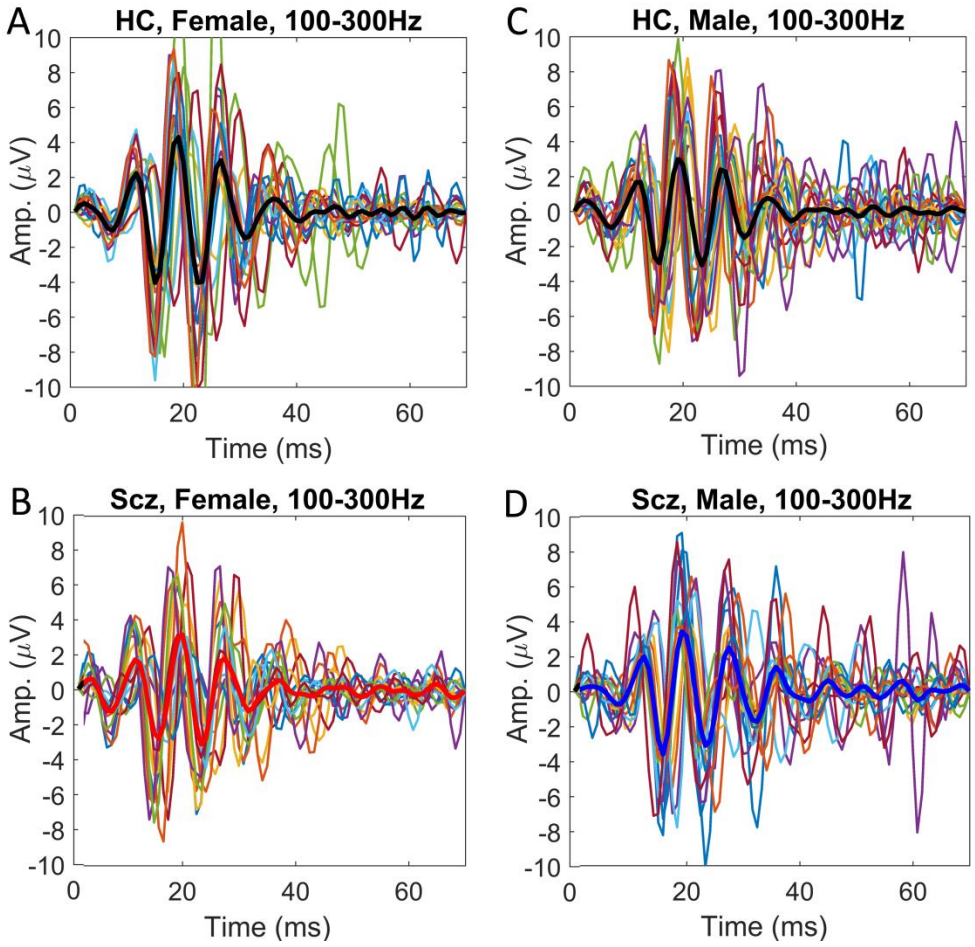

Supplemental Figure 4.4*: All oscillatory potentials at 100-300Hz for all subjects, each in a different color. The black trace is the mean of all subjects for each cohort. (A) Female control subjects (HC), (B) females with schizophrenia (Scz), (C) male control subjects (HC), and (D) males with schizophrenia (Scz). Amp is amplitude, given in microVolts (μV). Time is in milliseconds (ms). [This figure was co-developed by Nathalia and Pantea, and produced by Pantea Moghimi.]*

]

Chapter 5

Conclusion

The purpose of this work was to evaluate whether visual signals from the eye could identify NMDAR signal deficiencies. My interest was specifically in the outer retina, as fERG abnormalities in people with schizophrenia were observed early in the retinal pathway but the biological bases for them is not understood. However, it was unclear whether these changes would represent NMDAR functionality, given the implication of reduced NMDAR function in the etiological underpinnings of schizophrenia. Since it is well established that NMDARs contribute to the light-evoked responses from retinal ganglion cells (Coleman and Miller, 1978), reduction in retinal field potentials that are derived from the retinal ganglion cell layer would be expected. Surprisingly, a reduction in the a- and b-wave, derived from photoreceptors and bipolar cells respectively, was observed in people with schizophrenia. While there could be a myriad of reasons for a reduced a- and b-wave that does not pertain to the NMDAR, it is also known that functional NMDAR channels are expressed in horizontal cells (O'Dell and Christensen, 1989) and NMDAR subunits are expressed throughout the retina (Fletcher et al. 2002; Hartveit et al. 1994, Haverkar and Wässle, 2002), highlighting the possibility for changes in fERG to reflect one or more NMDAR components. This led me to inquire whether any of the abnormalities in the a- and b-wave in people with schizophrenia were due to NMDAR functional changes. Due to the presence of functional NMDAR in the outer retina, it is possible that light-evoked signal transmission is edited earlier in the retinal

pathway. In this work, I demonstrate that D-serine deprivation or excess affects outer retinal field potentials, which infers changes to NMDAR functioning due to D-serine's role as co-agonist for the glycine site. Alternatively, it could reflect a role for D-serine in the retina other than being a co-agonist for the NMDAR that has not been discovered yet. Furthermore, I demonstrate that effects of D-serine depend on the sex of the animal, with males showing the most pronounced change. Therefore, my work contributes to the hypothesis that the fERG could be a potential biomarker for schizophrenia. I summarize the findings below.

In chapter 1, I evaluated the fERG of NMDAR-hypofunction mouse model caused by D-serine deprivation ($SR^{-/-}$) to identify whether there is a significant NMDAR component in the outer retina, which would be reflected in the a- and b-wave. I demonstrate temporal delay and amplitude reduction in the outer retina of $SR^{-/-}$ mice, which is more significant in male $SR^{-/-}$ mice. These results suggest that D-serine deprivation effects the outer retina, and it is more prominent in male mice. This work mirrors the alterations in people with schizophrenia compared to age matched controls, highlighting the fERG potential as a biomarker for the disease. Furthermore, it demonstrates that NMDAR hypofunction-related changes can be observed in the outer retina, illuminating our understanding of D-serine in retinal network as whole.

The next steps for this work are to evaluate inner retinal functioning, which can be done through the measurement of the oscillatory potentials (OPs) in order to understand the full scope of abnormalities that are caused by D-serine deprivation. A second step is to investigate whether NMDAR expression patterns differ in the $SR^{-/-}$ mouse. Serine racemase and D-serine have a higher

expression level during the first month of life, but it is not clear why that is so and what the functional ramifications of these changes are. It is also unclear whether serine racemase and D-serine are necessary for appropriate expression of the NMDAR subunits in the retina (Dun et al., 2008; Romero et al., 2014). Immunofluorescent studies targeting NR1, NR2A, B, and C subunits would elucidate whether the NMDAR expression pattern changes due to developmental loss of serine racemase. Lastly, investigations on how hormones such as estrogen or testosterone could interact with D-serine is necessary to understand the sex differences observed. Knowing this could provide insight into differences in symptom onset between males and females afflicted with schizophrenia.

In chapter 2, I investigated whether exogenous delivery of D-serine would restore abnormalities in the fERG of $SR^{-/-}$ mouse. Topical 5mM delivery of D-serine in WT retinas created a pharmacologically-induced hyperfunction of the NMDAR in WT mice. Surprisingly, our results showed that male WT mice were affected profoundly by the exogenous delivery of D-serine, which delayed and reduced specific responses in the fERG. While exogenous D-serine did not statistically restore the abnormalities found in the experiments described in chapter 1 in $SR^{-/-}$ mice, it did improve the response of the retina toward normalcy. The next steps for this work are to control the concentration of D-serine by performing intravitreal injections of various concentrations of D-serine to evaluate the dose-dependent changes of D-serine in the fERG. In addition, these intravitreal injections will help us to understand whether these changes caused by D-serine are due to its role as NMDAR co-agonist, and this would be accomplished by delivering the following agents: a competitive antagonist of the

NMDAR glycine, 5,7-Dichlorokynurenic acid (DCK) and a competitive antagonist for the glutamate binding site of the NMDAR, 2*R*-amino-5-phosphonovaleric acid (AP5). These experiments would help clarify whether the changes in retinal function are mediated by the NMDAR, or if D-serine is acting on another receptor or cell. If it is in fact mediated by NMDAR, introduction of DCK and AP5 in WT mice should drastically reduce the b-wave amplitude of the fERG. Lastly, to investigate the male differences observed upon topical deliver of D-serine and in D-serine deprived mice ($SR^{-/-}$), it be worth measuring the amount of DAAO with capillary electrophoresis in all groups, to evaluate whether the sex differences in DAAO concentration observed in the kidney (Konno and Yasumura, 1983) is present in the retina.

In chapter 3, we evaluated whether there were any retinal ganglion cell abnormalities in people with schizophrenia. While reduced outer retina field potentials were observed in people with schizophrenia as reflected by a reduced a- and b-wave, retinal field potentials that derived from the inner retina, such as the photopic negative response and the pattern-electroretinogram, were only tested by one other laboratory and not found to be significant (Demmin et al., 2018). We observed statistically significant differences in the PhNR, but not the outer retina. Interestingly, this difference appeared to be more prominent in males with schizophrenia rather than females. Future work in people with schizophrenia, should conduct fERGs at different background light intensities. Based on our mouse studies, it may be that collecting fERGs under mesopic conditions is critical to parse out differences between control human retinal function and the retinas of people with schizophrenia. All the mouse studies were

performed under mesopic fERG, which is not incorporated in the ISCEV protocol (McCullock et al., 2015), but may illustrate mental health differences as visualized through retinal ERG analysis, that would not be seen under dark- or light-adapted conditions. This is supported by differences observed in 'Photopic 1 (P_1)' in people with schizophrenia (Demmin et al., 2018), which technically was mesopic because the background condition was insufficient to saturate rods. Furthermore, further studies in human subjects to identify abnormalities in the fERG of people with schizophrenia should include a wider-array of flash strengths in order to understand the intensity/response function of this population. Given the network changes that NMDARs play in the brain, it is worth investigating parameters provided by the Naka-Rushton equation, which identifies response parameters in response to light. For instance, the Naka-Rushton equation can provide the flash strength at which the response of the b-wave and the PhNR saturates (I_{max}) in people with schizophrenia or the maximum amplitude of the response (b_{max} and $PhNR_{max}$) attained, which can be used to understand the role of NMDAR in response to light intensity demands. Whole-cell patch clamp and extracellular recordings have demonstrated that D-serine plays a role in light intensity demands, likely from recruitment of the NMDAR (Stevens et al., 2011; Gustafson et al., 2015). This study suggests that the intensity/response function of people with schizophrenia would differ as they may not be able to meet the light intensity demands. Therefore, collecting a wider intensity array would elucidate how global- retinal changes occur in response to light demands in people with schizophrenia. Lastly, analyses of the fERG should

not pool males and females together when performing analyses, as it is quite apparent that there are sex differences in the ERG.

To conclude, the fERG holds promise in revealing NMDAR abnormalities that may play a role in the pathology that develops in people with schizophrenia. My work demonstrates that D-serine may interacts with sex hormones, which is reflected in the fERG response. Future studies will elucidate more clearly the role of the NMDAR in these processes.

Bibliography

Adams, S. A., & Nasrallah, H. A. (2018). Multiple retinal anomalies in schizophrenia. *Schizophrenia Research, 195*, 3-12.

Aizenman, E., Frosch, M., & Lipton, S. A. (1988). Responses mediated by excitatory amino acid receptors in solitary retinal ganglion cells from rat. *The Journal of Physiology, 396*(1), 75-91.

Aldebasi, Y. H., Drasdo, N., Morgan, J. E., & North, R. V. (2004). S-cone, L+ M-cone, and pattern, electroretinograms in ocular hypertension and glaucoma. *Vision Research, 44*(24), 2749-2756.

Anis, N. A., Berry, S. C., Burton, N. R., & Lodge, D. (1983). The dissociative anaesthetics, ketamine and phencyclidine, selectively reduce excitation of central mammalian neurones by N-methyl-aspartate. *British Journal of Pharmacology, 79*(2), 565-575.

Asi, H., & Perlman, I. (1992). Relationships between the electroretinogram a-wave, b-wave and oscillatory potentials and their application to clinical diagnosis. *Documenta Ophthalmologica, 79*(2), 125-139.

Association, A. P. (2013). *Diagnostic and statistical manual of mental disorders (DSM-5®)*: American Psychiatric Pub.

Bai, N., Aida, T., Yanagisawa, M., Katou, S., Sakimura, K., Mishina, M., & Tanaka, K. (2013). NMDA receptor subunits have different roles in NMDA-induced neurotoxicity in the retina. *Molecular Brain*, *6*(1), 34.

Bach, M., Brigell, M. G., Hawlina, M., Holder, G. E., Johnson, M. A., McCulloch, D. L., Viswanathan, S. (2013). ISCEV standard for clinical pattern electroretinography (PERG): 2012 update. *Documenta Ophthalmologica, 126*(1), 1-7.

Balogh, Z., Benedek, G., & Keri, S. (2008). Retinal dysfunctions in schizophrenia. *Prog Neuropsychopharmacology and Biological Psychiatry, 32*(1), 297-300. doi:10.1016/j.pnpbp.2007.08.024

Balu, D. T., & Coyle, J. T. (2015). The NMDA receptor 'glycine modulatory site' in schizophrenia: D-serine, glycine, and beyond. *Current Opinion in Pharmacology, 20*, 109-115.

Baron, M., Gruen, R., Asnis, L., & Kane, J. (1983). Age-of-onset in schizophrenia and schizotypal disorders. Clinical and genetic implications. *Neuropsychobiology, 10*(4), 199-204. doi:10.1159/000118011

Basu, A., Tsai, G., Ma, C., Ehmsen, J., Mustafa, A., Han, L., Lange, N. (2010). Targeted disruption of serine racemase affects glutamatergic neurotransmission and behavior. *Molecular Psychiatry, 14*(7), 719.

Bear, M. F., Kleinschmidt, A., Gu, Q. A., & Singer, W. (1990). Disruption of experience-dependent synaptic modifications in striate cortex by infusion of an NMDA receptor antagonist. *Journal of Neuroscience, 10*(3), 909-925.

Beard, M., Davies, T., Holloway, M., & Holtzman, E. (1988). Peroxisomes in pigment epithelium and Müller cells of amphibian retina possess D-amino acid oxidase as well as catalase. *Experimental Eye Research, 47*(6), 795-806.

Benchorin, G., Calton, M. A., Beaulieu, M. O., & Vollrath, D. (2017). Assessment of Murine Retinal Function by Electroretinography. *Bio-protocol, 7*(7).

Bendikov, I., Nadri, C., Amar, S., Panizzutti, R., De Miranda, J., Wolosker, H., & Agam, G. (2007). A CSF and postmortem brain study of D-serine metabolic parameters

in schizophrenia. *Schizophrenia Research, 90*(1-3), 41-51. doi:10.1016/j.schres.2006.10.010
Binns, A., Mortlock, K. E., & North, R. V. (2011). The relationship between stimulus intensity and response amplitude for the photopic negative response of the flash electroretinogram. *Documenta Ophthalmologica, 122*(1), 39-52.
Blanke, M. L., & Van Dongen, A. M. J. (2009). Activation Mechanisms of the NMDA Receptor, Chapter 13. *Biology of the NMDA Receptor*.
Blokhuis, C., Demirkaya, N., Cohen, S., Wit, F. W., Scherpbier, H. J., Reiss, P., Verbraak, F. D. (2016). The eye as a window to the brain: neuroretinal thickness is associated with microstructural white matter injury in HIV-infected children. *Investigative Ophthalmology and Visual Science, 57*(8), 3864-3871.
Brandstätter, J. H., Hartveit, E., Sassoè-Pognetto, M., & Wässle, H. (1994). Expression of NMDA and high-affinity kainate receptor subunit mRNAs in the adult rat retina. *European Journal of Neuroscience, 6*(7), 1100-1112.
Bresnick, G. H., & Palta, M. (1987). Oscillatory potential amplitudes: relation to severity of diabetic retinopathy. *Archives of Ophthalmology, 105*(7), 929-933.
Bresnick, G. H., & Palta, M. (1987). Temporal aspects of the electroretinogram in diabetic retinopathy. *Archives of Ophthalmology, 105*(5), 660-664.
Bristow, D. R., Bowery, N. G., & Woodruff, G. N. (1986). Light microscopic autoradiographic localisation of [3H] glycine and [3H] strychnine binding sites in rat brain. *European Journal of Pharmacology, 126*(3), 303-307.
Brown, K., & Wiesel, T. (1961). Localization of origins of electroretinogram components by intraretinal recording in the intact cat eye. *The Journal of Physiology, 158*(2), 257-280.
Chen, S., Zhi, Z. N., Ruan, Q. Q., Liu, Q. X., Li, F., Wan, F., Zhou, X. T. (2017). Bright light suppresses form-deprivation myopia development with activation of dopamine D1 receptor signaling in the ON pathway in retina. *Investigative Ophthalmology and Visual Science, 58*(4), 2306-2316. doi:10.1167/iovs.16-20402
Chong, H. Y., Teoh, S. L., Wu, D. B.-C., Kotirum, S., Chiou, C.-F., & Chaiyakunapruk, N. (2016). Global economic burden of schizophrenia: a systematic review. *Neuropsychiatric Disease and Treatment, 12*, 357.
Chu, E. M.-Y., Kolappan, M., Barnes, T. R., Joyce, E. M., & Ron, M. A. (2012). A window into the brain: an in vivo study of the retina in schizophrenia using optical coherence tomography. *Psychiatry Research: Neuroimaging, 203*(1), 89-94.
Chumakov, I., Blumenfeld, M., Guerassimenko, O., Cavarec, L., Palicio, M., Abderrahim, H., La Rosa, P. (2002). Genetic and physiological data implicating the new human gene G72 and the gene for D-amino acid oxidase in schizophrenia. *Proceedings of the National Academy of Sciences, 99*(21), 13675-13680.
Clark, L. C., Kochakian, C. D., & Fox, R. P. (1943). The effect of castration and testosterone propionate on d-amino acid oxidase activity in the mouse. *Science*, *98*(2534), 89-89.
Cloutier, M., Aigbogun, M. S., Guerin, A., Nitulescu, R., Ramanakumar, A. V., Kamat, S. A., Henderson, C. (2016). The economic burden of schizophrenia in the United States in 2013. *The Journal of Clinical Psychiatry, 77*(6), 764-771.

Cohen, E. D., & Miller, R. F. (1994). The role of NMDA and non-NMDA excitatory amino acid receptors in the functional organization of primate retinal ganglion cells. *Visual Neuroscience, 11*(2), 317-332.
Coleman, P. A., & Miller, R. F. (1988). Do N-methyl-D-aspartate receptors mediate synaptic responses in the mudpuppy retina? *Journal of Neuroscience, 8*(12), 4728-4733.
Corrigan, J. J. (1969). D-amino acids in animals. *Science, 164*(3876), 142-149.
Coull, B. M., & Cutler, R. W. (1978). Light-evoked release of endogenous glycine into the perfused vitreous of the intact rat eye. *Investigative Ophthalmology Visual Science, 17*(7), 682-684.
Coyle, J. T. (1996). The glutamatergic dysfunction hypothesis for schizophrenia. *Harvard Review of Psychiatry, 3*(5), 241-253.
Coyle, J. T. (2006). Glutamate and schizophrenia: beyond the dopamine hypothesis. *Cellular and Molecular Neurobiology, 26*(4-6), 363-382.
Cyr, M., Ghribi, O., Thibault, C., Morissette, M., Landry, M., & Di Paolo, T. (2001). Ovarian steroids and selective estrogen receptor modulators activity on rat brain NMDA and AMPA receptors. *Brain Research Reviews, 37*(1-3), 153-161.
Daniels, B. A., & Baldridge, W. H. (2010). D-Serine enhancement of NMDA receptor-mediated calcium increases in rat retinal ganglion cells. *Journal of Neurochemistry, 112*(5), 1180-1189.
Das, S., Sasaki, Y. F., Rothe, T., Premkumar, L. S., Takasu, M., Crandall, J. E., Nakanishi, N. (1998). Increased NMDA current and spine density in mice lacking the NMDA receptor subunit NR3A. *Nature, 393*(6683), 377-381. doi:10.1038/30748
Demmin, D. L., Davis, Q., Roche, M., & Silverstein, S. M. (2018). Electroretinographic anomalies in schizophrenia. *Journal of Abnormal Psychology, 127*(4), 417-428. doi:10.1037/abn0000347
Desai, P. R., Lawson, K. A., Barner, J. C., & Rascati, K. L. (2013). Estimating the direct and indirect costs for community-dwelling patients with schizophrenia. *Journal of Pharmaceutical Health Services Research, 4*(4), 187-194.
Diamond, J. S., & Copenhagen, D. R. (1993). The contribution of NMDA and non-NMDA receptors to the light-evoked input-output characteristics of retinal ganglion cells. *Neuron, 11*(4), 725-738.
Dimopoulos, I. S., Freund, P. R., Redel, T., Dornstauder, B., Gilmour, G., & Sauvé, Y. (2014). Changes in rod and cone-driven oscillatory potentials in the aging human retina. *Investigative Ophthalmology and Visual Science, 55*(8), 5058-5073.
Dixon, D. B., & Copenhagen, D. R. (1992). Two types of glutamate receptors differentially excite amacrine cells in the tiger salamander retina. *The Journal of Physiology, 449*(1), 589-606.
Driesen, N. R., McCarthy, G., Bhagwagar, Z., Bloch, M., Calhoun, V., D'Souza, D. C., Suckow, R. F. (2013). Relationship of resting brain hyperconnectivity and schizophrenia-like symptoms produced by the NMDA receptor antagonist ketamine in humans. *Molecular Psychiatry, 18*(11), 1199.
Dun, Y., Duplantier, J., Roon, P., Martin, P. M., Ganapathy, V., & Smith, S. B. (2008). Serine racemase expression and D-serine content are developmentally regulated in neuronal ganglion cells of the retina. *Journal Neurochemistry, 104*(4), 970-978. doi:10.1111/j.1471-4159.2007.05015.x

Faraone, S. V., Chen, W. J., Goldstein, J. M., & Tsuang, M. T. (1994). Gender differences in age at onset of schizophrenia. *British Journal of Psychiatry, 164*(5), 625-629.
Farshi, P., Fyk-Kolodziej, B., Krolewski, D. M., Walker, P. D., & Ichinose, T. (2016). Dopamine D1 receptor expression is bipolar cell type-specific in the mouse retina. *Journal of Comparative Neurology, 524*(10), 2059-2079.
Ferreira, I. L., Duarte, C. B., Santos, P. F., Carvalho, C. M., & Carvalho, A. P. (1994). Release of [3H] GABA evoked by glutamate receptor agonists in cultured chick retina cells: effect of Ca2+. *Brain Research, 664*(1-2), 252-256. doi:10.1016/0006-8993(94)91981-x
First, M. B., Regier, D. A., & Kupfer, D. J. (2002). *A Research Agenda for DSM-V*: Citeseer.
Fletcher, E. L., Hack, I., Brandstätter, J. H., & Wässle, H. (2000). Synaptic localization of NMDA receptor subunits in the rat retina. *Journal of Comparative Neurology, 420*(1), 98-112.
Flood, M. D., Moore-Dotson, J. M., & Eggers, E. D. (2018). Dopamine D1 receptor activation contributes to light-adapted changes in retinal inhibition to rod bipolar cells. *Journal Neurophysiology, 120*(2), 867-879. doi:10.1152/jn.00855.2017
Frishman, L., Sustar, M., Kremers, J., McAnany, J. J., Sarossy, M., Tzekov, R., & Viswanathan, S. (2018). ISCEV extended protocol for the photopic negative response (PhNR) of the full-field electroretinogram. *Documenta Ophthalmologica, 136*(3), 207-211.
Frishman, L. J., & Wang, M. H. (2011). Electroretinogram of human, monkey and mouse. *Adler's Physiology of the Eye, 24*, 480-501.
Föcking, M., Lopez, L. M., English, J. A., Dicker, P., Wolff, A., Brindley, E., Cotter, D. R. (2015). Proteomic and genomic evidence implicates the postsynaptic density in schizophrenia. *Molecular Psychiatry, 20*(4), 424.
Gao, W.-J., & Snyder, M. A. (2013). NMDA hypofunction as a convergence point for progression and symptoms of schizophrenia. *Frontiers in Cellular Neuroscience, 7*, 31.
Gauvin, M., Lina, J.-M., & Lachapelle, P. (2014). Advance in ERG analysis: from peak time and amplitude to frequency, power, and energy. *BioMed Research International, 2014*.
Gerbaldo, H., Thaker, G., Tittel, P. G., Layne-Gedge, J., Moran, M., & Demisch, L. (1992). Abnormal electroretinography in schizophrenic patients with a history of sun gazing. *Neuropsychobiology, 25*(2), 99-101.
Goff, D. C., Tsai, G., Levitt, J., Amico, E., Manoach, D., Schoenfeld, D. A., Coyle, J. T. (1999). A placebo-controlled trial of D-cycloserine added to conventional neuroleptics in patients with schizophrenia. *Archives of General Psychiatry, 56*(1), 21-27.
Goff, D. C., Tsai, G., Manoach, D. S., & Coyle, J. T. (1995). Dose-finding trial for D-cycloserine added to neuroleptics for negative symptoms in schizophrenia. *The American Journal of Psychiatry*.
Goltsov, A. Y., Loseva, J. G., Andreeva, T. V., Grigorenko, A. P., Abramova, L. I., Kaleda, V. G., Rogaev, E. I. (2006). Polymorphism in the 5′-promoter region of serine racemase gene in schizophrenia. *Molecular psychiatry, 11*(4), 325.

Gottesman, J. O. N., & Miller, R. F. (2003). N-methyl-D-aspartate receptors contribute to the baseline noise of retinal ganglion cells. *Visual Neuroscience, 20*(3), 329-333.
Granit, R. (1933). The components of the retinal action potential in mammals and their relation to the discharge in the optic nerve. *The Journal of Physiology, 77*(3), 207-239.
Grünert, U., Haverkamp, S., Fletcher, E. L., & Wässle, H. (2002). Synaptic distribution of ionotropic glutamate receptors in the inner plexiform layer of the primate retina. *Journal of Comparative Neurology, 447*(2), 138-151.
Gur, M., & Zeevi, Y. (1980). Frequency-domain analysis of the human electroretinogram. *JOSA, 70*(1), 53-59.
Gustafson, E. C., Stevens, E. R., Wolosker, H., & Miller, R. F. (2007). Endogenous D-serine contributes to NMDA-receptor-mediated light-evoked responses in the vertebrate retina. *Journal Neurophysiology, 98*(1), 122-130. doi:10.1152/jn.00057.2006
Gustafson, E. G., Stevens, E. S., & Miller, R. F. (2015). Dynamic regulation of D-serine release in the vertebrate retina. *Journal Physiology, 593*(4), 843-856. doi:10.1113/jphysiol.2014.283432
Hambrecht, M., Maurer, K., Häfner, H., & Sartorius, N. (1992). Transnational stability of gender differences in schizophrenia? *European Archives of Psychiatry and Clinical Neuroscience, 242*(1), 6-12.
Harsanyi, K., Wang, Y., & Mangel, S. C. (1996). Activation of NMDA receptors produces dopamine-mediated changes in fish retinal horizontal cell light responses. *Journal of Neurophysiology, 75*(2), 629-647.
Hartveit, E. (1996). Membrane currents evoked by ionotropic glutamate receptor agonists in rod bipolar cells in the rat retinal slice preparation. *Journal of Neurophysiology, 76*(1), 401-422.
Hartveit, E., Brandstätter, J. H., Sassoè-Pognetto, M., Laurie, D. J., Seeburg, P. H., & Wässle, H. (1994). Localization and developmental expression of the NMDA receptor subunit NR2A in the mammalian retina. *Journal of Comparative Neurology, 348*(4), 570-582.
Hartveit, E., & Veruki, M. L. (1997). AII amacrine cells express functional NMDA receptors. *Neuroreport, 8*(5), 1219-1223.
Hashimoto, A., Nishikawa, T., Hayashi, T., Fujii, N., Harada, K., Oka, T., & Takahashi, K. (1992a). The presence of free D-serine in rat brain. *FEBS Letters, 296*(1), 33-36.
Hashimoto, A., Nishikawa, T., Oka, T., & Takahashi, K. (1993). Endogenous D-serine in rat brain: N-methyl-D-aspartate receptor-related distribution and aging. *Journal of Neurochemistry, 60*(2), 783-786.
Hashimoto, A., Nishikawa, T., Oka, T., Takahashi, K., & Hayashi, T. (1992b). Determination of free amino acid enantiomers in rat brain and serum by high-performance liquid chromatography after derivatization with N-tert.-butyloxycarbonyl-L-cysteine and o-phthaldialdehyde. *Journal of Chromatography B: Biomedical Sciences and Applications, 582*(1-2), 41-48.
Hashimoto, K., Engberg, G., Shimizu, E., Nordin, C., Lindstrom, L. H., & Iyo, M. (2005). Reduced D-serine to total serine ratio in the cerebrospinal fluid of drug naive schizophrenic patients. *Progressive Neuropsychopharmacology Biological Psychiatry, 29*(5), 767-769. doi:10.1016/j.pnpbp.2005.04.023

Haverkamp, S., & Wässle, H. (2000). Immunocytochemical analysis of the mouse retina. *Journal of Comparative Neurology, 424*(1), 1-23.
Hebert, M., Gagne, A. M., Paradis, M. E., Jomphe, V., Roy, M. A., Merette, C., & Maziade, M. (2010). Retinal response to light in young nonaffected offspring at high genetic risk of neuropsychiatric brain disorders. *Biological Psychiatry, 67*(3), 270-274. doi:10.1016/j.biopsych.2009.08.016
Hebert, M., Merette, C., Paccalet, T., Emond, C., Gagne, A. M., Sasseville, A., & Maziade, M. (2015). Light evoked potentials measured by electroretinogram may tap into the neurodevelopmental roots of schizophrenia. *Schizophrenia Research, 162*(1-3), 294-295. doi:10.1016/j.schres.2014.12.030
Heinemann-Vernaleken, B., Palmowski, A., & Allgayer, R. (2000). The effect of time of day and repeat reliability on the fast flicker multifocal ERG. *Documenta Ophthalmologica, 101*(3), 247-255.
Holder, G. E. (2001). Pattern electroretinography (PERG) and an integrated approach to visual pathway diagnosis. *Progress in Retinal and Eye Research, 20*(4), 531-561.
Horn, F. K., Gottschalk, K., Mardin, C. Y., Pangeni, G., Jünemann, A. G., & Kremers, J. (2011). On and off responses of the photopic fullfield ERG in normal subjects and glaucoma patients. *Documenta Ophthalmologica, 122*(1), 53-62.
Hughes, T. E. (1997). Are there ionotropic glutamate receptors on the rod bipolar cell of the mouse retina? *Visual neuroscience, 14*(1), 103-109.
Häfner, H. (2003). Gender differences in schizophrenia. *Psychoneuroendocrinology*, 28 (Suppl2), 17-54. In.
Hébert, M., Gagné, A.-M., Paradis, M.-E., Jomphe, V., Roy, M.-A., Mérette, C., & Maziade, M. (2010). Retinal response to light in young nonaffected offspring at high genetic risk of neuropsychiatric brain disorders. *Biological Psychiatry, 67*(3), 270-274.
Hébert, M., Mérette, C., Paccalet, T., Émond, C., Gagné, A.-M., Sasseville, A., & Maziade, M. (2015). Light evoked potentials measured by electroretinogram may tap into the neurodevelopmental roots of schizophrenia. *Schizophrenia Research*, 162(1-3), 294-295. do10.1016/j.schres.2014.12.030
Javitt, D. C., & Zukin, S. R. (1991). Recent advances in the phencyclidine model of schizophrenia. *The American Journal of Psychiatry, 148*(10), 1308. doi:10.1176/ajp.148.10.1301.
Johnson, J. W., & Ascher, P. (1987). Glycine potentiates the NMDA response in cultured mouse brain neurons. *Nature, 325*(6104), 529.
Joshi, N. R., Ly, E., & Viswanathan, S. (2017). Intensity response function of the photopic negative response (PhNR): effect of age and test–retest reliability. *Documenta Ophthalmologica, 135*(1), 1-16.
Jules, R. S., Kennard, J., Setlik, W., & Holtzman, E. (1992). Frog cones as well as Müller cells have peroxisomes. *Experimental eye research, 54*(1), 1-8.
Kalbaugh, T. L., Zhang, J., & Diamond, J. S. (2009). Coagonist release modulates NMDA receptor subtype contributions at synaptic inputs to retinal ganglion cells. *Journal of Neuroscience, 29*(5), 1469-1479.
Kalloniatis, M., Sun, D., Foster, L., Haverkamp, S., & WÄssle, H. (2004). Localization of NMDA receptor subunits and mapping NMDA drive within the mammalian retina. *Visual Neuroscience, 21*(4), 587-597.

Kantrowitz, J. T., Malhotra, A. K., Cornblatt, B., Silipo, G., Balla, A., Suckow, R. F., Javitt, D. C. (2010). High dose D-serine in the treatment of schizophrenia. *Schizophrenia Research, 121*(1-3), 125-130. doi:10.1016/j.schres.2010.05.012

Karschin, A., & Wassle, H. (1990). Voltage-and transmitter-gated currents in isolated rod bipolar cells of rat retina. *Journal of Neurophysiology, 63*(4), 860-876.

Kendler, K. S., & Robinette, C. D. (1983). Schizophrenia in the national academy of sciences-national research council twin registry: a 16-year update. *American Journal Psychiatry, 140*(12), 1551-1563. doi:10.1176/ajp.140.12.1551

Kessler, R. C., Birnbaum, H., Demler, O., Falloon, I. R. H., Gagnon, E., Guyer, M., Walters, E. (2005). The prevalence and correlates of nonaffective psychosis in the National Comorbidity Survey Replication (NCS-R). *Biological Psychiatry, 58*(8), 668-676.

Kirov, G., Pocklington, A., Holmans, P., Ivanov, D., Ikeda, M., Ruderfer, D., Georgieva, L. (2012). De novo CNV analysis implicates specific abnormalities of postsynaptic signalling complexes in the pathogenesis of schizophrenia. *Molecular Psychiatry, 17*(2), 142.

Kishimoto, H., Simon, J. R., & Aprison, M. H. (1981). Determination of the equilibrium dissociation constants and number of glycine binding sites in several areas of the rat central nervous system, using a sodium-independent system. *Journal of Neurochemistry, 37*(4), 1015-1024.

Kleckner, N. W., & Dingledine, R. (1988). Requirement for glycine in activation of NMDA-receptors expressed in Xenopus oocytes. *Science, 241*(4867), 835-837.

Kofuji, P., Ceelen, P., Zahs, K. R., Surbeck, L. W., Lester, H. A., & Newman, E. A. (2000). Genetic inactivation of an inwardly rectifying potassium channel (Kir4. 1 subunit) in mice: phenotypic impact in retina. *Journal of Neuroscience, 20*(15), 5733-5740.

Kondo, M., Piao, C.-H., Tanikawa, A., Horiguchi, M., Terasaki, H., & Miyake, Y. (2000). Amplitude decrease of photopic ERG b-wave at higher stimulus intensities in humans. *Japanese Journal of Ophthalmology, 44*(1), 20-28.

Konno, R., & Yasumura, Y. (1983). Mouse mutant deficient in d-amino acid oxidase activity. *Genetics*, *103*(2), 277-285.

Krizaj, D. (2000). Mesopic state: Cellular mechanisms involved in pre-and post-synaptic mixing of rod and cone signals. *Microscopy Research and Technique, 50*(5), 347-359.

Kundra, H., Park, J. C., & McAnany, J. J. (2016). Comparison of photopic negative response measurements in the time and time–frequency domains. *Documenta Ophthalmologica, 133*(2), 91-98.

Labrie, V., Fukumura, R., Rastogi, A., Fick, L. J., Wang, W., Boutros, P. C., Baker, G. B. (2009). Serine racemase is associated with schizophrenia susceptibility in humans and in a mouse model. *Human Molecular Genetics, 18*(17), 3227-3243.

Lavoie, J., Gagné, A.-M., Lavoie, M.-P., Sasseville, A., Charron, M.-C., & Hébert, M. (2010). Circadian variation in the electroretinogram and the presence of central melatonin. *Documenta Ophthalmologica, 120*(3), 265-272.

Lavoie, J., Illiano, P., Sotnikova, T. D., Gainetdinov, R. R., Beaulieu, J. M., & Hebert, M. (2014). The electroretinogram as a biomarker of central dopamine and serotonin: potential relevance to psychiatric disorders. *Biological Psychiatry, 75*(6), 479-486. doi:10.1016/j.biopsych.2012.11.024

Lavoie, J., Maziade, M., & Hébert, M. (2014). The brain through the retina: the flash electroretinogram as a tool to investigate psychiatric disorders. *Progress in Neuro-Psychopharmacology and Biological Psychiatry, 48*, 129-134.
Leiderman, E., Zylberman, I., Zukin, S. R., Cooper, T. B., & Javitt, D. C. (1996). Preliminary investigation of high-dose oral glycine on serum levels and negative symptoms in schizophrenia: an open-label trial. *Biological Psychiatry, 39*(3), 213-215.
Lewis, D. A., & Lieberman, J. A. (2000). Catching up on schizophrenia: natural history and neurobiology. *Neuron, 28*(2), 325-334.
Li, B., Barnes, G., & Holt, W. (2005). The decline of the photopic negative response (PhNR) in the rat after optic nerve transection. *Documenta Ophthalmologica, 111*(1), 23-31.
Li, P., Snyder, G. L., & Vanover, K. E. (2016). Dopamine targeting drugs for the treatment of schizophrenia: Past, present and future. *Current Topics in Medicinal Chemistry, 16*(29), 3385-3403.
Loebel, A. D., Lieberman, J. A., Alvir, J. M., Mayerhoff, D. I., Geisler, S. H., & Szymanski, S. R. (1992). Duration of psychosis and outcome in first-episode schizophrenia. *The American Journal of Psychiatry*.
London, A., Benhar, I., & Schwartz, M. (2013). The retina as a window to the brain-from eye research to CNS disorders. *Nature Reviews Neurology, 9*(1), 44-53. doi:10.1038/nrneurol.2012.227
Loranger, A. W. (1984). Sex difference in age at onset of schizophrenia. *Archives of General Psychiatry, 41*(2), 157-161.
Luby, E. D., Gottlieb, J. S., Cohen, B. D., Rosenbaum, G., & Domino, E. F. (1962). Model psychoses and schizophrenia. *American Journal of Psychiatry, 119*(1), 61-67. doi:10.1176/ajp.119.1.61
Lukasiewicz, P. D., & McReynolds, J. S. (1985). Synaptic transmission at N-methyl-D-aspartate receptors in the proximal retina of the mudpuppy. *The Journal of Physiology, 367*(1), 99-115.
Luo, X., & Frishman, L. J. (2011). Retinal pathway origins of the pattern electroretinogram (PERG). *Investigative Ophthalmology and Visual Science, 52*(12), 8571-8584.
Machida, S. (2012). Clinical applications of the photopic negative response to optic nerve and retinal diseases. *Journal of Ophthalmology, 2012*.
Maffei, L., Fiorentini, A., Bisti, S., & Holländer, H. (1985). Pattern ERG in the monkey after section of the optic nerve. *Experimental Brain Research, 59*(2), 423-425.
Malenka, R. C., & Bear, M. F. (2004). LTP and LTD: an embarrassment of riches. *Neuron, 44*(1), 5-21.
Marcus, M., Cabael, L., & Marmor, M. F. (2004). Are circadian variations in the electroretinogram evident on routine testing? *Documenta Ophthalmologica, 108*(2), 165-169.
Marmor, M. F., Hock, P., Schechter, G., Pfefferbaum, A., Berger, P. A., & Maurice, R. (1988). Oscillatory potentials as a marker for dopaminergic disease. *Documenta Ophthalmologica, 69*(3), 255-261.
Massey, S. C., & Miller, R. F. (1990). N-methyl-D-aspartate receptors of ganglion cells in rabbit retina. *Journal of Neurophysiology, 63*(1), 16-30.

Matsui, Y., Katsumi, O., Sakaue, H., & Hirose, T. (1994). Electroretinogram b/a wave ratio improvement in central retinal vein obstruction. *British Journal of Ophthalmology, 78*(3), 191-198.

McCulloch, D. L., Marmor, M. F., Brigell, M. G., Hamilton, R., Holder, G. E., Tzekov, R., & Bach, M. (2015). ISCEV Standard for full-field clinical electroretinography (2015 update). *Documenta Ophthalmologica, 130*(1), 1-12.

McEwen, B. (2002). Estrogen actions throughout the brain. *Recent progress in Hormone Research, 57*, 357-384.

McRoberts, J. A., Li, J., Ennes, H. S., & Mayer, E. A. (2007). Sex-dependent differences in the activity and modulation of N-methyl-d-aspartic acid receptors in rat dorsal root ganglia neurons. *Neuroscience, 148*(4), 1015-1020.

Meguro, H., Mori, H., Araki, K., Kushiya, E., Kutsuwada, T., Yamazaki, M., Mishina, M. (1992). Functional characterization of a heteromeric NMDA receptor channel expressed from cloned cDNAs. *Nature, 357*(6373), 70-74.

Miller, R. F., & Slaughter, M. M. (1986). Excitatory amino acid receptors of the retina: diversity of subtypes and conductance mechanisms. *Trends in Neurosciences, 9*, 211-218.

Mittman, S., Taylor, W. R., & Copenhagen, D. R. (1990). Concomitant activation of two types of glutamate receptor mediates excitation of salamander retinal ganglion cells. *The Journal of Physiology, 428*(1), 175-197.

Miura, G., Wang, M. H., Ivers, K. M., & Frishman, L. J. (2009). Retinal pathway origins of the pattern ERG of the mouse. *Experimental Eye Research, 89*(1), 49-62.

Moghaddam, B., & Javitt, D. (2012). From revolution to evolution: the glutamate hypothesis of schizophrenia and its implication for treatment. *Neuropsychopharmacology, 37*(1), 4.

Mojumder, D. K., Sherry, D. M., & Frishman, L. J. (2008). Contribution of voltage-gated sodium channels to the b-wave of the mammalian flash electroretinogram. *The Journal of Physiology, 586*(10), 2551-2580.

Monsalve, P., Triolo, G., Toft-Nielsen, J., Bohorquez, J., Henderson, A. D., Delgado, R., Porciatti, V. (2017). Next generation PERG method: expanding the response dynamic range and capturing response adaptation. *Translational Vision Science & Technology, 6*(3), 5-5.

Moriyoshi, K., Masu, M., Ishii, T., Shigemoto, R., Mizuno, N., & Nakanishi, S. (1991). Molecular cloning and characterization of the rat NMDA receptor. *Nature, 354*(6348), 31-37.

Mothet, J.-P., Parent, A. T., Wolosker, H., Brady, R. O., Linden, D. J., Ferris, C. D., . . . Snyder, S. H. (2000). D-serine is an endogenous ligand for the glycine site of the N-methyl-D-aspartate receptor. *Proceedings of the National Academy of Sciences, 97*(9), 4926-4931.

Neims, A. H., Zieverink, W. D., & Smilack, J. D. (1966). Distribution of d-amino acid oxidase in bovine and human nervous tissues. *Journal of Neurochemistry, 13*(3), 163-168.

Nguyen, C. T., Hui, F., Charng, J., Velaedan, S., van Koeverden, A. K., Lim, J. K., . . . Bui, B. V. (2017). Retinal biomarkers provide “insight” into cortical pharmacology and disease. *Pharmacology and Therapeutics, 175*, 151-177.

O'Dell, T. J., & Christensen, B. N. (1989). Horizontal cells isolated from catfish retina contain two types of excitatory amino acid receptors. *Journal of Neurophysiology, 61*(6), 1097-1109.
Ochoa, S., Usall, J., Cobo, J., Labad, X., & Kulkarni, J. (2012). Gender differences in schizophrenia and first-episode psychosis: a comprehensive literature review. *Schizophrenia Research and Treatment, 2012*.
Olney, J. W., & Farber, N. B. (1995). Glutamate receptor dysfunction and schizophrenia. *Archives of General Psychiatry, 52*(12), 998-1007.
Özdamar, Ö., Toft-Nielsen, J., Bohórquez, J., & Porciatti, V. (2014). Relationship between transient and steady-state pattern electroretinograms: theoretical and experimental assessment. *Investigative Ophthalmology and Visual Science, 55*(12), 8560-8570.
Paoletti, P. (2011). Molecular basis of NMDA receptor functional diversity. *European Journal of Neuroscience, 33*(8), 1351-1365.
Penn, R., & Hagins, W. (1969). Signal transmission along retinal rods and the origin of the electroretinographic a-wave. *Nature, 223*(5202), 201.
Penn, R., & Hagins, W. (1972). Kinetics of the photocurrent of retinal rods. *Biophysical Journal, 12*(8), 1073-1094.
Peterson, H. (1968). The normal B-potential in the single-flash clinical electroretinogram. A computer technique study of the influence of sex and age. *Acta Ophthalmol (Copenh)*, Suppl 99:97-77.
Plonsey, R., & Barr, R. C. (2007). *Bioelectricity: a quantitative approach*: Springer Science & Business Media.
Porciatti, V. (2015). Electrophysiological assessment of retinal ganglion cell function. *Experimental eye research, 141*, 164-170.
Prager, T. C., Garcia, C. A., Mincher, C. A., Mishra, J., & Chu, H.-H. (1990). The pattern electroretinogram in diabetes. *American Journal of Ophthalmology, 109*(3), 279-284.
Preiser, D., Lagreze, W. A., Bach, M., & Poloschek, C. M. (2013). Photopic negative response versus pattern electroretinogram in early glaucoma. *Investigative Ophthalmology and Visual Science, 54*(2), 1182-1191.
Purcell, S. M., Moran, J. L., Fromer, M., Ruderfer, D., Solovieff, N., Roussos, P., Kähler, A. (2014). A polygenic burden of rare disruptive mutations in schizophrenia. *Nature, 506*(7487), 185.
Raese, J. D., King, R. J., Barnes, D., Berger, P. A., Marmor, M. F., & Hock, P. (1982). Retinal oscillatory potentials in schizophrenia: Implications for the assessment of dopamine transmission in man. *Pharmacology Bulletin, 18*, 72-78.
Rapoport, J. L., Giedd, J. N., & Gogtay, N. (2012). Neurodevelopmental model of schizophrenia: update 2012. *Molecular Psychiatry, 17*(12), 1228-1238. doi:10.1038/mp.2012.23
Reed, B. T., Sullivan, S. J., Tsai, G., Coyle, J. T., Esguerra, M., & Miller, R. F. (2009). The glycine transporter GlyT1 controls N-methyl-D-aspartic acid receptor coagonist occupancy in the mouse retina. *European Journal of Neuroscience, 30*(12), 2308-2317.
Robson, J., & Frishman, L. (1995). Response linearity and kinetics of the cat retina: the bipolar cell component of the dark-adapted electroretinogram. *Visual Neuroscience, 12*(5), 837-850.

Romero, G. E., Lockridge, A. D., Morgans, C. W., Bandyopadhyay, D., & Miller, R. F. (2014). The postnatal development of D-Serine in the retinas of two mouse strains, including a mutant mouse with a deficiency in D-amino acid oxidase and a serine racemase knockout mouse. *ACS Chemical Neuroscience, 5*(9), 848-854.

Rufiange, M., Dassa, J., Dembinska, O., Koenekoop, R. K., Little, J. M., Polomeno, R. C., Lachapelle, P. (2003). The photopic ERG luminance-response function (photopic hill): method of analysis and clinical application. *Vision research, 43*(12), 1405-1412.

Rufiange, M., Dumont, M., & Lachapelle, P. (2002). Correlating retinal function with melatonin secretion in subjects with an early or late circadian phase. *Investigative Ophthalmology and Visual Science, 43*(7), 2491-2499.

Sabates, R., Hirose, T., & McMeel, J. W. (1983). Electroretinography in the prognosis and classification of central retinal vein occlusion. *Archives of Ophthalmology, 101*(2), 232-235.

Sannita, W. G., Maggi, L., Germini, P. L., & Fioretto, M. (1989). Correlation with age and sex of flash-evoked electroretinogram and retinal oscillatory potentials recorded with skin electrodes. *Documenta Ophthalmologica, 71*(4), 413-419.

Savill, M., D'Ambrosio, J., Cannon, T. D., & Loewy, R. L. (2018). Psychosis risk screening in different populations using the Prodromal Questionnaire: A systematic review. *Early Intervention in Psychiatry, 12*(1), 3-14.

Schechter, G., Hock, P., Rodgers, K., Pfefferbaum, A., Marmor, M., & Berger, P. (1987). Electroretinographic assessment in schizophrenia. *Electroencephalography and Clinical Neurophysiology. Supplement, 40*, 746-751.

Schell, M. J., Brady Jr, R. O., Molliver, M. E., & Snyder, S. H. (1997). D-serine as a neuromodulator: regional and developmental localizations in rat brain glia resemble NMDA receptors. *Journal of Neuroscience, 17*(5), 1604-1615.

Schell, M. J., Molliver, M. E., & Snyder, S. H. (1995). D-serine, an endogenous synaptic modulator: localization to astrocytes and glutamate-stimulated release. *Proceedings of the National Academy of Sciences, 92*(9), 3948-3952.

Schlaggar, B. L., Fox, K., & O'Leary, D. D. (1993). Postsynaptic control of plasticity in developing somatosensory cortex. *Nature, 364*(6438), 623-626.

Schönfeldt-Lecuona, C., Kregel, T., Schmidt, A., Pinkhardt, E. H., Lauda, F., Kassubek, J., Gahr, M. (2015). From imaging the brain to imaging the retina: optical coherence tomography (OCT) in schizophrenia. *Schizophrenia Bulletin, 42*(1), 9-14.

Shen, Y., Liu, X.-L., & Yang, X.-L. (2006). N-methyl-D-aspartate receptors in the retina. *Molecular Neurobiology, 34*(3), 163-179.

Shepherd, M., Watt, D., Falloon, I., & Smeeton, N. (1989). The natural history of schizophrenia: a five-year follow-up study of outcome and prediction in a representative sample of schizophrenics. *Psychological Medicine Monograph Supplement, 15*, 1-46.

Silverstein, S. M., & Rosen, R. (2015). Schizophrenia and the eye. *Schizophrenia Research: Cognition, 2*(2), 46-55.

Slaughter, M. M., & Miller, R. F. (1983). The role of excitatory amino acid transmitters in the mudpuppy retina: an analysis with kainic acid and N-methyl aspartate. *J Neuroscience, 3*(8), 1701-1711.

Slikker Jr, W. (2018). Biomarkers and their impact on precision medicine. In: SAGE Publications Sage UK: London, England.
Snyder, S. H. (1976). The dopamine hypothesis of schizophrenia: focus on the dopamine receptor. *American Journal Psychiatry, 133*(2), 197-202. doi:10.1176/ajp.133.2.197
Stevens, E. R., Esguerra, M., Kim, P. M., Newman, E. A., Snyder, S. H., Zahs, K. R., & Miller, R. F. (2003). D-serine and serine racemase are present in the vertebrate retina and contribute to the physiological activation of NMDA receptors. *Proceedings of the National Academy of Sciences, 100*(11), 6789-6794.
Stevens, E. R., Gustafson, E. C., Sullivan, S. J., Esguerra, M., & Miller, R. F. (2010). Light-evoked NMDA receptor-mediated currents are reduced by blocking D-serine synthesis in the salamander retina. *Neuroreport, 21*(4), 239.
Stockton, R. A., & Slaughter, M. M. (1989). B-wave of the electroretinogram. A reflection of ON bipolar cell activity. *The Journal of General Physiology, 93*(1), 101-122.
Sugihara, H., Moriyoshi, K., Ishii, T., Masu, M., & Nakanishi, S. (1992). Structures and properties of seven isoforms of the NMDA receptor generated by alternative splicing. *Biochem Biophys Res Commun, 185*(3), 826-832. doi:10.1016/0006-291x(92)91701-q
Sullivan, S. J., Esguerra, M., Wickham, R. J., Romero, G. E., Coyle, J. T., & Miller, R. F. (2011). Serine racemase deletion abolishes light-evoked NMDA receptor currents in retinal ganglion cells. *The Journal of physiology, 589*(24), 5997-6006.
Sullivan, S. J., & Miller, R. F. (2012). AMPA receptor-dependent, light-evoked D-serine release acts on retinal ganglion cell NMDA receptors. *Journal Neurophysiology, 108*(4), 1044-1051. doi:10.1152/jn.00264.2012
Tahara, K., Matsuura, T., & Otori, T. (1993). Diagnostic evaluation of diabetic retinopathy by 30-Hz flicker electroretinography. *Japanese Journal of Ophthalmology, 37*(2), 204-210.
Tomasetti, C., Iasevoli, F., Buonaguro, E., De Berardis, D., Fornaro, M., Fiengo, A., Di Giannantonio, M. (2017). Treating the synapse in major psychiatric disorders: the role of postsynaptic density network in dopamine-glutamate interplay and psychopharmacologic drugs molecular actions. *International Journal of Molecular Sciences, 18*(1), 135.
Torres Jimenez, N., Lines, J.W., Kueppers, R.B., Kofuji, P., Wei, H., Rankila, A., Coyle, J.T., McLoon, L.K., Miller, R.F. (2019). Electroretinographic abnormalities and sex differences in an NMDAR hypofunction mouse model of schizophrenia: A and B wave analysis. *Investigative Ophthalmology and Visual Science*.
Tsai, G., Passani, L. A., Slusher, B. S., Carter, R., Baer, L., Kleinman, J. E., & Coyle, J. T. (1995). Abnormal excitatory neurotransmitter metabolism in schizophrenic brains. *Archives of General Psychiatry, 52*(10), 829-836.
Vainio-Mattila, B. (1951). The clinical electroretinogram: II. The difference between the electroretinogram in men and in women. *Acta Ophthalmologica, 29*(1), 25-32.
Ventura, J., Lukoff, D., Nuechterlein, K., Liberman, R., Green, M., & Shaner, A. (1993). Appendix 1: Brief Psychiatric Rating Scale (BPRS) expanded version (4.0) scales, anchor points and administration manual. *International Journal Methods Psychiatric Research, 3*(227), 43.
Ventura, L. M., & Porciatti, V. (2006). Pattern electroretinogram in glaucoma. *Current Opinion in Ophthalmology, 17*(2), 196.

Viswanathan, S., Frishman, L. J., Robson, J. G., Harwerth, R. S., & Smith, E. r. (1999). The photopic negative response of the macaque electroretinogram: reduction by experimental glaucoma. *Investigative Ophthalmology and Visual Science, 40*(6), 1124-1136.

Vorwerk, C. K., Naskar, R., Schuettauf, F., Quinto, K., Zurakowski, D., Gochenauer, G., Dreyer, E. B. (2000). Depression of retinal glutamate transporter function leads to elevated intravitreal glutamate levels and ganglion cell death. *Investigative Ophthalmology Visual Science, 41*(11), 3615-3621.

Wachtmeister, L. (1998). Oscillatory potentials in the retina: what do they reveal. *Progress in Retinal and Eye Research, 17*(4), 485-521.

Wali, N., & Leguire, L. E. (1992). The photopic hill: a new phenomenon of the light adapted electroretinogram. *Documenta Ophthalmologica, 80*(4), 335-342.

Warner, R., Laugharne, J., Peet, M., Brown, L., & Rogers, N. (1999). Retinal function as a marker for cell membrane omega–3 fatty acid depletion in schizophrenia: a pilot study. *Biological Psychiatry, 45*(9), 1138-1142.

Watanabe, M., Mishina, M., & Inoue, Y. (1994). Differential distributions of the NMDA receptor channel subunit mRNAs in the mouse retina. *Brain Research, 634*(2), 328-332.

Weickert, C. S., Fung, S., Catts, V., Schofield, P., Allen, K., Moore, L., Catts, S. (2013). Molecular evidence of N-methyl-D-aspartate receptor hypofunction in schizophrenia. *Molecular Psychiatry, 18*(11), 1185.

Weickert, C. S., Weickert, T. W., Pillai, A., & Buckley, P. F. (2013). Biomarkers in schizophrenia: a brief conceptual consideration. *Disease Markers, 35*(1), 3-9.

Weymouth, A., & Vingrys, A. (2008). Rodent electroretinography: methods for extraction and interpretation of rod and cone responses. *Progress in Retinal and Eye Research, 27*(1), 1-44.

Wolosker, H., Blackshaw, S., & Snyder, S. H. (1999). Serine racemase: a glial enzyme synthesizing D-serine to regulate glutamate-N-methyl-D-aspartate neurotransmission. *Proceedings of the National Academy of Sciences, 96*(23), 13409-13414.

Woodward, W. R., Choi, D., Grose, J., Malmin, B., Hurst, S., Pang, J., Pillers, D.-A. M. (2007). Isoflurane is an effective alternative to ketamine/xylazine/acepromazine as an anesthetic agent for the mouse electroretinogram. *Documenta Ophthalmologica, 115*(3), 187-201.

Woolley, C. S. (1998). Estrogen-mediated structural and functional synaptic plasticity in the female rat hippocampus. *Hormones and Behavior, 34*(2), 140-148.

Wu, E. Q., Birnbaum, H. G., Shi, L., Ball, D. E., Kessler, R. C., Moulis, M., & Aggarwal, J. (2005). The economic burden of schizophrenia in the United States in 2002. *Journal of Clinical Psychiatry, 66*(9), 1122-1129.

Wu, E. Q., Shi, L., Birnbaum, H., Hudson, T., & Kessler, R. (2006). Annual prevalence of diagnosed schizophrenia in the USA: a claims data analysis approach. *Psychological Medicine, 36*(11), 1535-1540.

Yamada, K., Ohnishi, T., Hashimoto, K., Ohba, H., Iwayama-Shigeno, Y., Toyoshima, M., Minabe, Y. (2005). Identification of multiple serine racemase (SRR) mRNA isoforms and genetic analyses of SRR and DAO in schizophrenia and D-serine levels. *Biological psychiatry, 57*(12), 1493-1503.

Yurgelun-Todd, D. A., Coyle, J. T., Gruber, S. A., Renshaw, P. F., Silveri, M. M., Amico, E., . . . Goff, D. C. (2005). Functional magnetic resonance imaging studies of schizophrenic patients during word production: effects of D-cycloserine. *Psychiatry Research: Neuroimaging, 138*(1), 23-31.

Zita, B., Benedek, G., Kéri, S. (2008). Retinal dysfunctions in schizophrenia. *Progress in Neuro-Psychopharmacology and Biological Psychiatry, 32*(1), 297 - 300. doi:10.1016/j.pnpbp.2007.08.024

Zeidler, I. (1959). The clinical electroretinogram: IX. The normal electroretinogram: Value of the b-potential in different age groups and its differences in men and women. *Acta Ophthalmologica, 37*(3), 294-301.

Zhang, D.-Q., Wong, K. Y., Sollars, P. J., Berson, D. M., Pickard, G. E., & McMahon, D. G. (2008). Intraretinal signaling by ganglion cell photoreceptors to dopaminergic amacrine neurons. *Proceedings of the National Academy of Sciences, 105*(37), 14181-14186.

Zhang, J., & Diamond, J. S. (2006). Distinct perisynaptic and synaptic localization of NMDA and AMPA receptors on ganglion cells in rat retina. *Journal of Comparative Neurology, 498*(6), 810-820.

Zhou, W., Rangaswamy, N., Ktonas, P., & Frishman, L. J. (2007). Oscillatory potentials of the slow-sequence multifocal ERG in primates extracted using the Matching Pursuit method. *Vision research, 47*(15), 2021-2036.